

## Supporting Information

### Chiral CNN Pincer Palladium(II) Complexes with 2-Aryl -6-(Oxazolinyl)pyridine Ligands: Synthesis, Characterization, and Application to Enantioselective Allylation of Isatins and Suzuki-Miyaura Coupling Reaction

Tao Wang, Xin-Qi Hao, Juan-Juan Huang, Kai Wang, Jun-Fang Gong,<sup>\*</sup>  
and Mao-Ping Song<sup>\*</sup>

*College of Chemistry and Molecular Engineering, Henan Key Laboratory of Chemical  
Biology and Organic Chemistry, Zhengzhou University, Zhengzhou 450001, People's  
Republic of China*

Crystallographic Details for Complexes <b>3c-f</b> .....	S-2
Additional Catalytical Results on the Allylation of a Ketimine Derived from N-benzyl Isatin.....	S-3
Proposed Reaction Mechanisms for the Asymmetric Allylation of Isatins and Suzuki-Miyaura Reaction.....	S-6
Characterization Data of the Known Catalysis Products.....	S-9
Copies of the <sup>1</sup> H and <sup>13</sup> C NMR Spectra of New Compounds <b>1-3</b> .....	S-15
Copies of the NMR Spectra of the Catalysis Products.....	S-28
HPLC Spectra of the Catalysis Products.....	S-54

---

\* Tel./Fax: (+86)-371-6778-3012. E-mail: mpsong@zzu.edu.cn (M.-P. Song) or gongjf@zzu.edu.cn (J.-F. Gong).

**Table S1. Summary of Crystallographic Details for Complexes 3c-f**

	<b>3c</b>	<b>3d</b>	<b>3e·(n-hexane)</b>	<b>(2 x 3f)·CH<sub>2</sub>Cl<sub>2</sub></b>
formula	C <sub>20</sub> H <sub>15</sub> ClN <sub>2</sub> OPd	C <sub>21</sub> H <sub>17</sub> ClN <sub>2</sub> OPd	C <sub>32</sub> H <sub>33</sub> ClN <sub>2</sub> OPd	C <sub>49</sub> H <sub>36</sub> Cl <sub>4</sub> N <sub>4</sub> O <sub>2</sub> Pd <sub>2</sub>
<i>M<sub>r</sub></i>	441.19	455.22	603.45	1067.42
temp (K)	291(2)	291(0)	291(2)	291(2)
cryst syst	orthorhombic	monoclinic	monoclinic	orthorhombic
space group	P2 <sub>1</sub> 2 <sub>1</sub> 2 <sub>1</sub>	P2 <sub>1</sub>	P2 <sub>1</sub>	P2 <sub>1</sub> 2 <sub>1</sub> 2 <sub>1</sub>
cryst size (mm)	0.24 x 0.20 x 0.20	0.24 x 0.22 x 0.20	0.5272 x 0.3018 x 0.1313	0.20 x 0.20 x 0.18
<i>a</i> (Å)	10.100(2)	7.1915(2)	6.0672(6)	12.8040(4)
<i>b</i> (Å)	11.2001(12)	21.4390(7)	17.9824(12)	13.5812(4)
<i>c</i> (Å)	15.725(2)	12.2763(3)	12.2022(9)	24.3928(5)
$\alpha$ (deg)	90.00	90.00	90.00	90.00
$\beta$ (deg)	90.00	101.495(3)	100.610(8)	90.00
$\gamma$ (deg)	90.00	90.00	90.00	90.00
<i>V</i> (Å <sup>3</sup> )	1778.9(5)	1854.79(9)	1308.54(19)	4241.75(19)
<i>Z</i>	4	4	2	4
<i>D</i> <sub>calcd</sub> (g cm <sup>-3</sup> )	1.647	1.630	1.532	1.671
$\mu$ (mm <sup>-1</sup> )	1.203	1.156	0.840	1.147
$\theta$ range (deg)	3.01-26.37	3.04-26.39	3.4-26.37	3.0-26.37
index range	-12 ≤ <i>h</i> ≤ 6, -14 ≤ <i>k</i> ≤ 12, -10 ≤ <i>l</i> ≤ 19	-8 ≤ <i>h</i> ≤ 8, -26 ≤ <i>k</i> ≤ 26, -8 ≤ <i>l</i> ≤ 15	-7 ≤ <i>h</i> ≤ 7, -22 ≤ <i>k</i> ≤ 22, -15 ≤ <i>l</i> ≤ 14	-16 ≤ <i>h</i> ≤ 15, -16 ≤ <i>k</i> ≤ 16, -28 ≤ <i>l</i> ≤ 30
no. of data collected	7100	8473	11301	18581
no. of unique data	3625	6363	5355	8666
final R indices ( <i>I</i> > $2\sigma(I)$ ) R1	0.0268	0.0388	0.0442	0.0437
wR2	0.0486	0.0784	0.1121	0.0570
R indices (all data) R1	0.0311	0.0463	0.0512	0.0702
wR2	0.0504	0.0835	0.1186	0.0633
<i>F</i> (000)	880	912	620	2136
peak/hole (e·Å <sup>-3</sup> )	0.243/-0.307	0.484/-0.464	0.736/-0.325	0.680/-0.458

**Additional Catalytical Results on the Allylation of a Ketimine Derived from N-benzyl Isatin.**

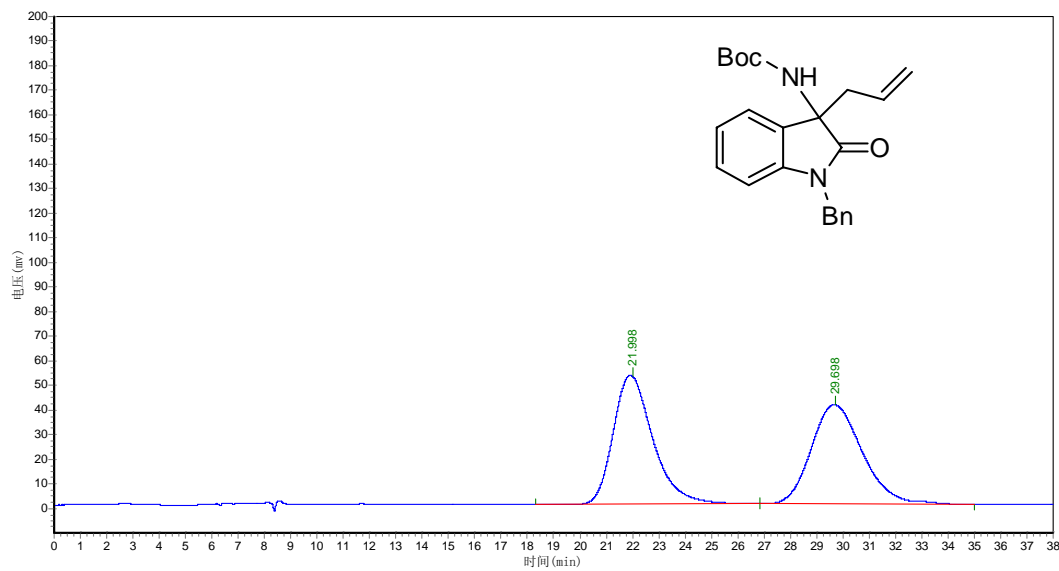
**Table S2. The Asymmetric Allylation of a Ketimine Derived from N-benzyl Isatin Catalyzed by the Chiral CNN Pincer Pd(II) Complexes 3<sup>a</sup>**

Entry	Cat.	Solvent	Temp. (°C)	Yield (%) <sup>b</sup>	ee (%) <sup>c,d</sup>
1	<b>3b</b>	CH <sub>2</sub> Cl <sub>2</sub>	-60	0	--
2	<b>3b</b>	CH <sub>2</sub> Cl <sub>2</sub>	RT	98	39
3	<b>3b</b>	CH <sub>2</sub> Cl <sub>2</sub>	-10	77	51
4	<b>3b</b>	THF	-10	85	0
5 <sup>e</sup>	<b>3b</b>	CH <sub>2</sub> Cl <sub>2</sub>	-30	80	58
6 <sup>e</sup>	<b>3e</b>	CH <sub>2</sub> Cl <sub>2</sub>	-30	84	69
7 <sup>e,f</sup>	<b>3e</b>	CH <sub>2</sub> Cl <sub>2</sub>	-30	81	9
8 <sup>e</sup>	<b>3e</b>	CH <sub>2</sub> Cl <sub>2</sub>	-40	53	72
9 <sup>e</sup>	<b>3e</b>	CH <sub>2</sub> Cl <sub>2</sub>	-50	37	72

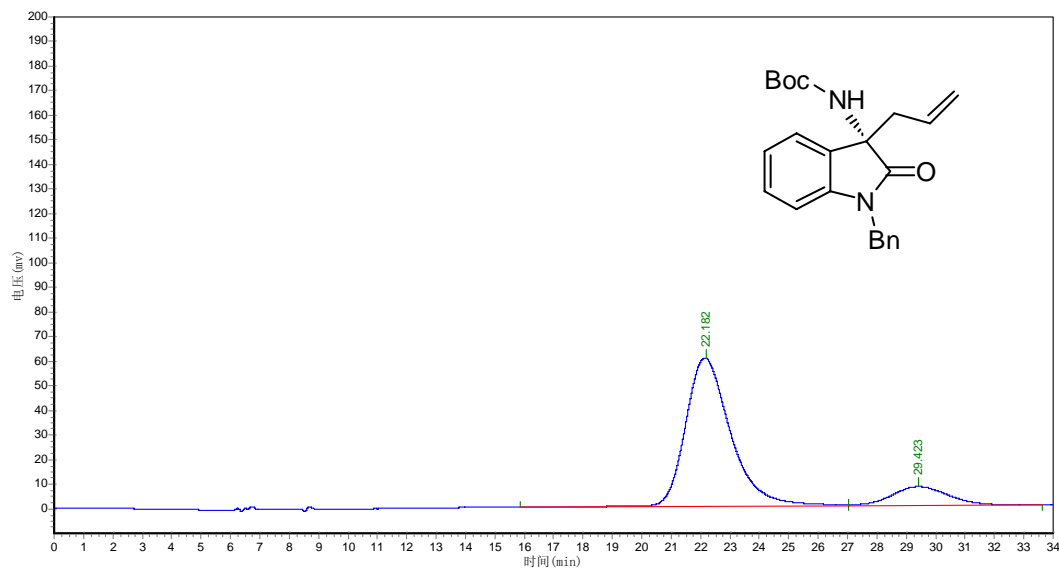
<sup>a</sup>Reaction conditions: ketimine (0.20 mmol), allyltributyltin (0.30 mmol), cat. **3** (5 mol %), solvent (1 mL), 12 h. <sup>b</sup>Isolated yields. <sup>c</sup>Determined by chiral HPLC. <sup>d</sup>The absolute configuration of the product was assigned to be *S* by comparison of optical rotation with that in the literature (*Chem. Eur. J.* **2013**, *19*, 7304). <sup>e</sup>36 h. <sup>f</sup>Allyltrimethylsilane (0.30 mmol) as the allyl source in the presence of AgF (0.20 mmol) as an additive.

**(S)-tert-Butyl (3-allyl-1-benzyl-2-oxoindolin-3-yl)carbamate:** White solid (40.1 mg, 0.106 mmol; 53%). The enantiomeric excess was determined on a Daicel Chiraldpak AS-H column with hexane/2-propanol = 90/10, flow = 0.5 mL/min, and detected at a UV wave length of 254 nm. Retention times: 22.2 min (major), 29.4 min, 72% ee.  $[\alpha]_D^{20} = -8.5$  (*c* 1.000, CHCl<sub>3</sub>). <sup>1</sup>H NMR (400 MHz, CDCl<sub>3</sub>):  $\delta$  7.36 (d, *J* = 7.3 Hz, 2H, ArH), 7.30 (t, *J* = 7.3 Hz, 2H, ArH), 7.25 (d, *J* = 6.6 Hz, 2H, ArH), 7.16 (t, *J* = 7.5 Hz, 1H, ArH), 7.02 (t, *J* = 7.4 Hz, 1H, ArH), 6.70 (d, *J* = 7.7 Hz, 1H, ArH), 5.76-5.65 (m, 1H, CH<sub>2</sub>CH=CH<sub>2</sub>),

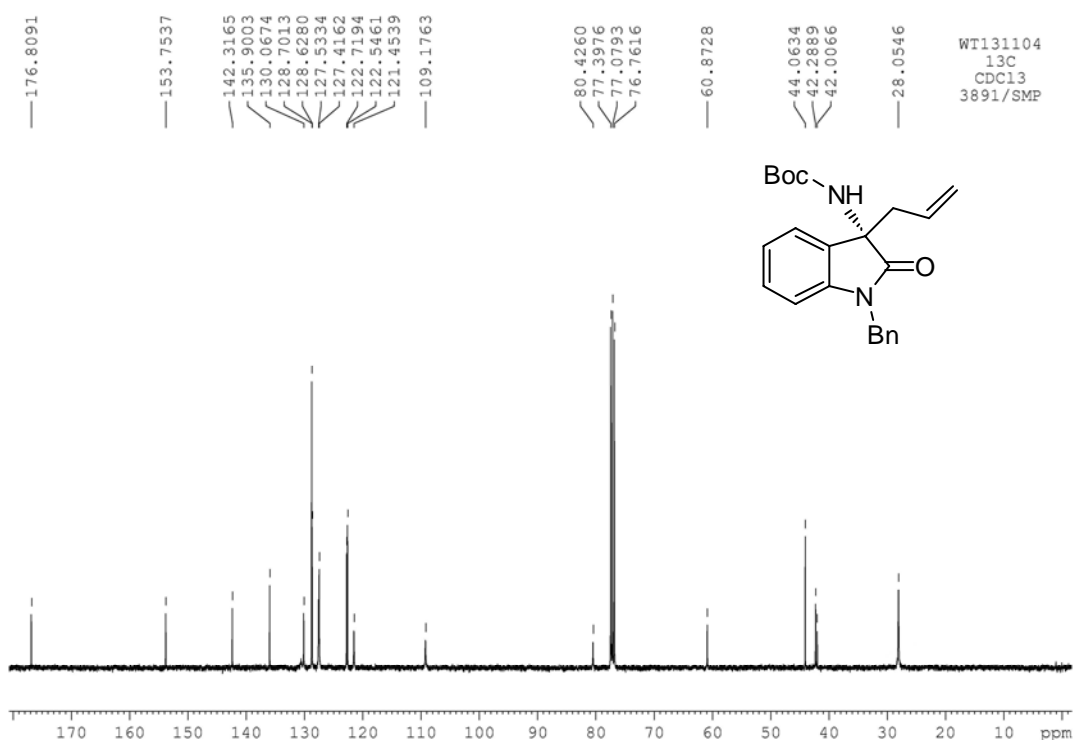
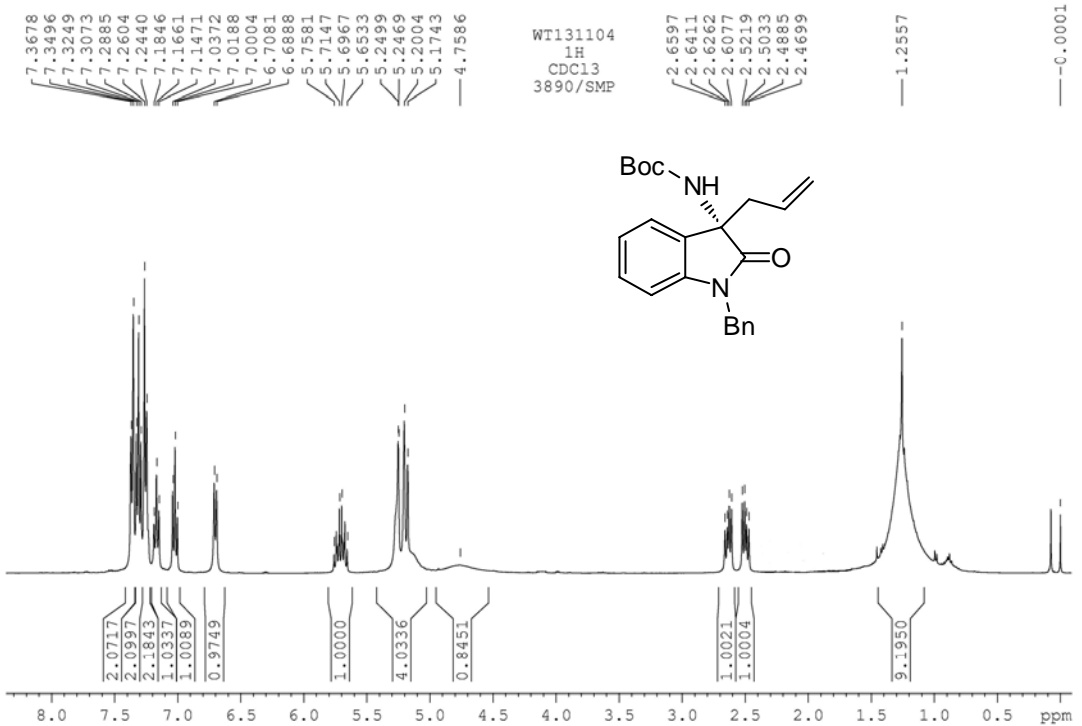
5.25-5.17 (m, 4H, NCH<sub>2</sub>, CH<sub>2</sub>CH=CH<sub>2</sub>), 4.76 (br s, 1H, NH), 2.66-2.61 (m, 1H, CH<sub>2</sub>CH=CH<sub>2</sub>), 2.52-2.47 (m, 1H, CH<sub>2</sub>CH=CH<sub>2</sub>), 1.26 (s, 9H, C(CH<sub>3</sub>)<sub>3</sub>). <sup>13</sup>C NMR (100 MHz, CDCl<sub>3</sub>): δ 176.8, 153.8, 142.3, 135.9, 130.1, 128.7, 128.6, 127.5, 127.4, 122.7, 122.5, 121.5, 109.2, 80.4, 60.9, 44.1, 42.3, 42.0, 28.1.



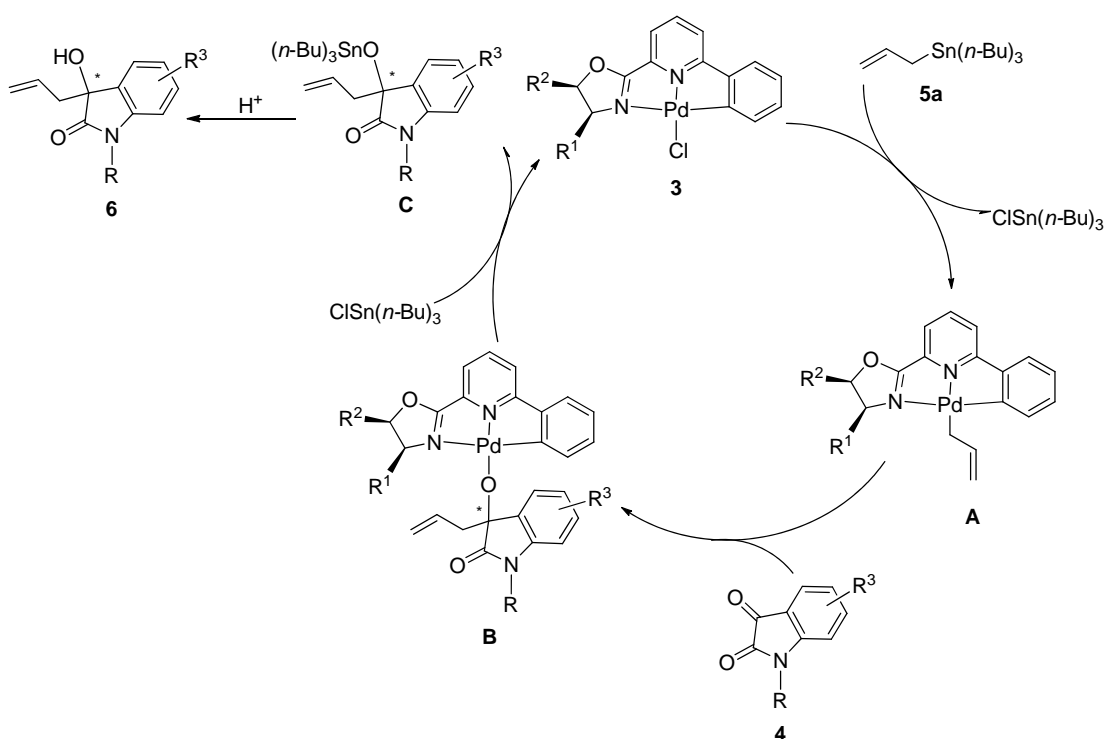
PeakNO.	Ret.Time	PeakHeight	PeakArea	Area%
1	21.998	52458.590	5524363.500	50.3503
2	29.698	40321.773	5447492.500	49.6497



PeakNO.	Ret.Time	PeakHeight	PeakArea	Area%
1	22.182	60394.984	6477737.500	85.7681
2	29.423	7767.010	1074884.625	14.2319



**Proposed Reaction Cycle for the Asymmetric Allylation of Isatins Catalyzed by the Chiral CNN Pincer Pd(II) Complexes 3.** A catalytic cycle (Scheme S1) for the allylation of isatins with allyltributyltin catalyzed by the chiral CNN pincer Pd(II) complexes **3** is proposed based on the related literature reports.<sup>1</sup> The chloride on the Pd(II) complex **3** reacts with allyltributyltin to give an  $\eta^1$ -allyl palladium(II) complex **A**. Then the nucleophilic reaction of allyl-palladium species **A** with isatin results in the intermediate **B**, which subsequently undergoes transmetallation with chlorotributyltin giving complex **C** and regenerating the pincer Pd(II) catalyst **3**. Finally, further acidification of the complex **C** affords the 3-allyl-3-hydroxyoxindole product **6**.

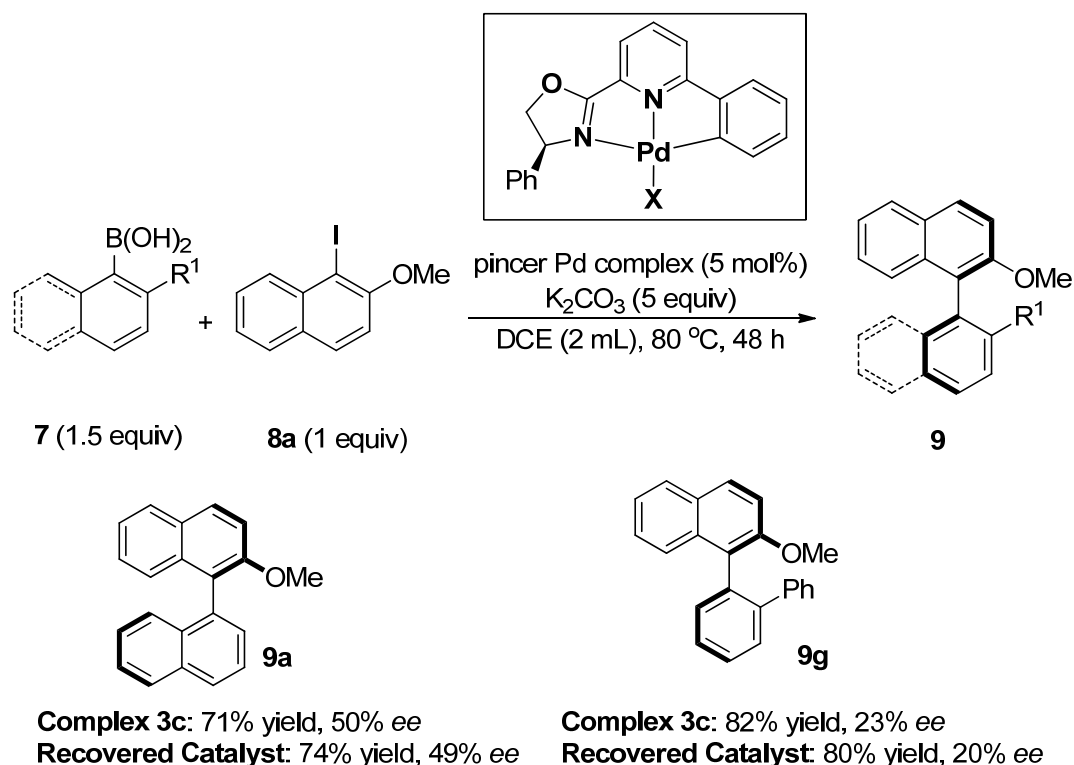


**Scheme S1. Proposed Reaction Cycle for the Asymmetric Allylation of Isatins Catalyzed by the Chiral CNN Pincer Pd(II) Complexes 3**

## References

- (1) (a) Nakamura, S.; Hyodo, K.; Nakamura, M.; Nakane, D.; Masuda, H. *Chem. Eur. J.* **2013**, *19*, 7304. (b) Li, J.; Minnaard, A. J.; Klein Gebbink, R. J. M.; van Koten, G. *Tetrahedron Lett.* **2009**, *50*, 2232. (c) Aydin, J.; Kumar, K. S.; Sayah, M. J.; Wallner, O. A.; Szabó, K. J. *J. Org. Chem.* **2007**, *72*, 4689. (d) Yao, Q.; Sheets, M. *J. Org. Chem.* **2006**, *71*, 5384. (e) Solin, N.; Kjellgren, J.; Szabó, K. J. *J. Am. Chem. Soc.* **2004**, *126*, 7026.

**Proposed Mechanism of Asymmetric Suzuki-Miyaura Reaction.** To gain some insights into the mechanism of Suzuki-Miyaura reaction catalyzed by the chiral CNN pincer Pd(II) complexes **3**, the recycling of the catalyst was investigated. It was found that the catalyst could be recovered when preparative TLC on silica gel plates was performed to isolate the axially chiral biaryl products. In the couplings of 1-iodo-2-methoxynaphthalene with 1-naphthaleneboronic acid and 2-phenylbenzeneboronic acid, the recovered catalyst exhibited comparable activity and enantioselectivities (Scheme S2). The NMR spectra of the recovered catalyst are very similar to those of the CNN-PdCl complex **3c**, but not the same. Although satisfactory elemental analysis of the recovered catalyst was not obtained (ESI-MS did not provide useful information, either), it was tentatively identified as the corresponding CNN-PdI complex on the basis of the NMR spectra and literature report.<sup>2</sup> In addition, palladium blacking out was not observed throughout the reaction process. The above results suggest that the current asymmetric Suzuki-Miyaura reaction may include a Pd(II)-Pd(IV) catalytic cycle instead of a Pd(0)-Pd(II) cycle, as reported by Iwasa and Nishiyama in the NCN bis(oxazolinyl)phenyl pincer Pd(II)-catalyzed Suzuki-Miyaura reaction.<sup>2</sup>

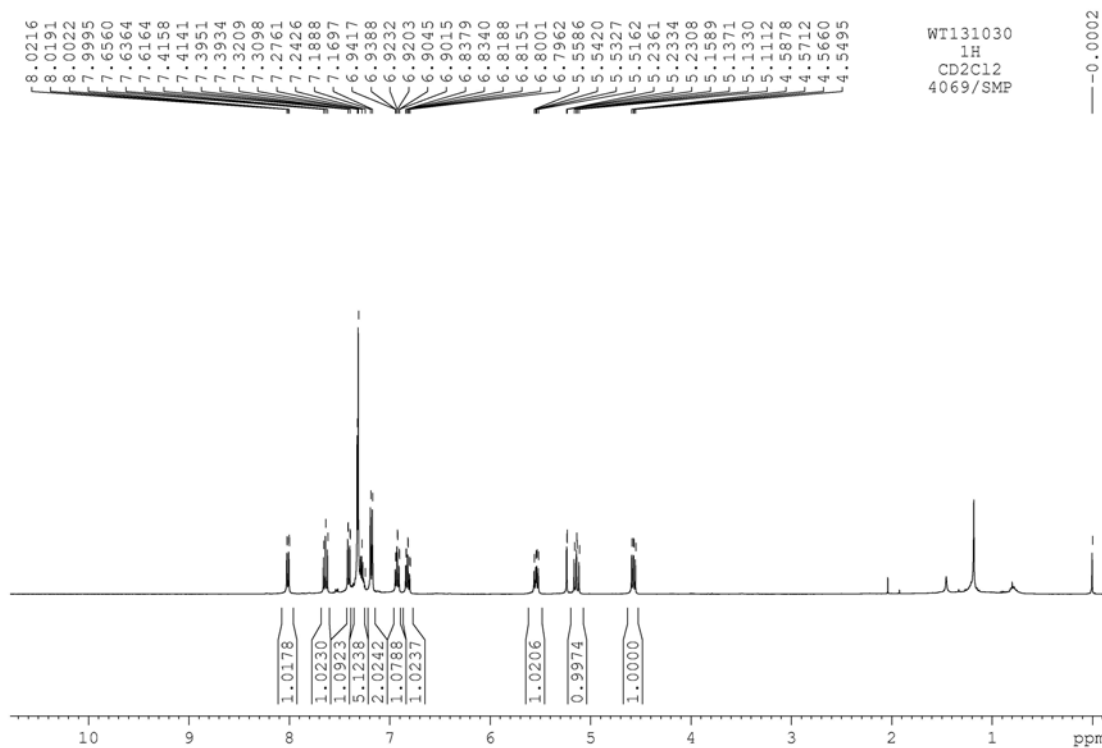


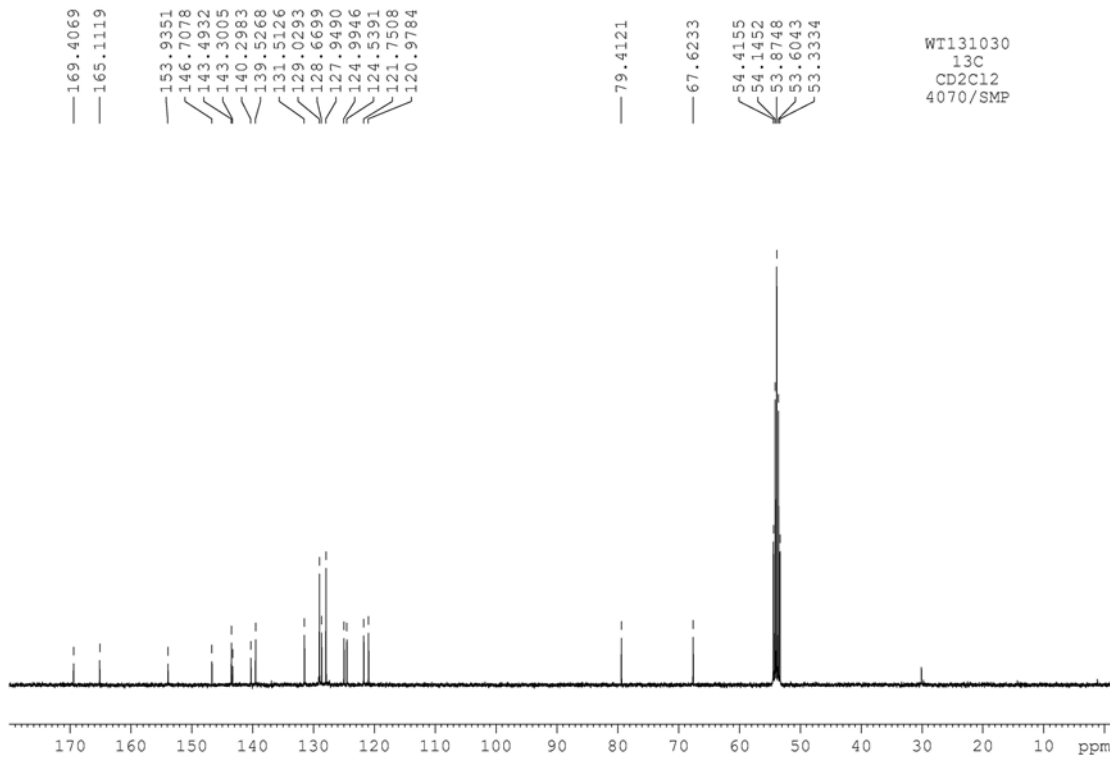
**Scheme S2.**

## Reference

(2) Takemoto, T.; Iwasa, S.; Hamada, H.; Shibatomi, K.; Kameyama, M.; Motoyama, Y.; Nishiyama, H. *Tetrahedron Lett.* **2007**, *48*, 3397.

**Recovered catalyst:**  $^1\text{H}$  NMR (400 MHz,  $\text{CD}_2\text{Cl}_2$ ):  $\delta$  8.01 (dd,  $J = 1.0, 7.8$  Hz, 1H, ArH), 7.64 (t,  $J = 7.8$  Hz, 1H, ArH), 7.40 (dd,  $J = 0.7, 8.3$  Hz, 1H, ArH), 7.32-7.24 (m, 5H, ArH), 7.18 (d,  $J = 7.6$  Hz, 2H, ArH), 6.92 (dt,  $J = 1.2, 7.4$  Hz, 1H, ArH), 6.82 (dt,  $J = 1.6, 7.6$  Hz, 1H, ArH), 5.54 (dd,  $J = 6.6, 10.4$  Hz, 1H, OxH), 5.13 (dd,  $J = 8.7, 10.4$  Hz, 1H, OxH), 4.57 (dd,  $J = 6.6, 8.7$  Hz, 1H, OxH).  $^{13}\text{C}$  NMR (100 MHz,  $\text{CD}_2\text{Cl}_2$ ):  $\delta$  169.4, 165.1, 153.9, 146.7, 143.4, 143.3, 140.3, 139.5, 131.5, 129.0, 128.7, 127.9, 125.0, 124.5, 121.8, 121.0, 79.4, 67.6.





## Characterization Data of the Known Catalysis Products

**(S)-3-Allyl-1-benzyl-3-hydroxyindolin-2-one (6a):** White solid (52.5 mg, 0.188 mmol; 94%). M.p.: 147-149 °C. The enantiomeric excess was determined on a Daicel Chiralcel OJ-H column with hexane/2-propanol = 90/10, flow = 0.8 mL/min, and detected at a UV wave length of 254 nm. Retention times: 13.5 min, 21.6 min (major), 78% ee.  $[\alpha]_D^{20} = -1.4$  (*c* 0.908, CH<sub>2</sub>Cl<sub>2</sub>). <sup>1</sup>H NMR (400 MHz, CDCl<sub>3</sub>): δ 7.40 (dd, *J* = 0.6, 7.3 Hz, 1H, ArH), 7.31-7.24 (m, 5H, ArH), 7.21-7.16 (m, 1H, ArH), 7.07-7.03 (m, 1H, ArH), 6.68 (d, *J* = 7.8 Hz, 1H, ArH), 5.65-5.54 (m, 1H, CH<sub>2</sub>CH=CH<sub>2</sub>), 5.14-5.05 (m, 2H, CH<sub>2</sub>CH=CH<sub>2</sub>), 5.01 (d, *J* = 15.7 Hz, 1H, CH<sub>2</sub>Ph), 4.70 (d, *J* = 15.7 Hz, 1H, CH<sub>2</sub>Ph), 3.76 (br s, 1H, OH), 2.85-2.81 (m, 1H, CH<sub>2</sub>CH=CH<sub>2</sub>), 2.74-2.69 (m, 1H, CH<sub>2</sub>CH=CH<sub>2</sub>).

**(S)-3-Allyl-3-hydroxyindolin-2-one (6d):** White solid (34.1 mg, 0.180 mmol; 90%). M.p.: 124-125 °C. The enantiomeric excess was determined on a Daicel Chiralcel OD-H column

with hexane/2-propanol = 90/10, flow = 1.0 mL/min, and detected at a UV wave length of 254 nm. Retention times: 9.4 min (major), 12.0 min, 60% *ee*.  $[\alpha]_D^{20} = +99.7$  (*c* 0.464,  $\text{CH}_2\text{Cl}_2$ ).  $^1\text{H}$  NMR (400 MHz,  $\text{CDCl}_3$ ):  $\delta$  8.70 (br s, 1H, NH), 7.35 (d, *J* = 7.3 Hz, 1H, ArH), 7.26-7.22 (m, 1H, ArH), 7.08-7.04 (m, 1H, ArH), 6.87 (d, *J* = 7.8 Hz, 1H, ArH), 5.69-5.58 (m, 1H,  $\text{CH}_2\text{CH}=\text{CH}_2$ ), 5.11-5.07 (m, 2H,  $\text{CH}_2\text{CH}=\text{CH}_2$ ), 3.82 (br s, 1H, OH), 2.77-2.72 (m, 1H,  $\text{CH}_2\text{CH}=\text{CH}_2$ ), 2.63-2.58 (m, 1H,  $\text{CH}_2\text{CH}=\text{CH}_2$ ).

**(S)-3-Allyl-3-hydroxy-1-methylindolin-2-one (6e):** White solid (36.6 mg, 0.180 mmol; 90%). M.p.: 150-152 °C. The enantiomeric excess was determined on a Daicel Chiralcel OJ-H column with hexane/2-propanol = 95/5, flow = 1.0 mL/min, and detected at a UV wave length of 254 nm. Retention times: 16.2 min, 17.8 min (major), 82% *ee*.  $[\alpha]_D^{20} = -17.5$  (*c* 0.634,  $\text{CH}_2\text{Cl}_2$ ).  $^1\text{H}$  NMR (400 MHz,  $\text{CDCl}_3$ ):  $\delta$  7.38 (d, *J* = 7.3 Hz, 1H, ArH), 7.31 (t, *J* = 7.7 Hz, 1H, ArH), 7.09 (t, *J* = 7.5 Hz, 1H, ArH), 6.81 (d, *J* = 7.8 Hz, 1H, ArH), 5.66-5.56 (m, 1H,  $\text{CH}_2\text{CH}=\text{CH}_2$ ), 5.10-5.05 (m, 2H,  $\text{CH}_2\text{CH}=\text{CH}_2$ ), 3.70 (br s, 1H, OH), 3.15 (s, 3H,  $\text{CH}_3$ ), 2.78-2.73 (m, 1H,  $\text{CH}_2\text{CH}=\text{CH}_2$ ), 2.65-2.59 (m, 1H,  $\text{CH}_2\text{CH}=\text{CH}_2$ ).

**(S)-3-Allyl-1-benzyl-3-hydroxy-5-methylindolin-2-one (6j):** White solid (55.7 mg, 0.190 mmol; 95%). M.p.: 148-150 °C. The enantiomeric excess was determined on a Daicel Chiralcel OJ-H column with hexane/2-propanol = 90/10, flow = 1.0 mL/min, and detected at a UV wave length of 254 nm. Retention times: 8.2 min, 14.7 min (major), 86% *ee*.  $[\alpha]_D^{20} = -10.4$  (*c* 0.432,  $\text{CH}_2\text{Cl}_2$ ).  $^1\text{H}$  NMR (400 MHz,  $\text{CDCl}_3$ ):  $\delta$  7.31-7.22 (m, 6H, ArH), 6.98 (dd, *J* = 0.9, 8.0 Hz, 1H, ArH), 6.57 (d, *J* = 8.0 Hz, 1H, ArH), 5.67-5.56 (m, 1H,  $\text{CH}_2\text{CH}=\text{CH}_2$ ), 5.17-5.07 (m, 2H,  $\text{CH}_2\text{CH}=\text{CH}_2$ ), 4.98 (d, *J* = 15.7 Hz, 1H,  $\text{CH}_2\text{Ph}$ ), 4.69 (d, *J* = 15.7 Hz, 1H,  $\text{CH}_2\text{Ph}$ ), 3.40 (br s, 1H, OH), 2.83-2.78 (m, 1H,  $\text{CH}_2\text{CH}=\text{CH}_2$ ), 2.73-2.68 (m, 1H,  $\text{CH}_2\text{CH}=\text{CH}_2$ ), 2.30 (s, 3H,  $\text{CH}_3$ ).

**(S)-3-Allyl-3-hydroxy-1,5-dimethylindolin-2-one (6l):** White solid (40.8 mg, 0.188 mmol; 94%). M.p.: 145-147 °C. The enantiomeric excess was determined on a Daicel Chiralcel OJ-H column with hexane/2-propanol = 90/10, flow = 1.0 mL/min, and detected at a UV wave length of 254 nm. Retention times: 7.3 min, 10.9 min (major), 85% ee.  $[\alpha]_D^{20} = -5.9$  (*c* 0.732, CH<sub>2</sub>Cl<sub>2</sub>). <sup>1</sup>H NMR (400 MHz, CDCl<sub>3</sub>): δ 7.21 (s, 1H, ArH), 7.11 (d, *J* = 7.8 Hz, 1H, ArH), 6.70 (d, *J* = 7.9 Hz, 1H, ArH), 5.66-5.56 (m, 1H, CH<sub>2</sub>CH=CH<sub>2</sub>), 5.12-5.05 (m, 2H, CH<sub>2</sub>CH=CH<sub>2</sub>), 3.64 (br s, 1H, OH), 3.13 (s, 3H, NCH<sub>3</sub>), 2.76-2.71 (m, 1H, CH<sub>2</sub>CH=CH<sub>2</sub>), 2.65-2.59 (m, 1H, CH<sub>2</sub>CH=CH<sub>2</sub>), 2.34 (s, 3H, CH<sub>3</sub>).

**(S)-3-Allyl-1-benzyl-3-hydroxy-5-methoxyindolin-2-one (6m):** White solid (56.9 mg, 0.184 mmol; 92%). M.p.: 150-151 °C. The enantiomeric excess was determined on a Daicel Chiralcel OJ-H column with hexane/2-propanol = 90/10, flow = 1.0 mL/min, and detected at a UV wave length of 254 nm. Retention times: 14.8 min, 20.9 min (major), 81% ee.  $[\alpha]_D^{20} = -3.5$  (*c* 0.958, CH<sub>2</sub>Cl<sub>2</sub>). <sup>1</sup>H NMR (400 MHz, CDCl<sub>3</sub>): δ 7.29-7.21 (m, 5H, ArH), 7.02 (d, *J* = 2.5 Hz, 1H, ArH), 6.69 (dd, *J* = 2.6, 8.5 Hz, 1H, ArH), 6.56 (d, *J* = 8.5 Hz, 1H, ArH), 5.64-5.54 (m, 1H, CH<sub>2</sub>CH=CH<sub>2</sub>), 5.15-5.05 (m, 2H, CH<sub>2</sub>CH=CH<sub>2</sub>), 4.96 (d, *J* = 15.7 Hz, 1H, CH<sub>2</sub>Ph), 4.65 (d, *J* = 15.7 Hz, 1H, CH<sub>2</sub>Ph), 4.04 (br s, 1H, OH), 3.73 (s, 3H, OCH<sub>3</sub>), 2.85-2.80 (m, 1H, CH<sub>2</sub>CH=CH<sub>2</sub>), 2.75-2.70 (m, 1H, CH<sub>2</sub>CH=CH<sub>2</sub>).

**(S)-3-Allyl-1-benzyl-5-fluoro-3-hydroxyindolin-2-one (6n):** White solid (56.5 mg, 0.190 mmol; 95%). M.p.: 126-127 °C. The enantiomeric excess was determined on a Daicel Chiralcel OJ-H column with hexane/2-propanol = 90/10, flow = 1.0 mL/min, and detected at a UV wave length of 254 nm. Retention times: 10.7 min, 14.3 min (major), 76% ee.  $[\alpha]_D^{20} = -5.5$  (*c* 0.930, CH<sub>2</sub>Cl<sub>2</sub>). <sup>1</sup>H NMR (400 MHz, CDCl<sub>3</sub>): δ 7.31-7.23 (m, 5H, ArH), 7.14 (dd, *J* = 2.6, 7.6 Hz, 1H, ArH), 6.89-6.84 (m, 1H, ArH), 6.58 (dd, *J* = 4.0, 8.6 Hz, 1H,

ArH), 5.63-5.53 (m, 1H,  $\text{CH}_2\text{CH}=\text{CH}_2$ ), 5.15-5.07 (m, 2H,  $\text{CH}_2\text{CH}=\text{CH}_2$ ), 4.97 (d,  $J = 15.7$  Hz, 1H,  $\text{CH}_2\text{Ph}$ ), 4.67 (d,  $J = 15.8$  Hz, 1H,  $\text{CH}_2\text{Ph}$ ), 4.15 (br s, 1H, OH), 2.85-2.80 (m, 1H,  $\text{CH}_2\text{CH}=\text{CH}_2$ ), 2.74-2.69 (m, 1H,  $\text{CH}_2\text{CH}=\text{CH}_2$ ).

**(S)-3-Allyl-1-benzyl-5-chloro-3-hydroxyindolin-2-one (6o):** White solid (57.7 mg, 0.184 mmol; 92%). M.p.: 117-119 °C. The enantiomeric excess was determined on a Daicel Chiralcel OJ-H column with hexane/2-propanol = 90/10, flow = 1.0 mL/min, and detected at a UV wave length of 254 nm. Retention times: 9.8 min, 14.8 min (major), 80% ee.  $[\alpha]_D^{20} = -14.5$  ( $c$  0.408,  $\text{CH}_2\text{Cl}_2$ ).  $^1\text{H}$  NMR (400 MHz,  $\text{CDCl}_3$ ):  $\delta$  7.37 (d,  $J = 2.0$  Hz, 1H, ArH), 7.32-7.23 (m, 5H, ArH), 7.15 (dd,  $J = 2.1, 8.3$  Hz, 1H, ArH), 6.59 (d,  $J = 8.3$  Hz, 1H, ArH), 5.66-5.55 (m, 1H,  $\text{CH}_2\text{CH}=\text{CH}_2$ ), 5.17-5.10 (m, 2H,  $\text{CH}_2\text{CH}=\text{CH}_2$ ), 4.98 (d,  $J = 15.8$  Hz, 1H,  $\text{CH}_2\text{Ph}$ ), 4.70 (d,  $J = 15.8$  Hz, 1H,  $\text{CH}_2\text{Ph}$ ), 3.57 (br s, 1H, OH), 2.82-2.78 (m, 1H,  $\text{CH}_2\text{CH}=\text{CH}_2$ ), 2.72-2.67 (m, 1H,  $\text{CH}_2\text{CH}=\text{CH}_2$ ).

**(S)-3-Allyl-1-benzyl-5-bromo-3-hydroxyindolin-2-one (6q):** White solid (63.8 mg, 0.178 mmol; 89%). M.p.: 121-123 °C. The enantiomeric excess was determined on a Daicel Chiralcel OJ-H column with hexane/2-propanol = 90/10, flow = 1.0 mL/min, and detected at a UV wave length of 254 nm. Retention times: 11.4 min, 17.7 min (major), 80% ee.  $[\alpha]_D^{20} = -12.4$  ( $c$  0.696,  $\text{CH}_2\text{Cl}_2$ ).  $^1\text{H}$  NMR (400 MHz,  $\text{CDCl}_3$ ):  $\delta$  7.51 (d,  $J = 1.9$  Hz, 1H, ArH), 7.31-7.22 (m, 6H, ArH), 6.54 (d,  $J = 8.3$  Hz, 1H, ArH), 5.63-5.52 (m, 1H,  $\text{CH}_2\text{CH}=\text{CH}_2$ ), 5.16-5.09 (m, 2H,  $\text{CH}_2\text{CH}=\text{CH}_2$ ), 4.96 (d,  $J = 15.7$  Hz, 1H,  $\text{CH}_2\text{Ph}$ ), 4.66 (d,  $J = 15.8$  Hz, 1H,  $\text{CH}_2\text{Ph}$ ), 3.83 (br s, 1H, OH), 2.83-2.78 (m, 1H,  $\text{CH}_2\text{CH}=\text{CH}_2$ ), 2.73-2.68 (m, 1H,  $\text{CH}_2\text{CH}=\text{CH}_2$ ).

**(S)-3-Allyl-1-benzyl-6-bromo-3-hydroxyindolin-2-one (6r):** White solid (65.9 mg, 0.184 mmol; 92%). M.p.: 152-155 °C. The enantiomeric excess was determined on a Daicel

Chiralpak AD-H column with hexane/2-propanol = 95/5, flow = 1.0 mL/min, and detected at a UV wave length of 254 nm. Retention times: 24.3 min, 27.6 min (major), 70% *ee*.  $[\alpha]_D^{20} = -3.0$  (*c* 0.968, CH<sub>2</sub>Cl<sub>2</sub>). <sup>1</sup>H NMR (400 MHz, CDCl<sub>3</sub>):  $\delta$  7.33-7.23 (m, 6H, ArH), 7.18 (dd, *J* = 1.6, 7.9 Hz, 1H, ArH), 6.81 (d, *J* = 1.5 Hz, 1H, ArH), 5.60-5.50 (m, 1H, CH<sub>2</sub>CH=CH<sub>2</sub>), 5.14-5.05 (m, 2H, CH<sub>2</sub>CH=CH<sub>2</sub>), 4.95 (d, *J* = 15.8 Hz, 1H, CH<sub>2</sub>Ph), 4.62 (d, *J* = 15.8 Hz, 1H, CH<sub>2</sub>Ph), 4.00 (br s, 1H, OH), 2.82-2.77 (m, 1H, CH<sub>2</sub>CH=CH<sub>2</sub>), 2.71-2.65 (m, 1H, CH<sub>2</sub>CH=CH<sub>2</sub>).

**(S)-2-Methoxy-1,1'-binaphthalene (9a):** White solid (40.4 mg, 0.142 mmol; 71%). M.p.: 118-119 °C. The enantiomeric excess was determined on a Daicel Chiralpak AD-H column with hexane/2-propanol = 98/2, flow = 0.25 mL/min, and detected at a UV wave length of 254 nm. Retention times: 20.9 min, 24.4 min (major), 52% *ee*.  $[\alpha]_D^{20} = +24.4$  (*c* 0.446, CH<sub>2</sub>Cl<sub>2</sub>). <sup>1</sup>H NMR (400 MHz, CDCl<sub>3</sub>):  $\delta$  7.97 (d, *J* = 9.0 Hz, 1H, ArH), 7.93 (dd, *J* = 4.2, 8.2 Hz, 2H, ArH), 7.86 (d, *J* = 8.2 Hz, 1H, ArH), 7.61 (dd, *J* = 7.0, 8.2 Hz, 1H, ArH), 7.47-7.42 (m, 3H, ArH), 7.34-7.14 (m, 5H, ArH), 3.75 (s, 3H, OCH<sub>3</sub>).

**(S)-2-Ethoxy-1,1'-binaphthalene (9b):** White solid (46.5 mg, 0.156 mmol; 78%). M.p.: 113-114 °C. The enantiomeric excess was determined on a Daicel Chiralcel OJ-H column with hexane/2-propanol = 90/10, flow = 1.0 mL/min, and detected at a UV wave length of 254 nm. Retention times: 7.3 min (major), 11.5 min, 54% *ee*.  $[\alpha]_D^{20} = +44.9$  (*c* 0.406, CH<sub>2</sub>Cl<sub>2</sub>). <sup>1</sup>H NMR (400 MHz, CDCl<sub>3</sub>):  $\delta$  7.92 (dd, *J* = 3.9, 9.1 Hz, 3H, ArH), 7.85 (d, *J* = 8.2 Hz, 1H, ArH), 7.59 (dd, *J* = 7.0, 8.2 Hz, 1H, ArH), 7.46-7.39 (m, 3H, ArH), 7.34-7.16 (m, 5H, ArH), 4.07-3.95 (m, 2H, OCH<sub>2</sub>CH<sub>3</sub>), 1.02 (t, *J* = 7.0 Hz, 3H, OCH<sub>2</sub>CH<sub>3</sub>).

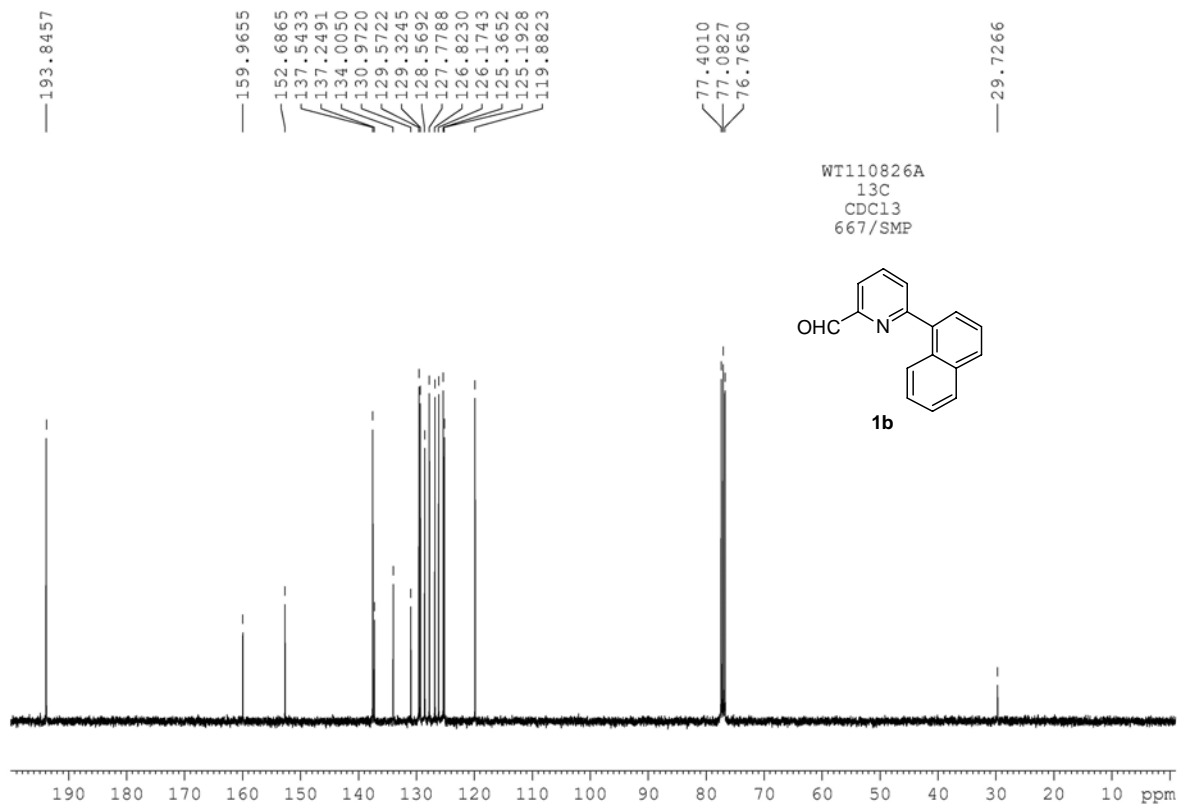
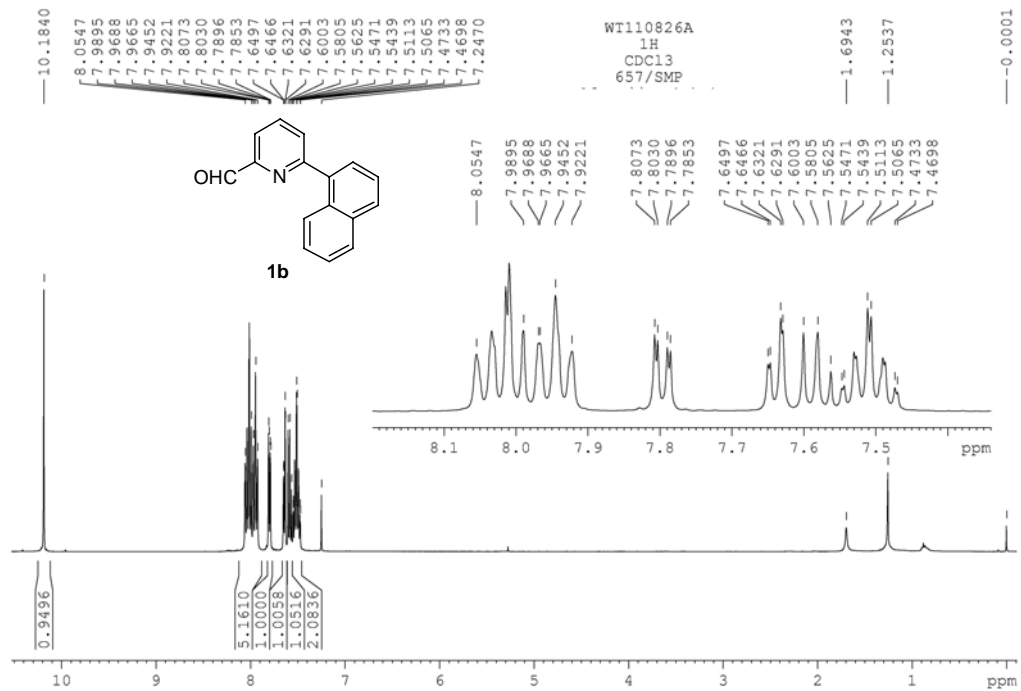
**(S)-2-(Benzylxy)-1,1'-binaphthalene (9c):** White solid (53.3 mg, 0.148 mmol; 74%). M.p.: 78-79 °C. The enantiomeric excess was determined on a Daicel Chiralpak AD-H

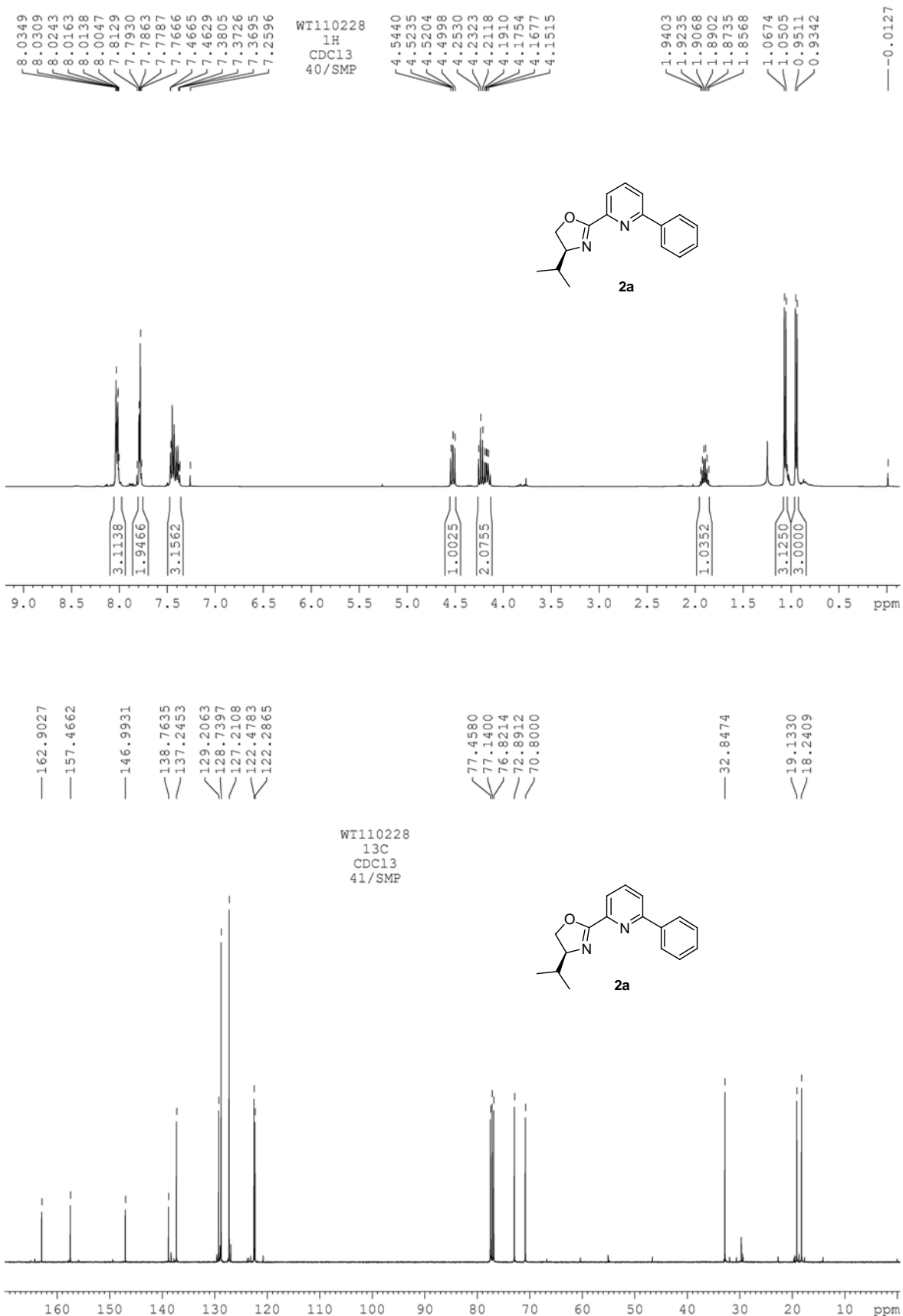
column with hexane/2-propanol = 98/2, flow = 0.5 mL/min, and detected at a UV wave length of 254 nm. Retention times: 20.8 min, 32.2 min (major), 51% *ee*.  $[\alpha]_D^{20} = +38.7$  (*c* 0.350,  $\text{CH}_2\text{Cl}_2$ ).  $^1\text{H}$  NMR (400 MHz,  $\text{CDCl}_3$ ):  $\delta$  7.95 (dd, *J* = 1.5, 8.1 Hz, 2H, ArH), 7.91 (d, *J* = 9.0 Hz, 1H, ArH), 7.85 (d, *J* = 8.1 Hz, 1H, ArH), 7.61 (dd, *J* = 7.0, 8.1 Hz, 1H, ArH), 7.48-7.41 (m, 3H, ArH), 7.37-7.25 (m, 3H, ArH), 7.23-7.22 (m, 2H, ArH), 7.15-7.10 (m, 3H, ArH), 6.95-6.92 (m, 2H, ArH), 5.05 (d, *J* = 12.5 Hz, 1H,  $\text{OCHHC}_6\text{H}_5$ ), 5.00 (d, *J* = 12.5 Hz, 1H,  $\text{OCHHC}_6\text{H}_5$ ).

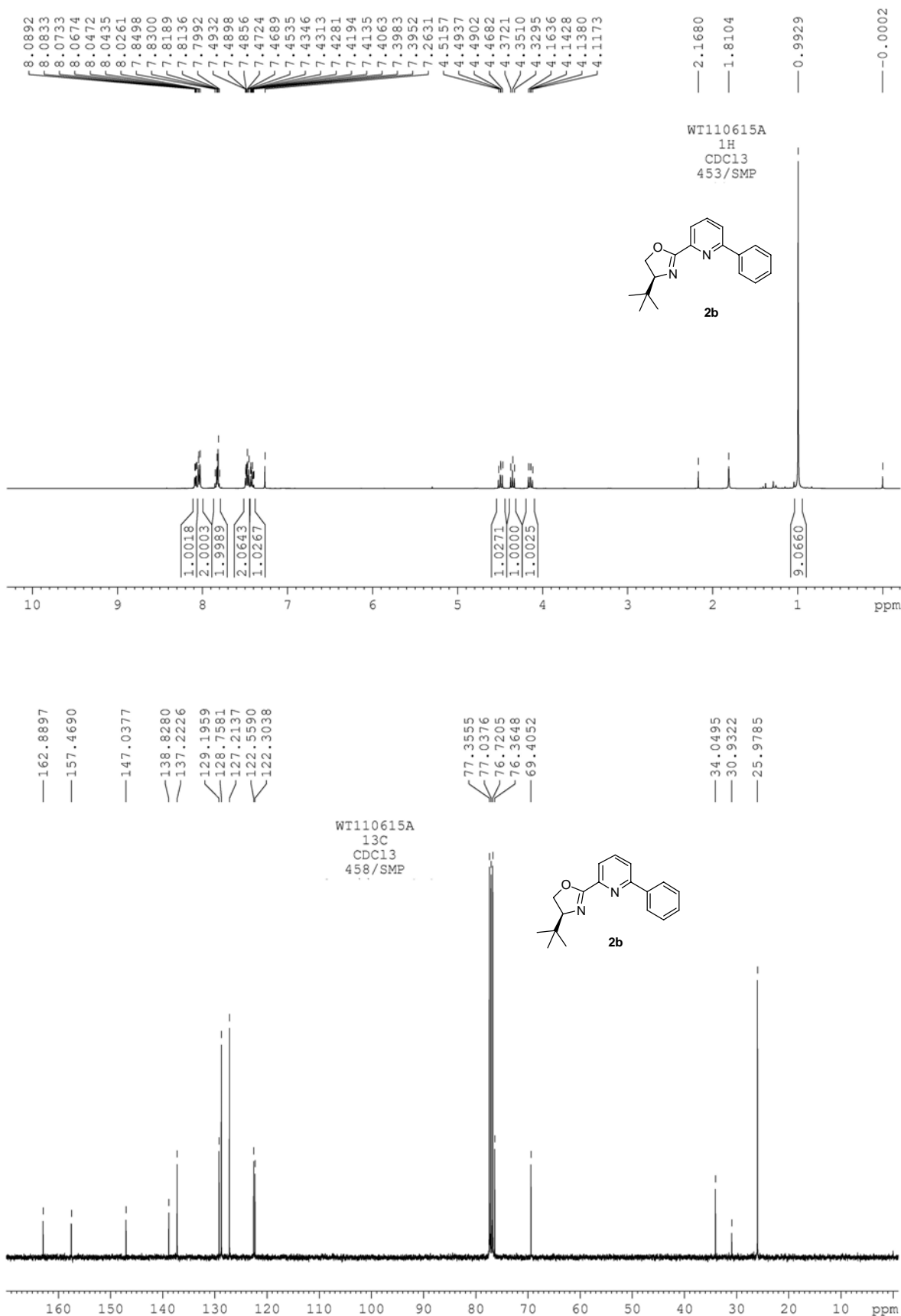
**(S)-2-Methoxy-1-(o-tolyl)naphthalene (9d):** White solid (45.2 mg, 0.182 mmol; 91%). M.p.: 89-90 °C. The enantiomeric excess was determined on a Daicel Chiralcel OJ-H column with hexane/2-propanol = 98/2, flow = 1.0 mL/min, and detected at a UV wave length of 254 nm. Retention times: 9.0 min (major), 14.0 min, 23% *ee*.  $[\alpha]_D^{20} = +14.2$  (*c* 0.774,  $\text{CH}_2\text{Cl}_2$ ).  $^1\text{H}$  NMR (400 MHz,  $\text{CDCl}_3$ ):  $\delta$  7.87 (d, *J* = 9.0 Hz, 1H, ArH), 7.83-7.80 (m, 1H, ArH), 7.37-7.33 (m, 3H, ArH), 7.32-7.24 (m, 4H, ArH), 7.20-7.17 (m, 1H, ArH), 3.82 (s, 3H,  $\text{OCH}_3$ ), 1.99 (s, 3H,  $\text{CH}_3$ ).

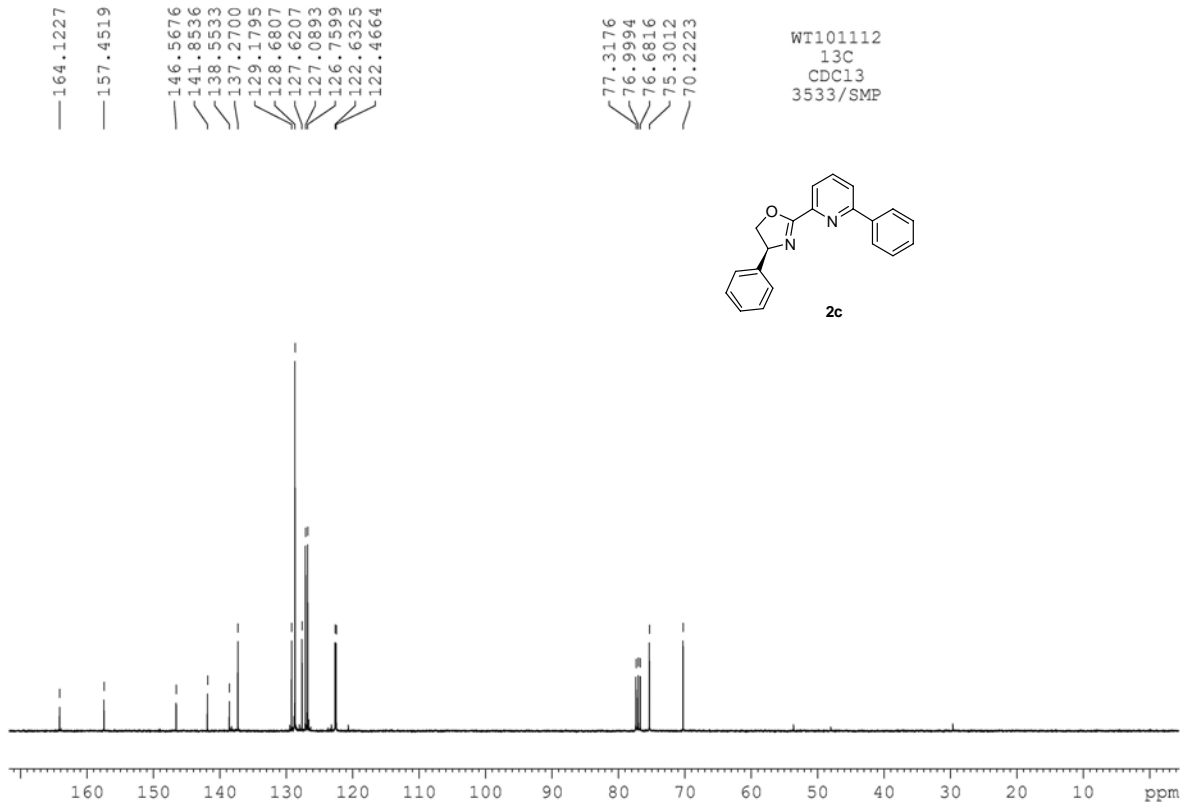
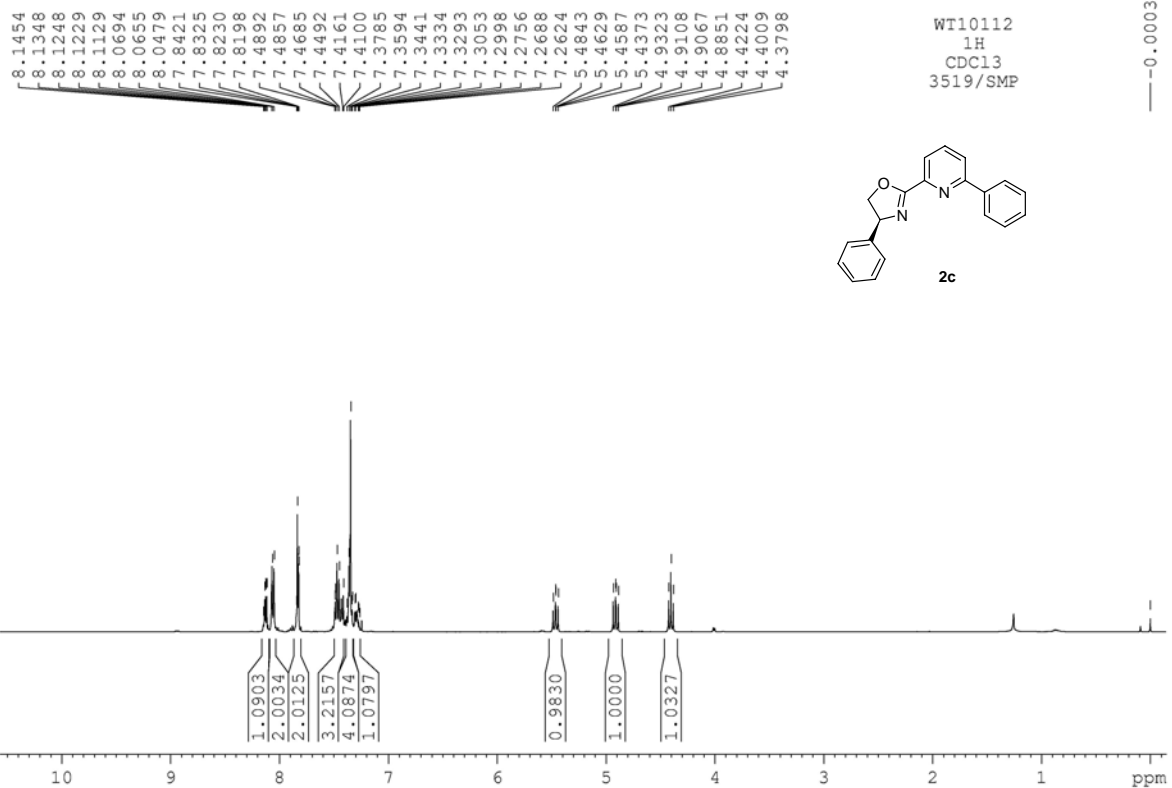
**(R)-1-([1,1'-Biphenyl]-2-yl)-2-methoxynaphthalene (9g):** White solid (50.9 mg, 0.164 mmol; 82%). M.p.: 93-95 °C. The enantiomeric excess was determined on a Daicel Chiraldak AD-H column with hexane/2-propanol = 98/2, flow = 0.8 mL/min, and detected at a UV wave length of 254 nm. Retention times: 6.0 min, 6.6 min (major), 23% *ee*.  $[\alpha]_D^{20} = -9.5$  (*c* 0.970,  $\text{CH}_2\text{Cl}_2$ ).  $^1\text{H}$  NMR (400 MHz,  $\text{CDCl}_3$ ):  $\delta$  7.74 (d, *J* = 8.8 Hz, 2H, ArH), 7.54-7.43 (m, 4H, ArH), 7.34-7.26 (m, 3H, ArH), 7.08 (d, *J* = 9.0 Hz, 1H, ArH), 7.05-6.99 (m, 5H, ArH), 3.48 (s, 3H,  $\text{OCH}_3$ ).

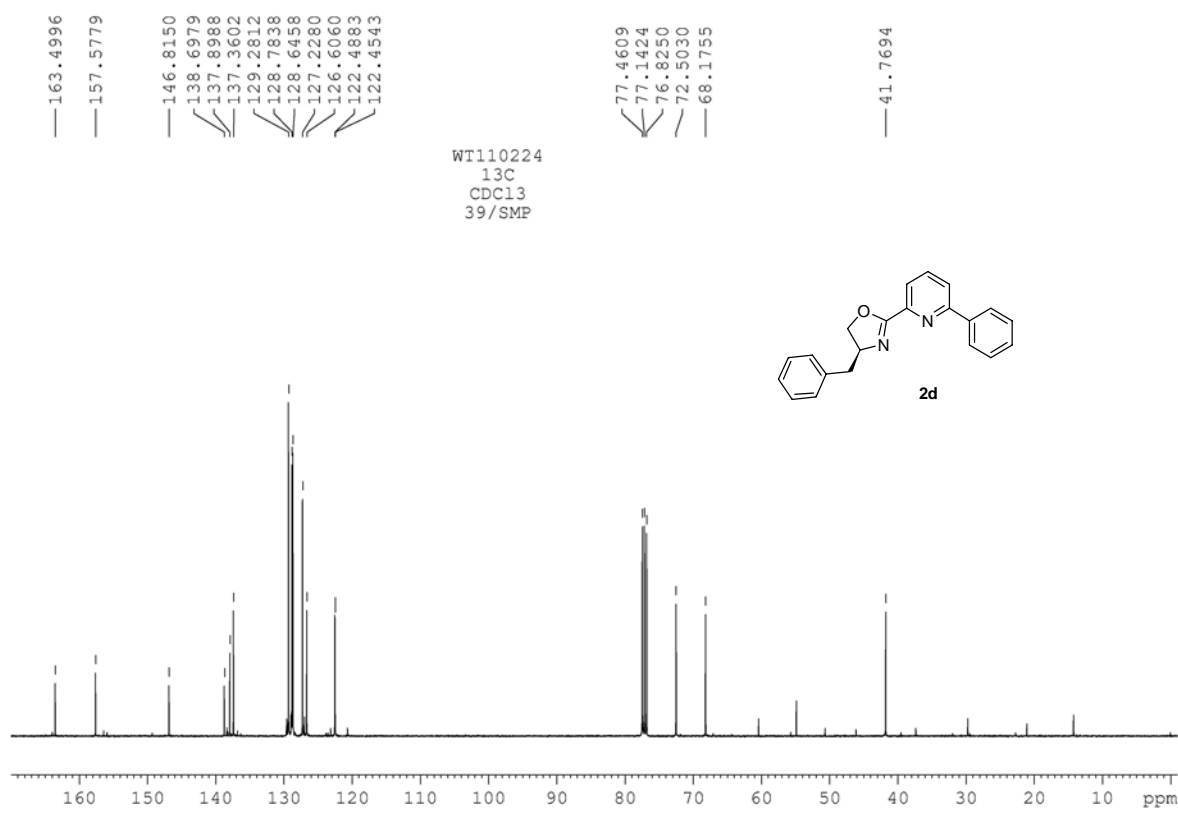
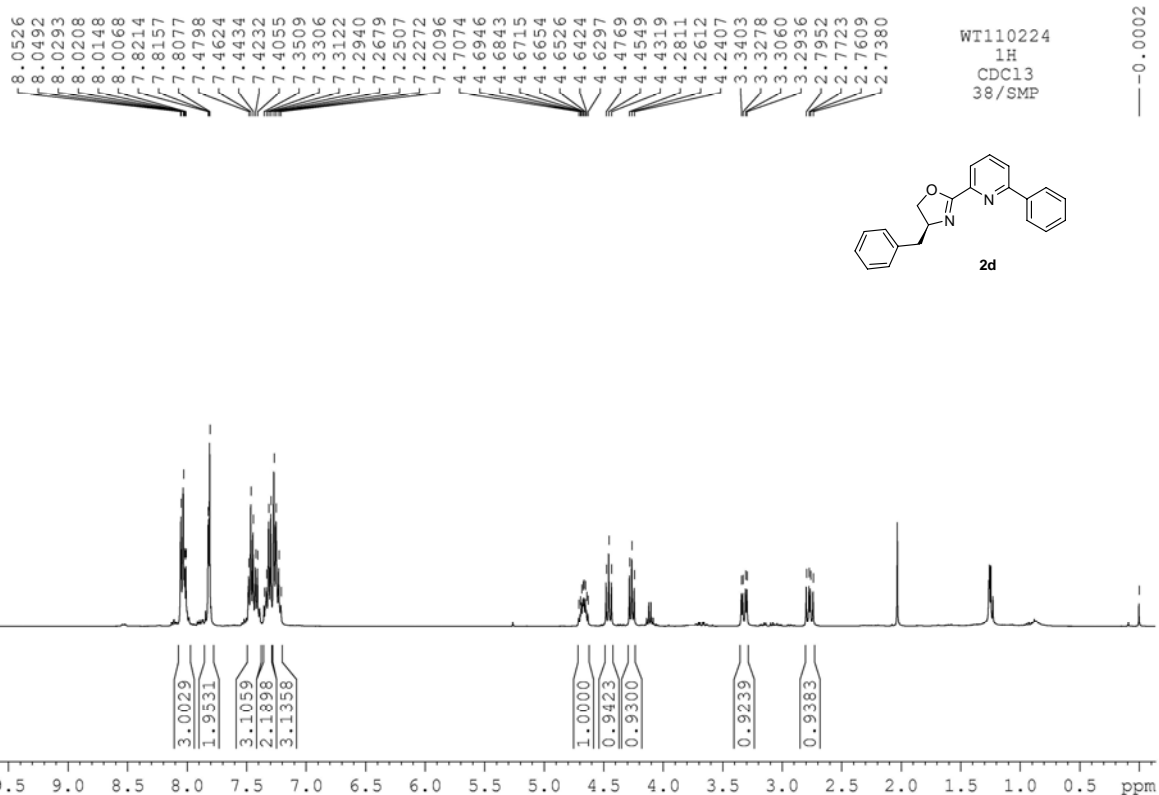
## Copies of the $^1\text{H}$ and $^{13}\text{C}$ NMR Spectra of New Compounds 1-3

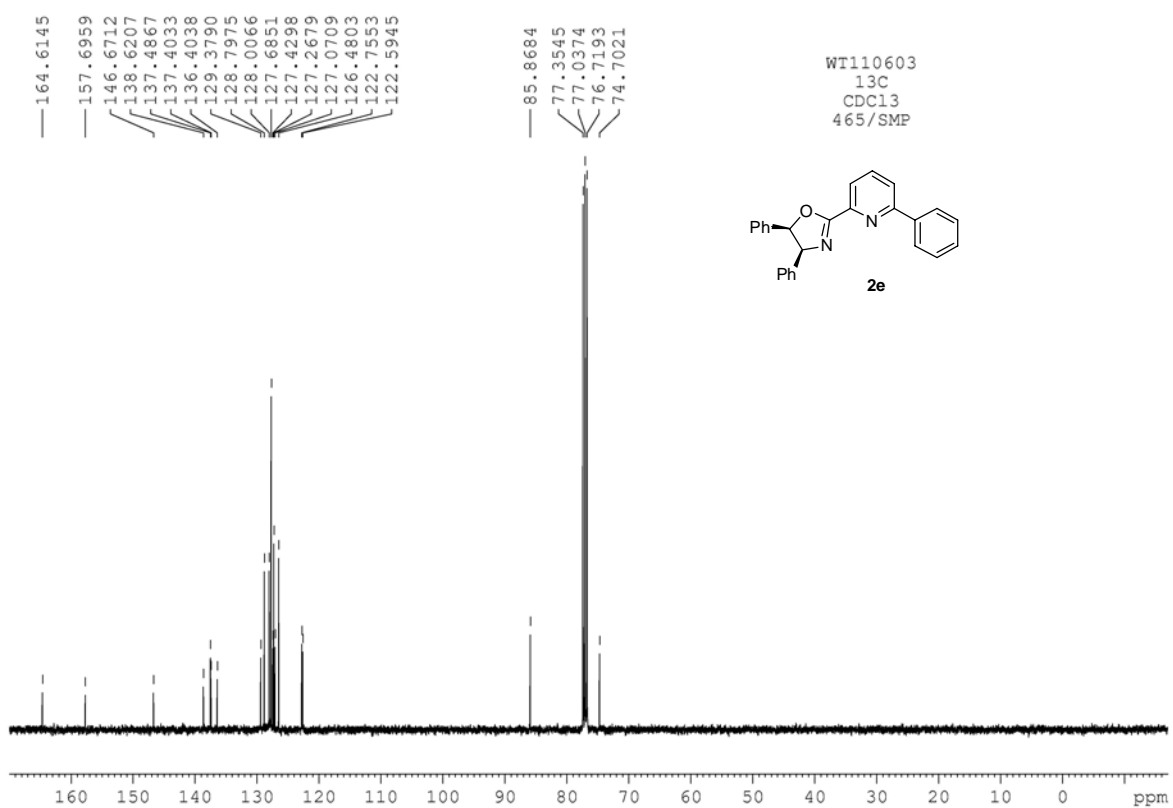
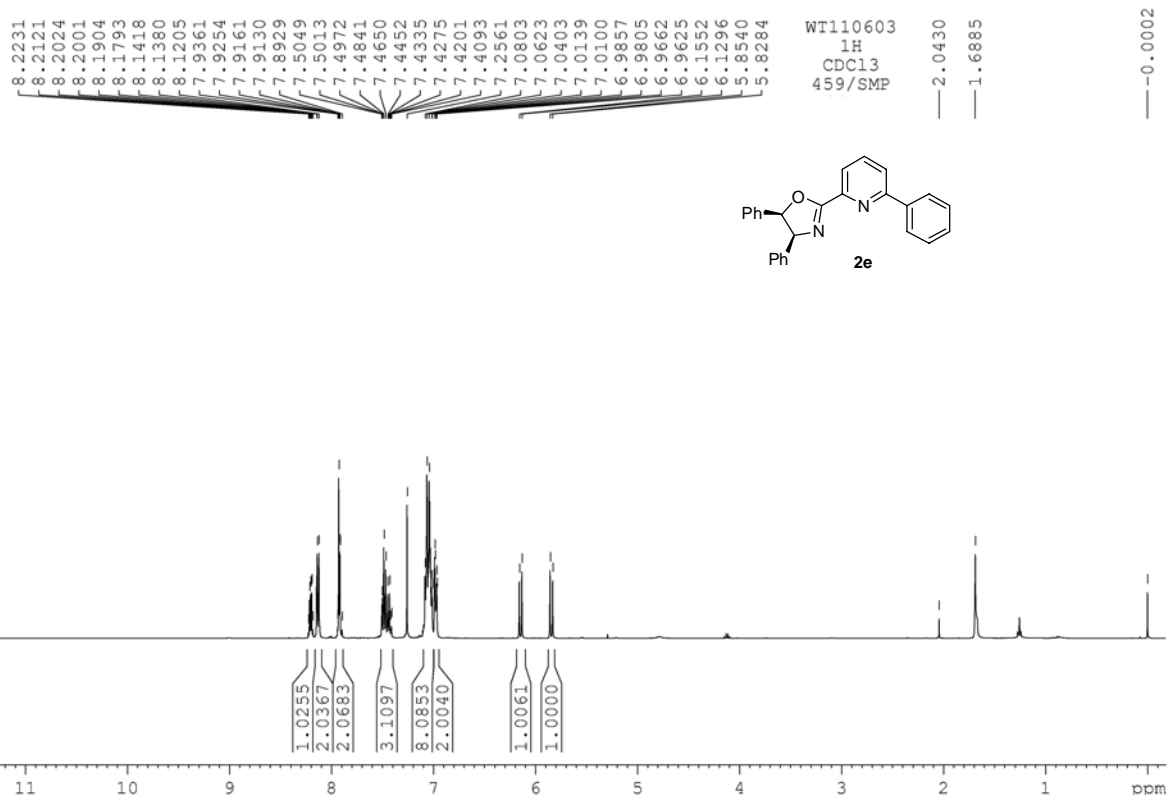


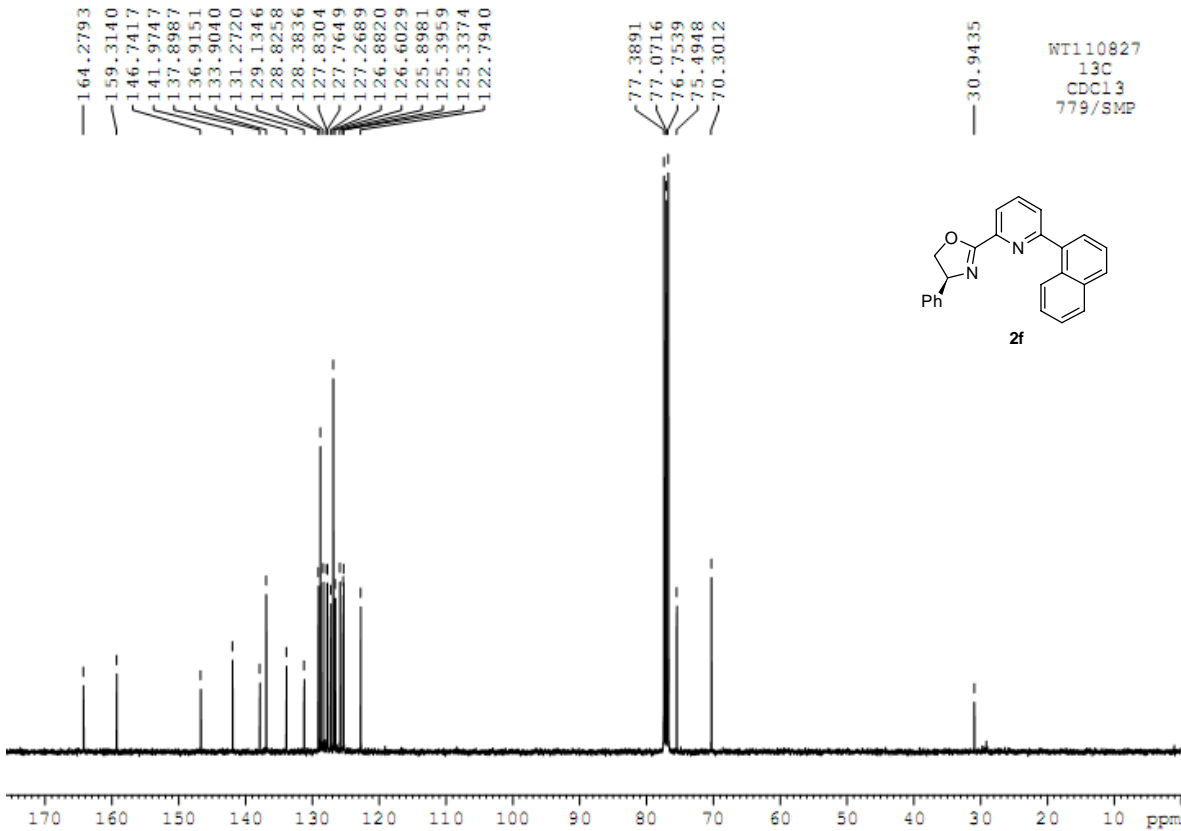
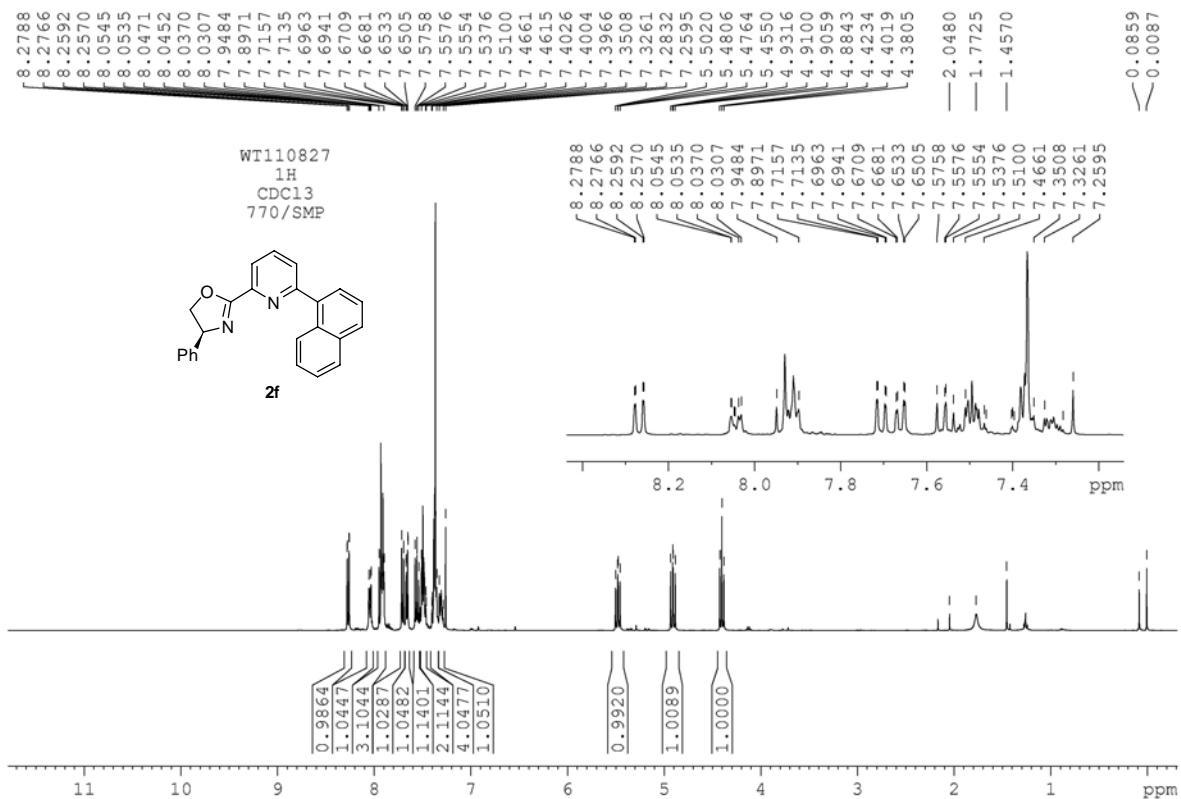


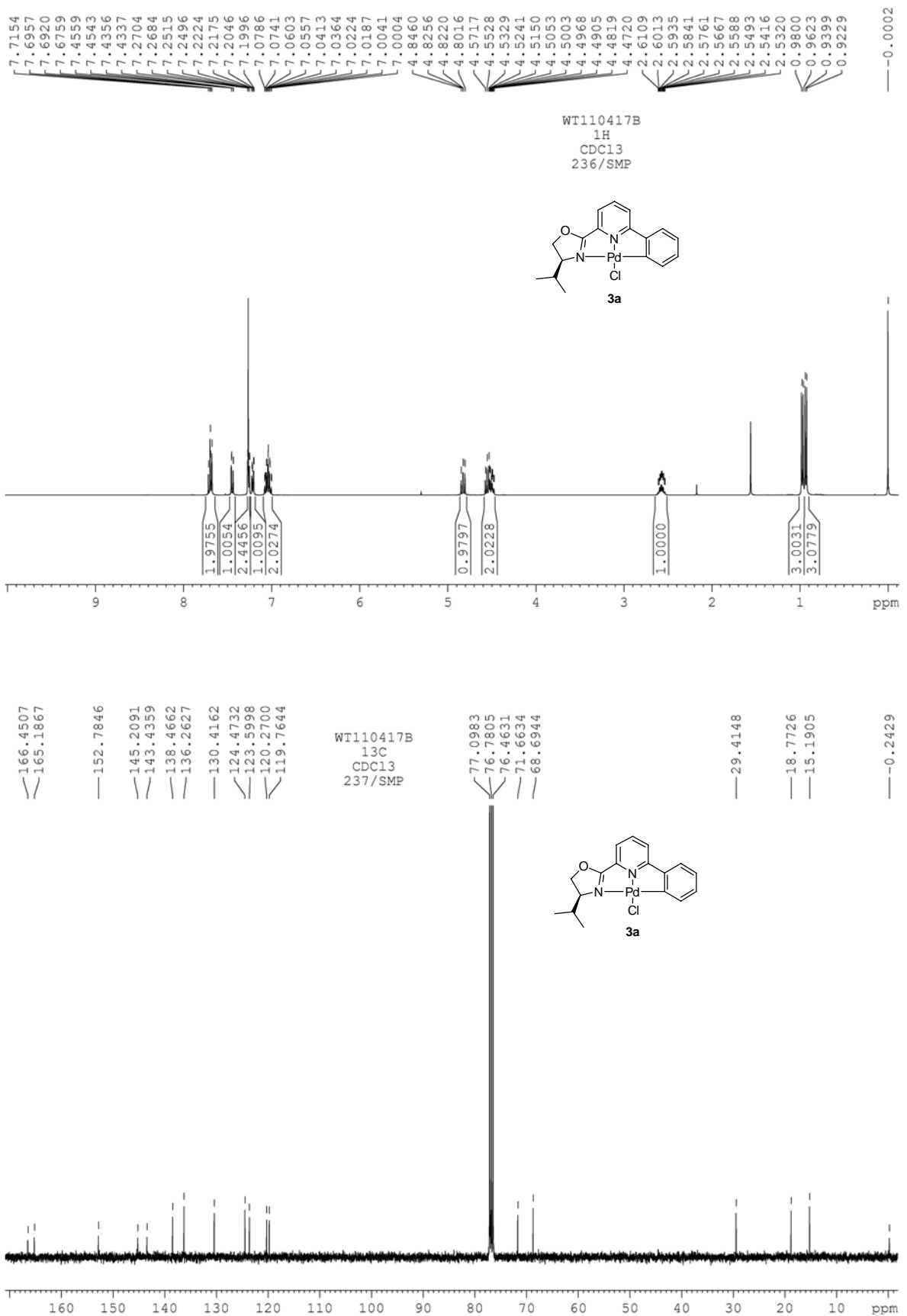


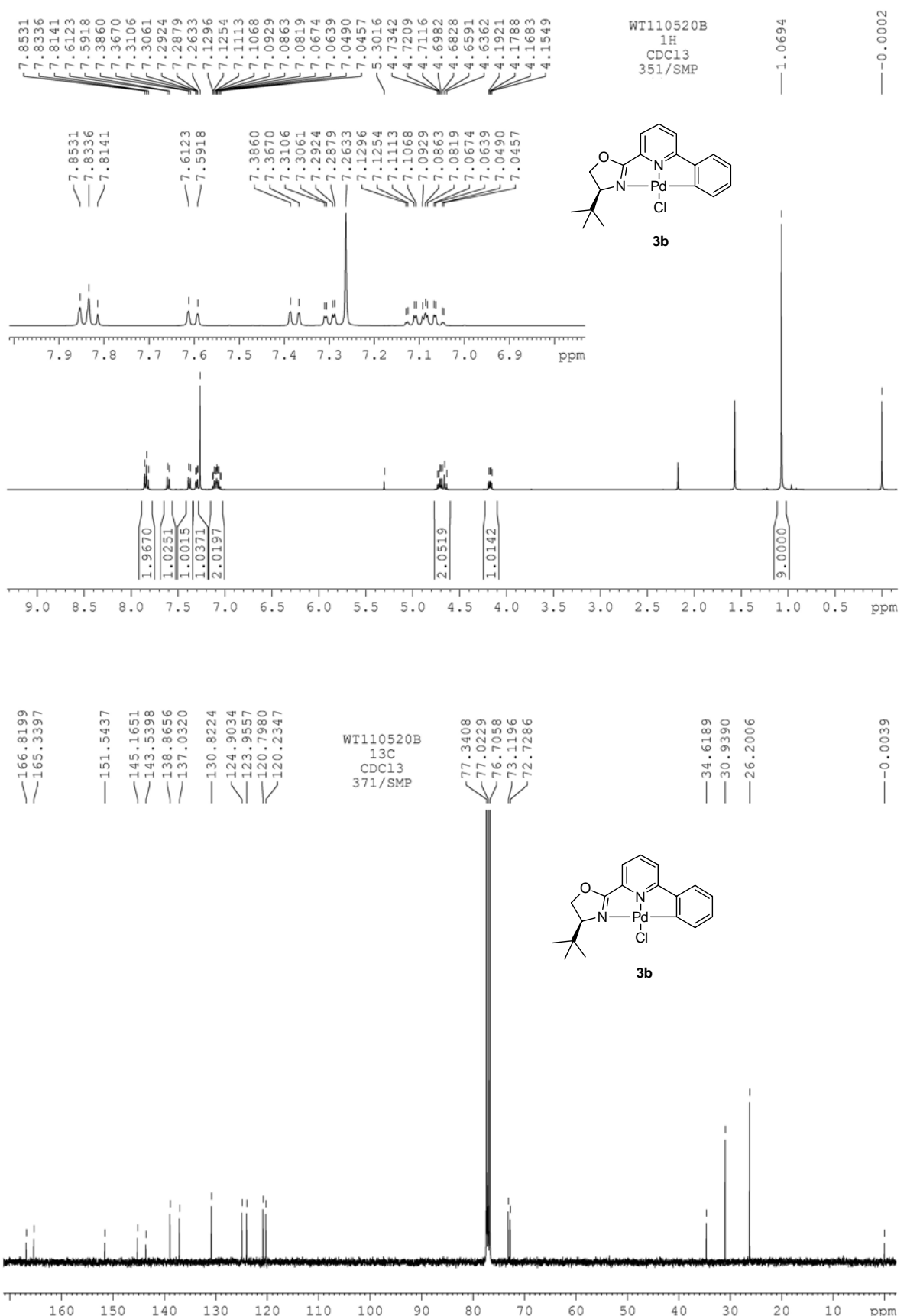


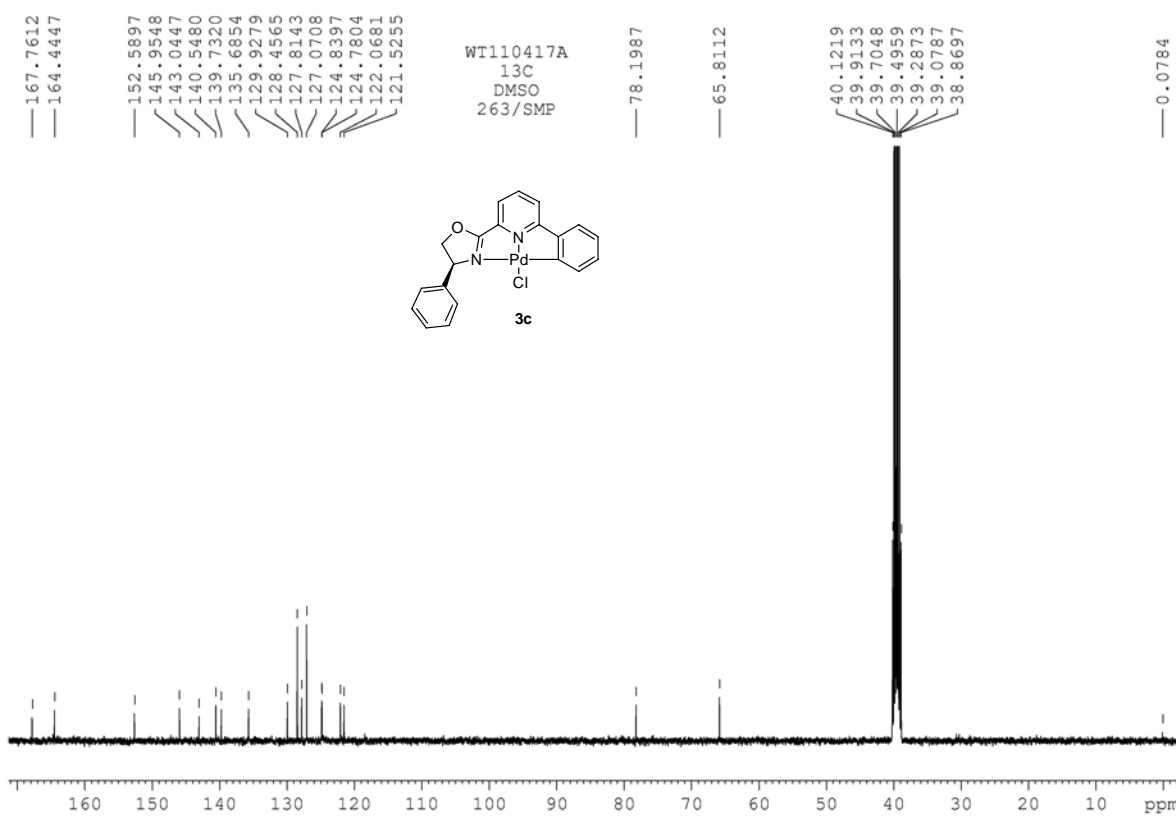
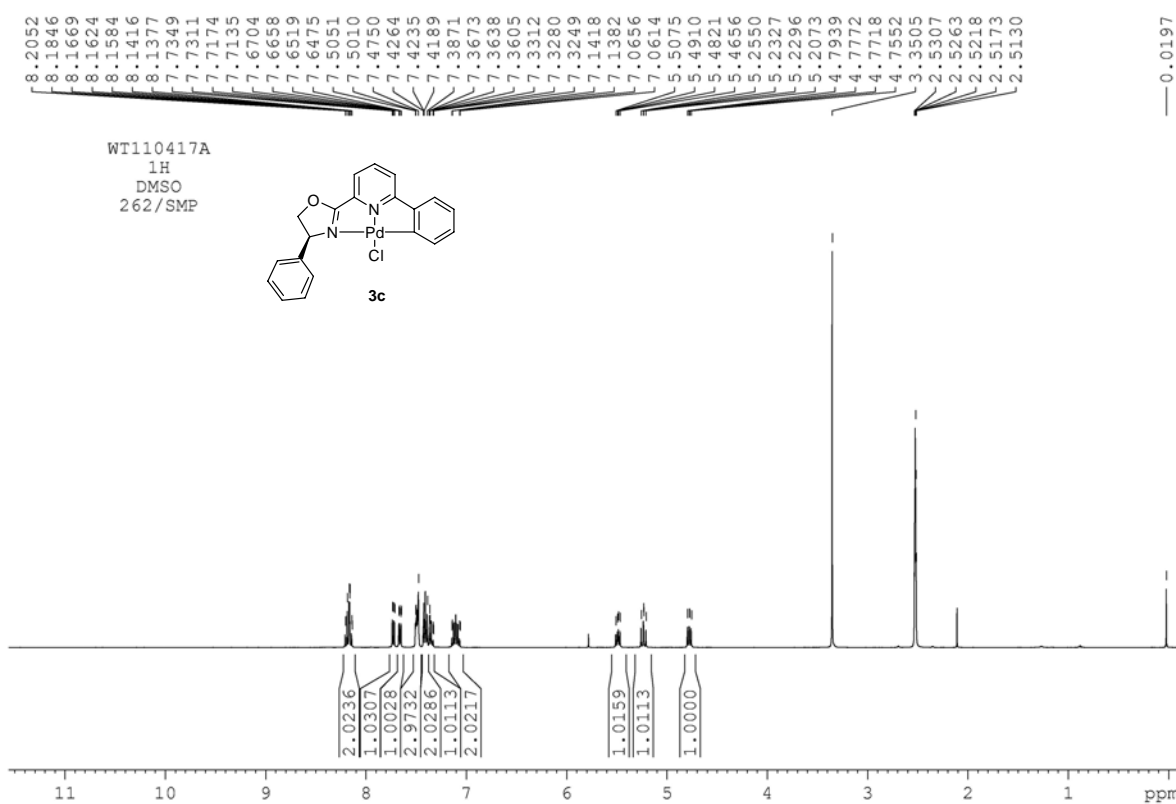


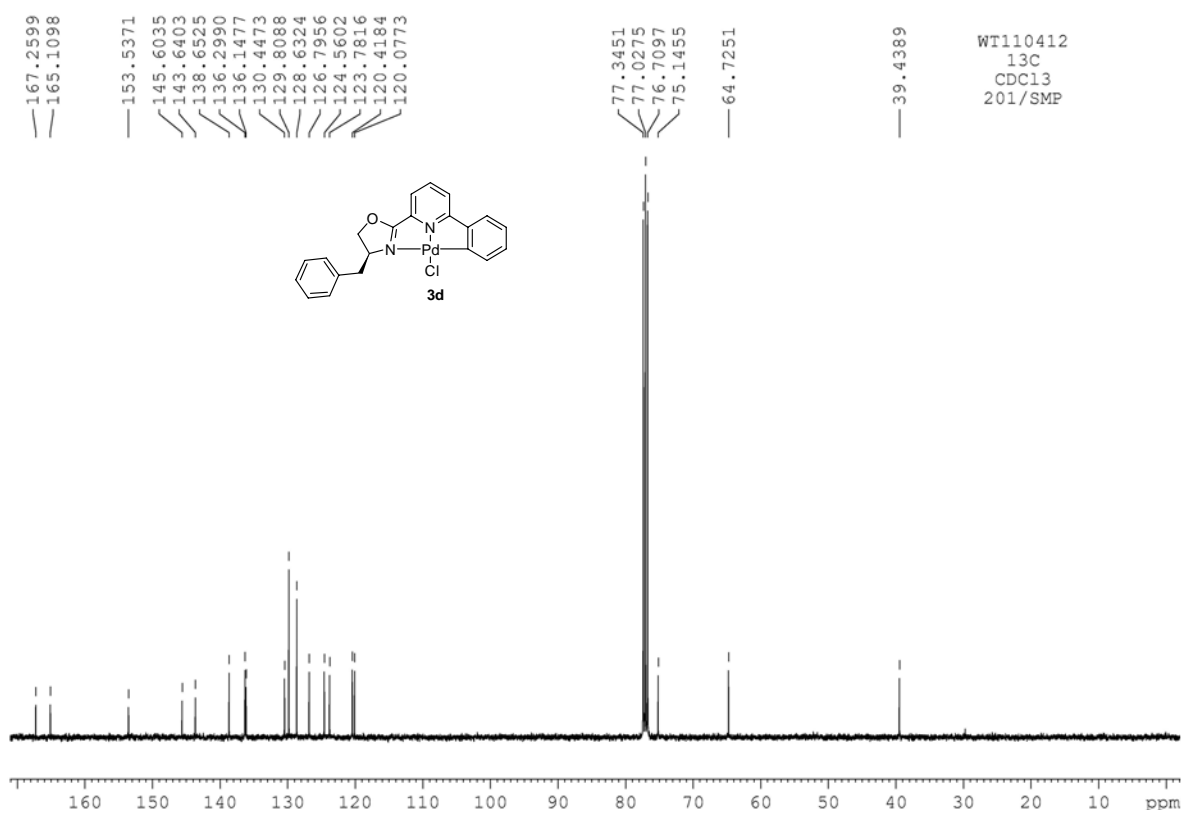
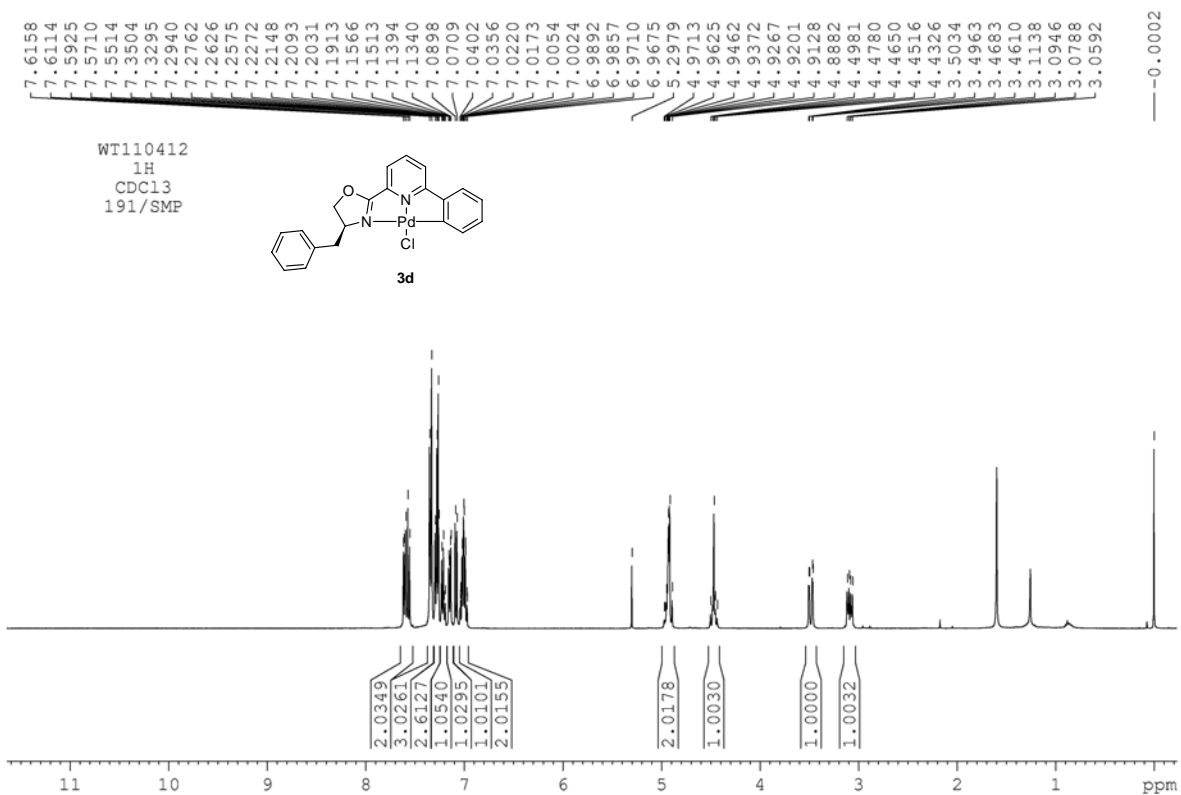


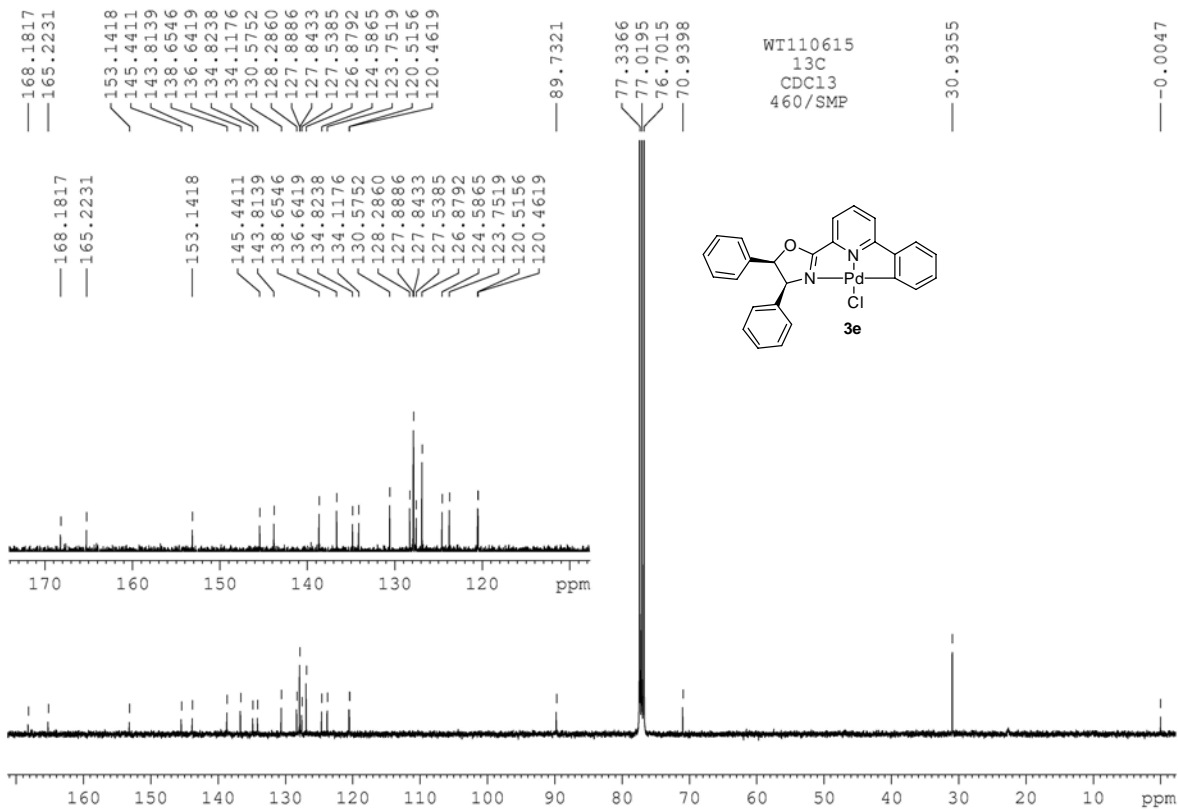
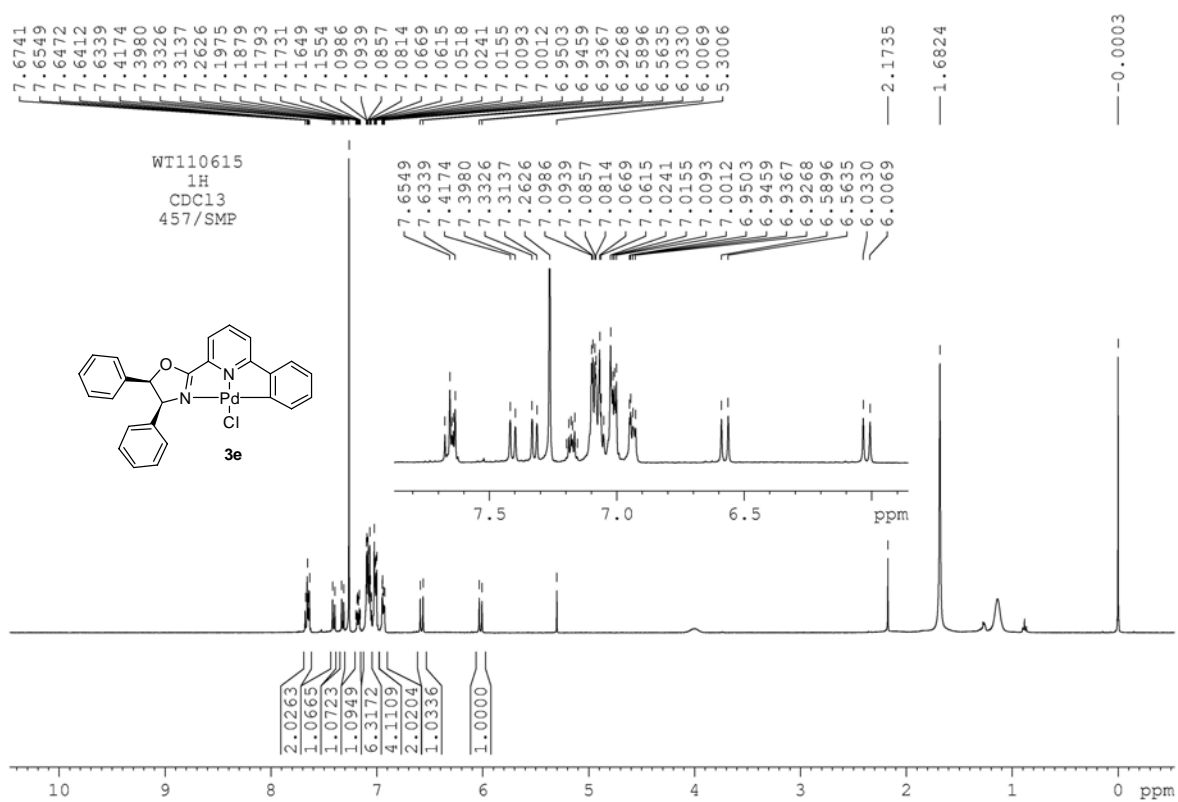


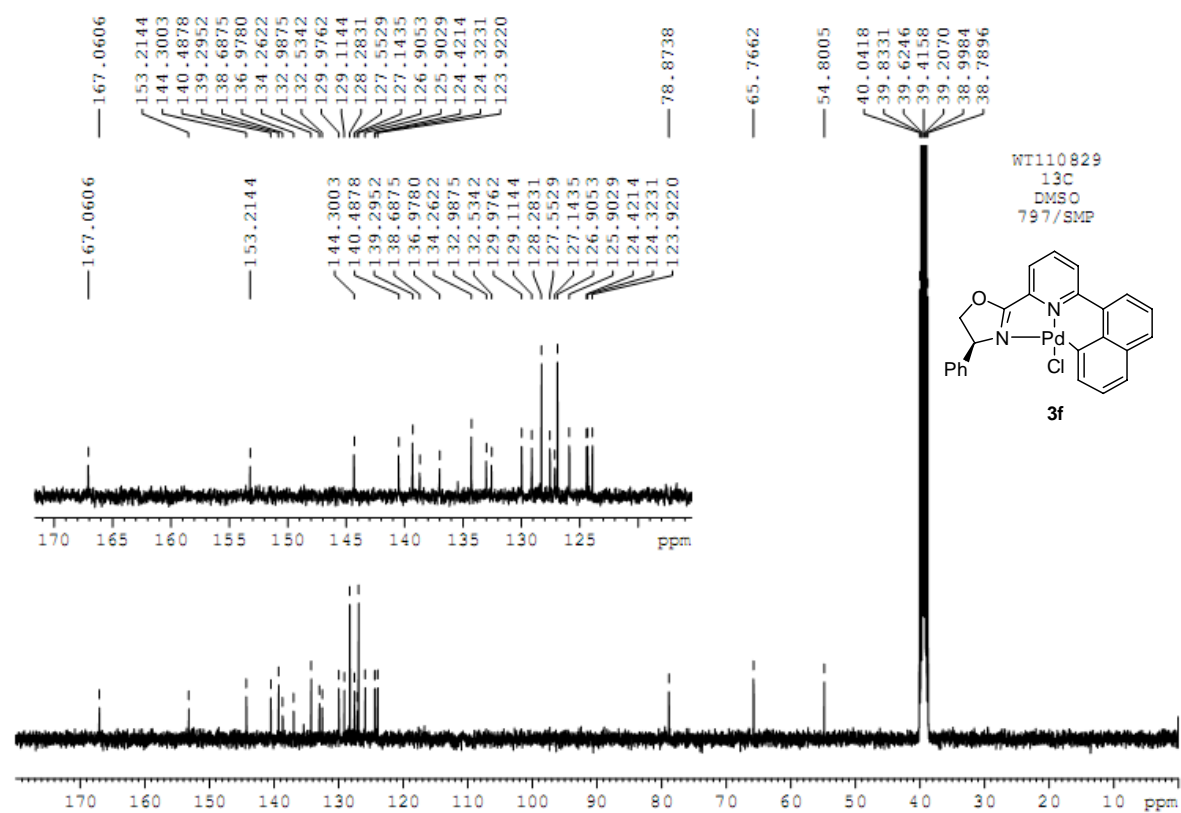
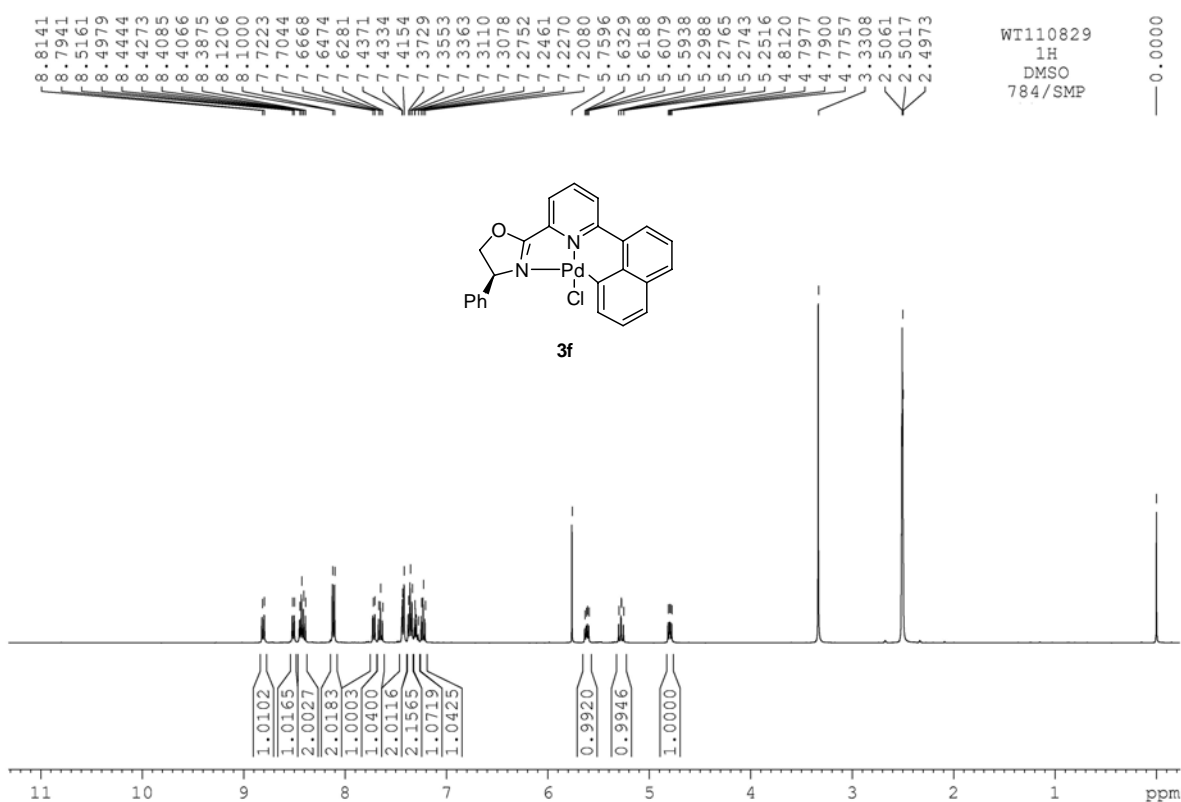




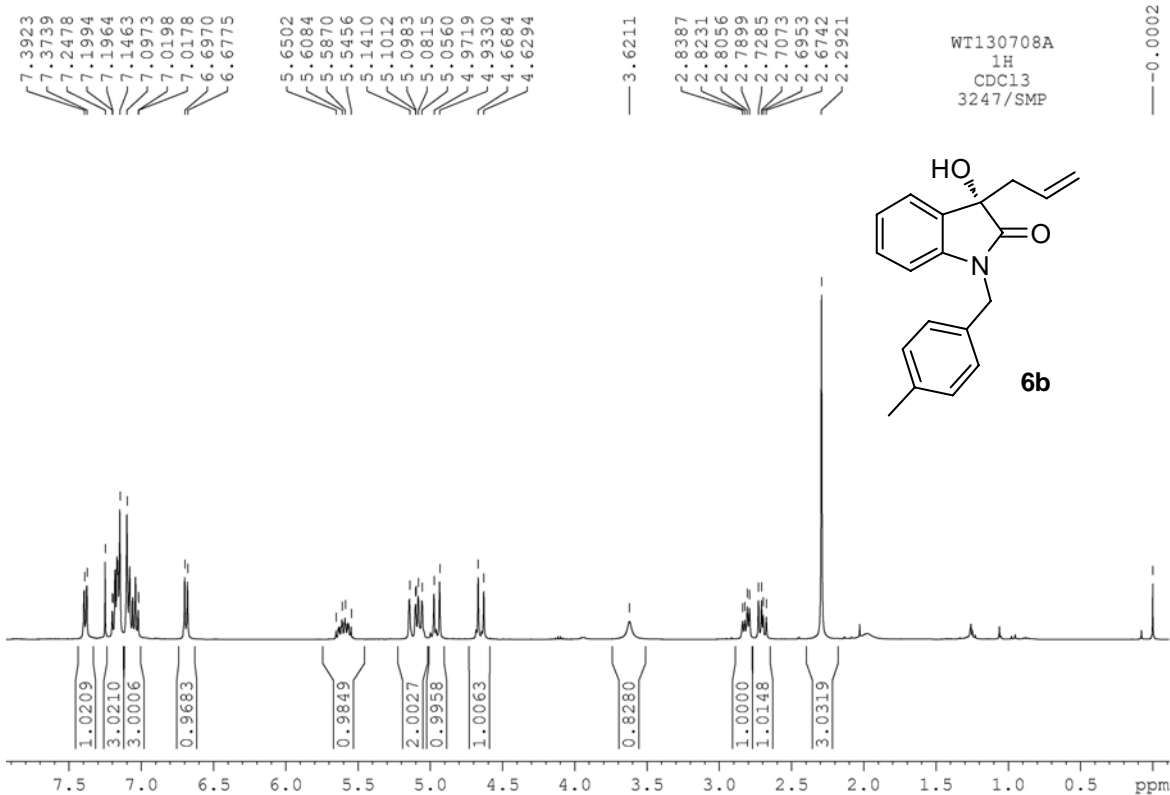
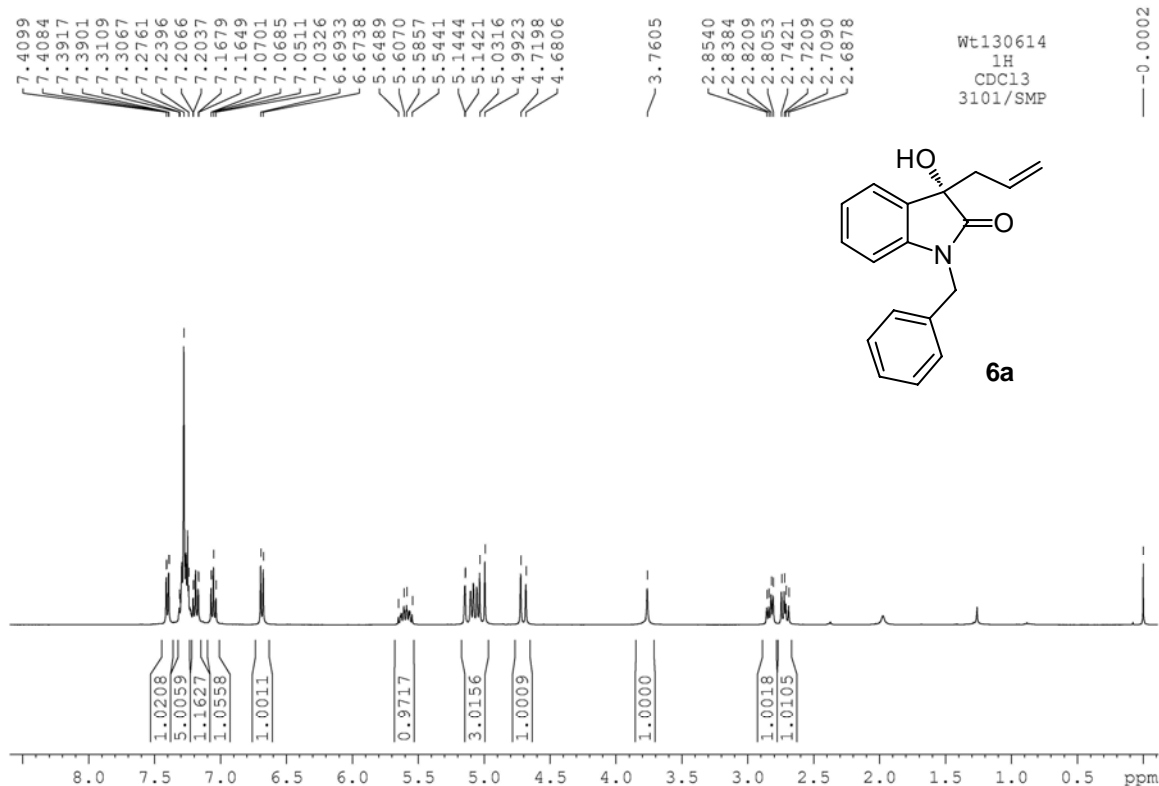


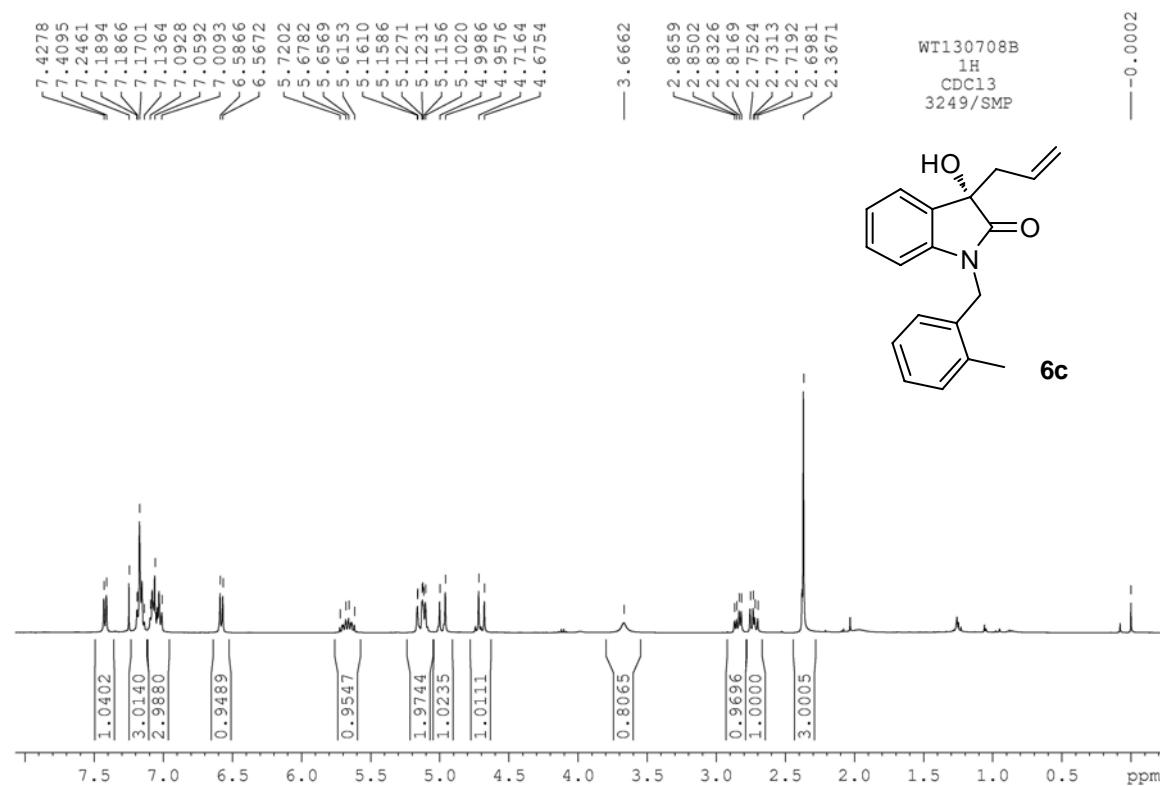
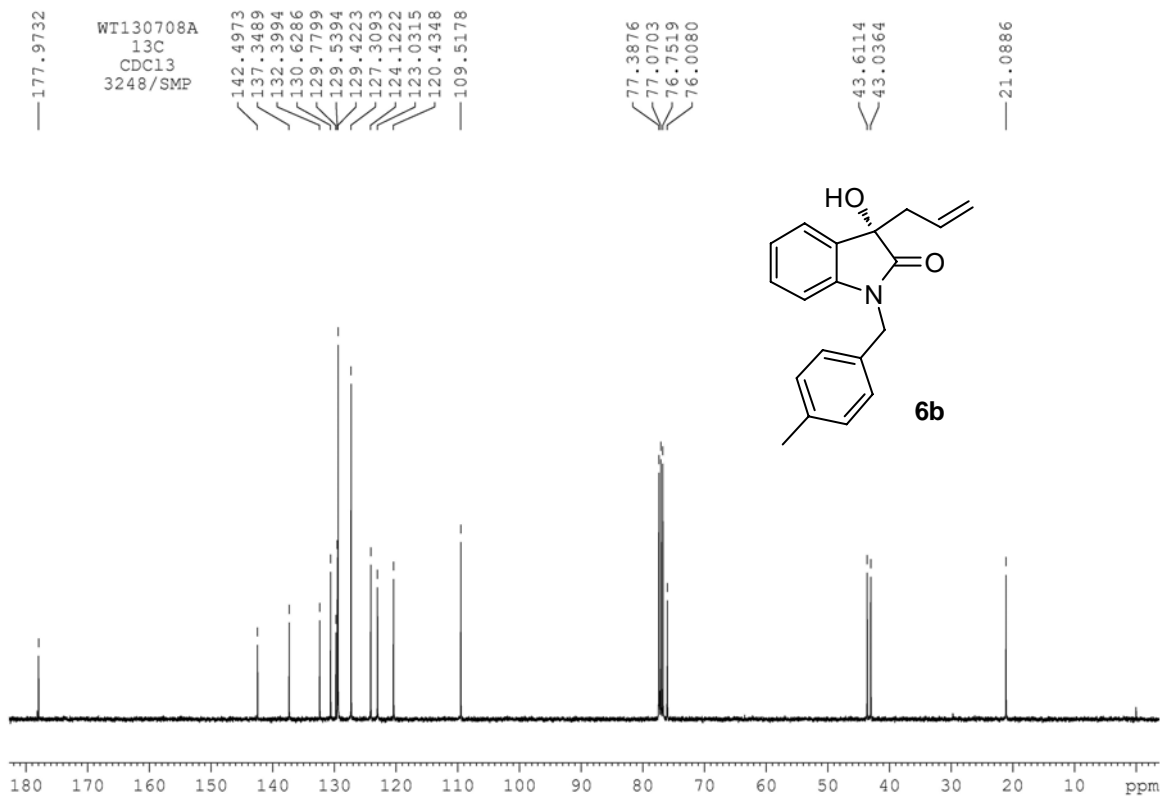


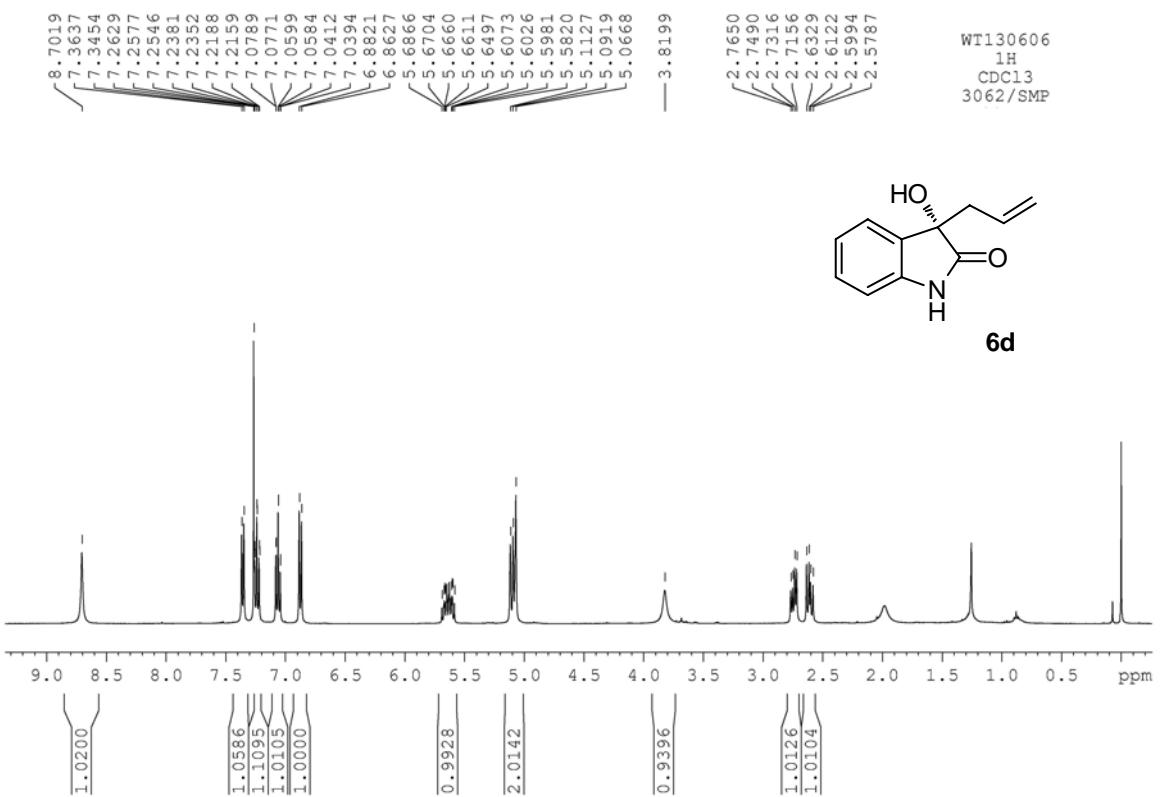
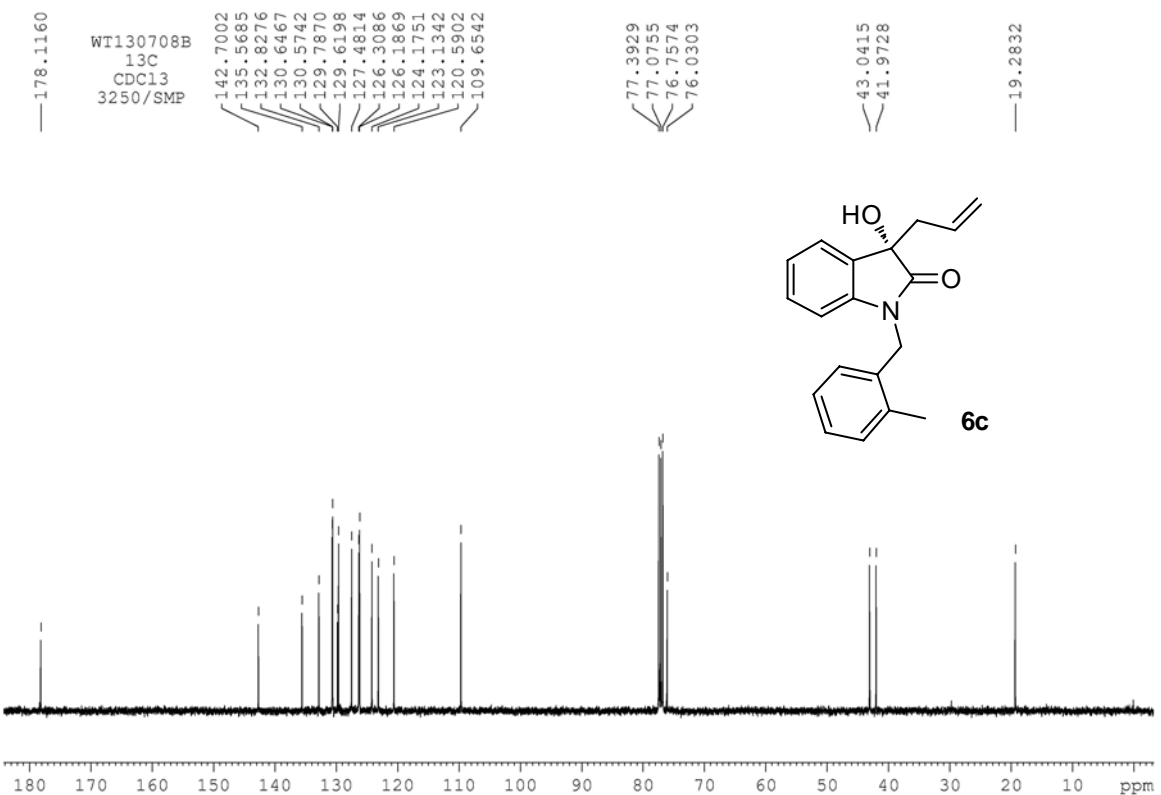


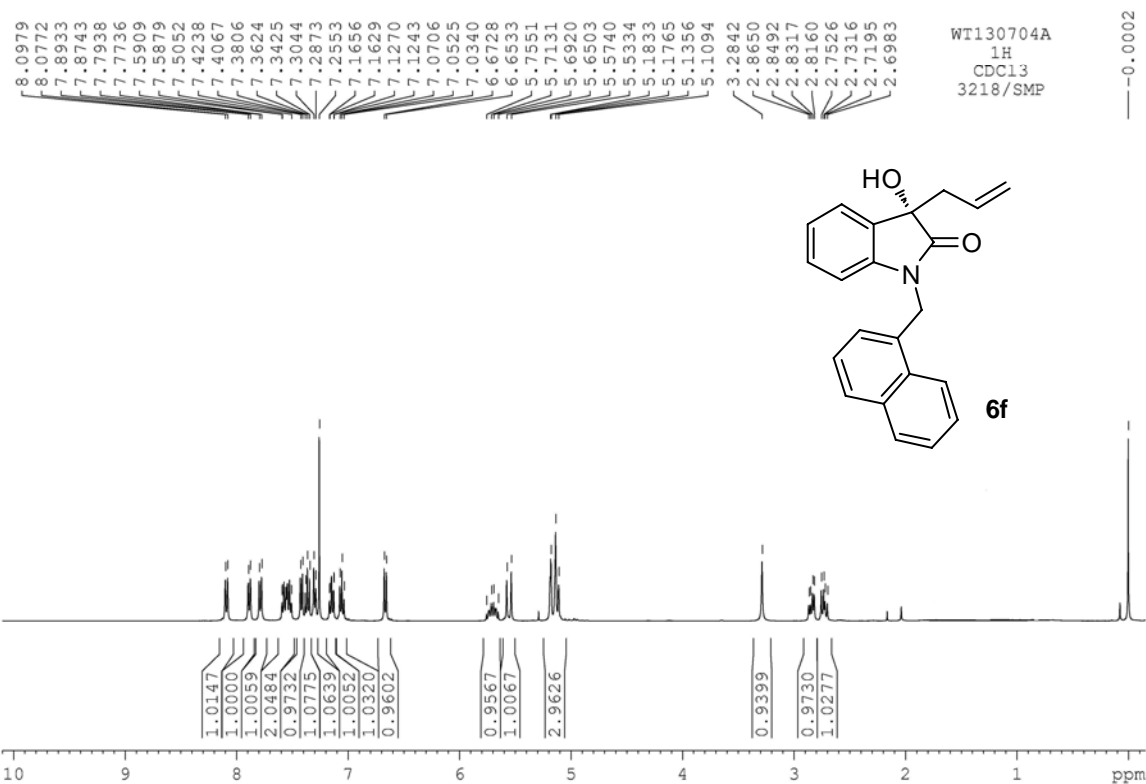
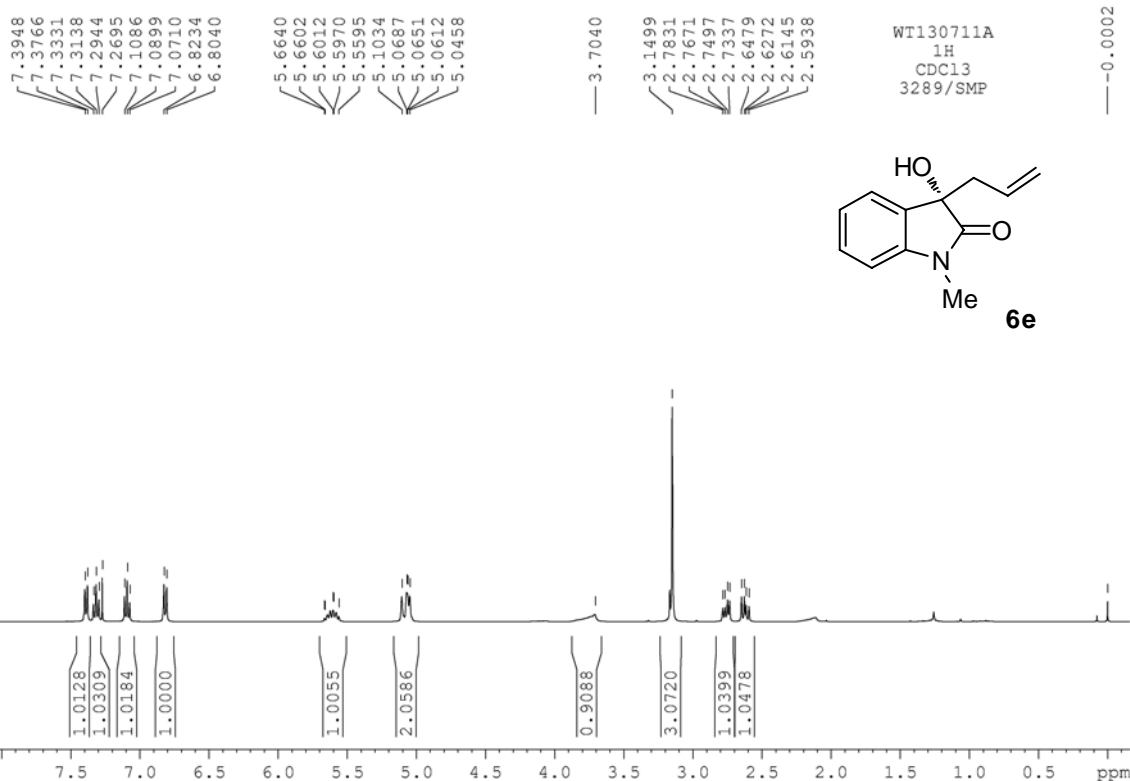


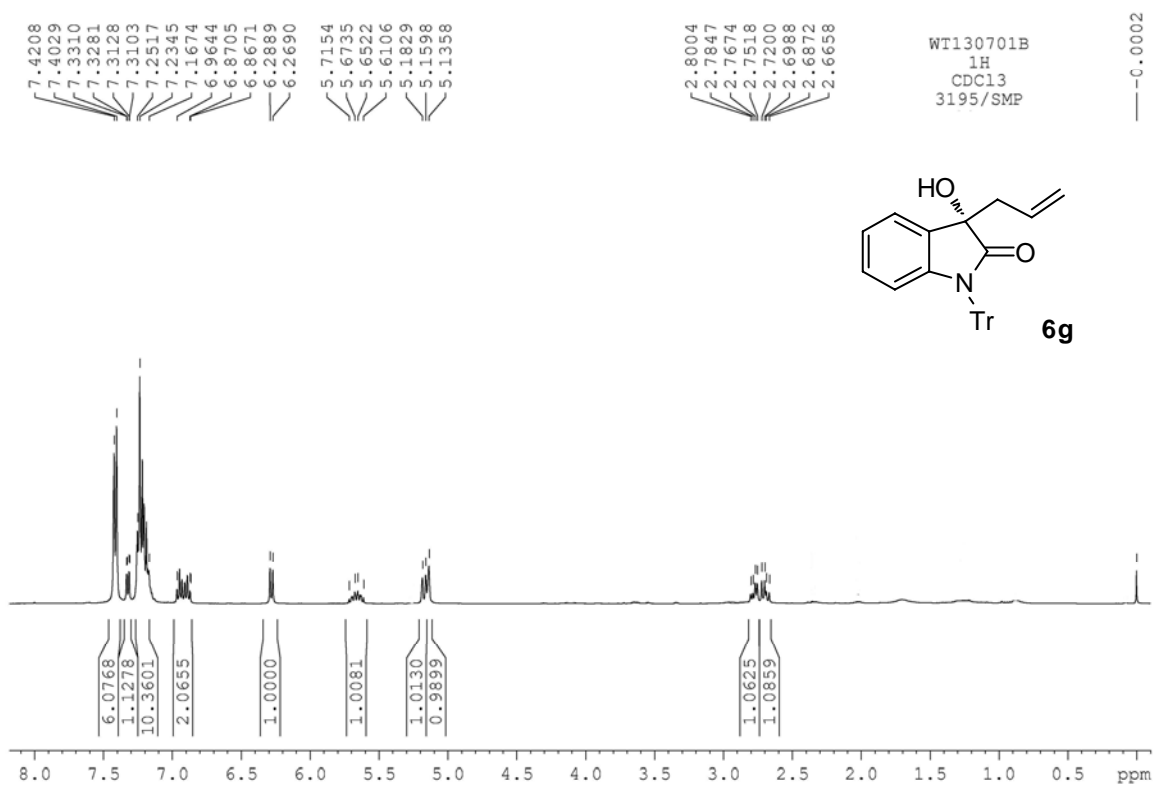
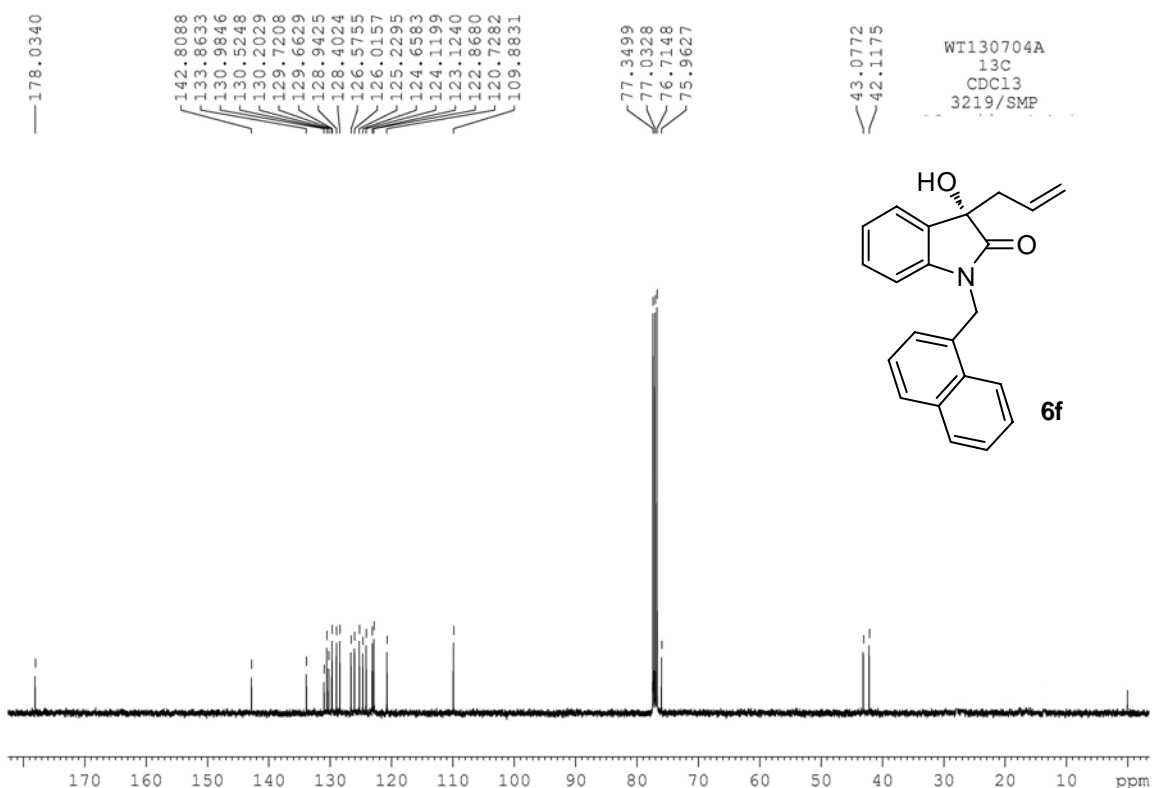
## Copies of the NMR Spectra of the Catalysis Products

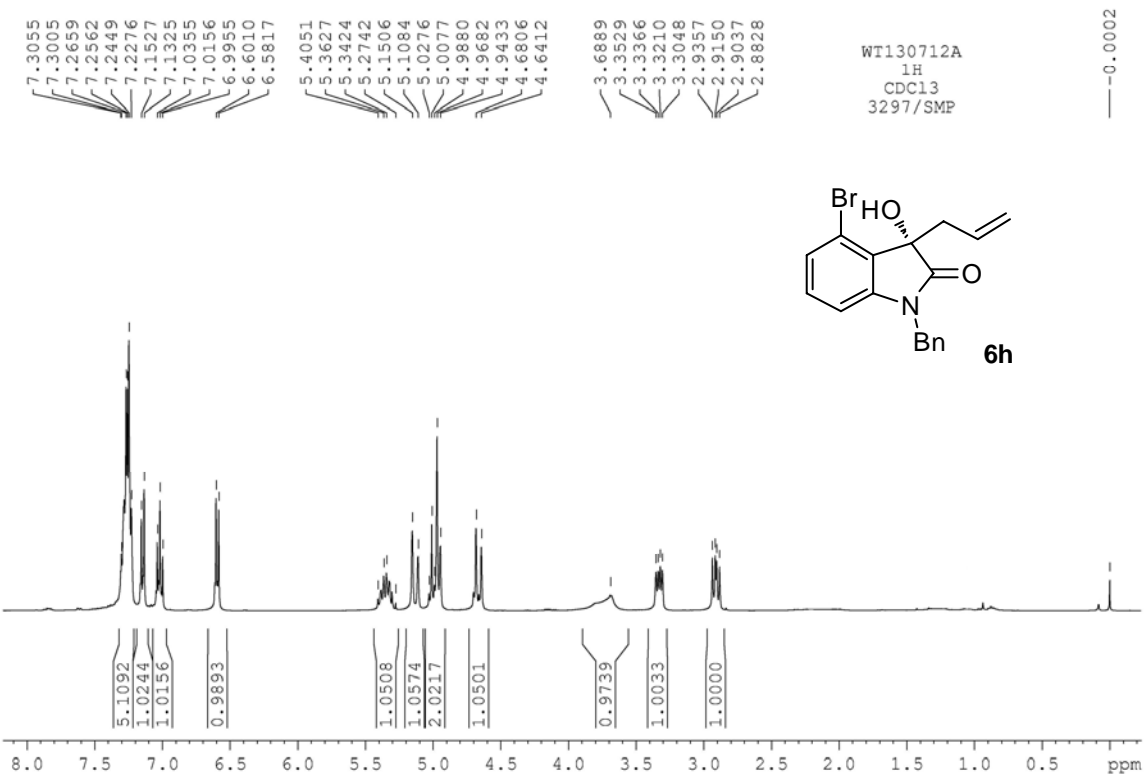
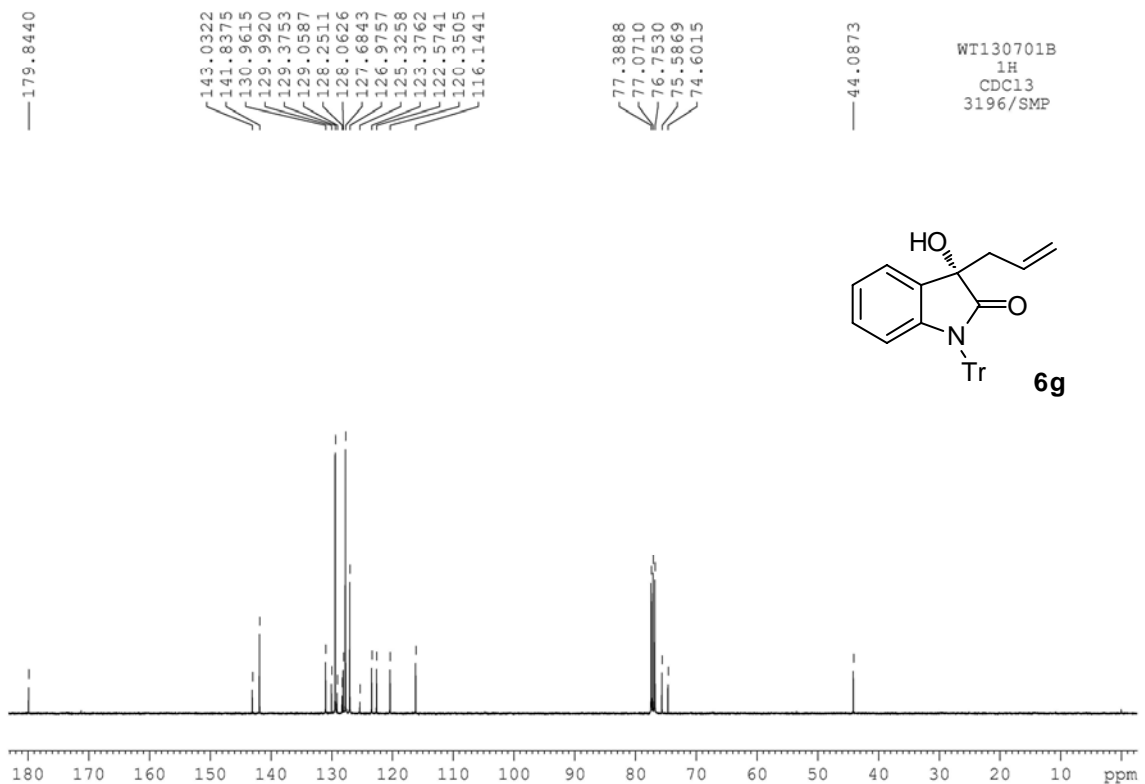


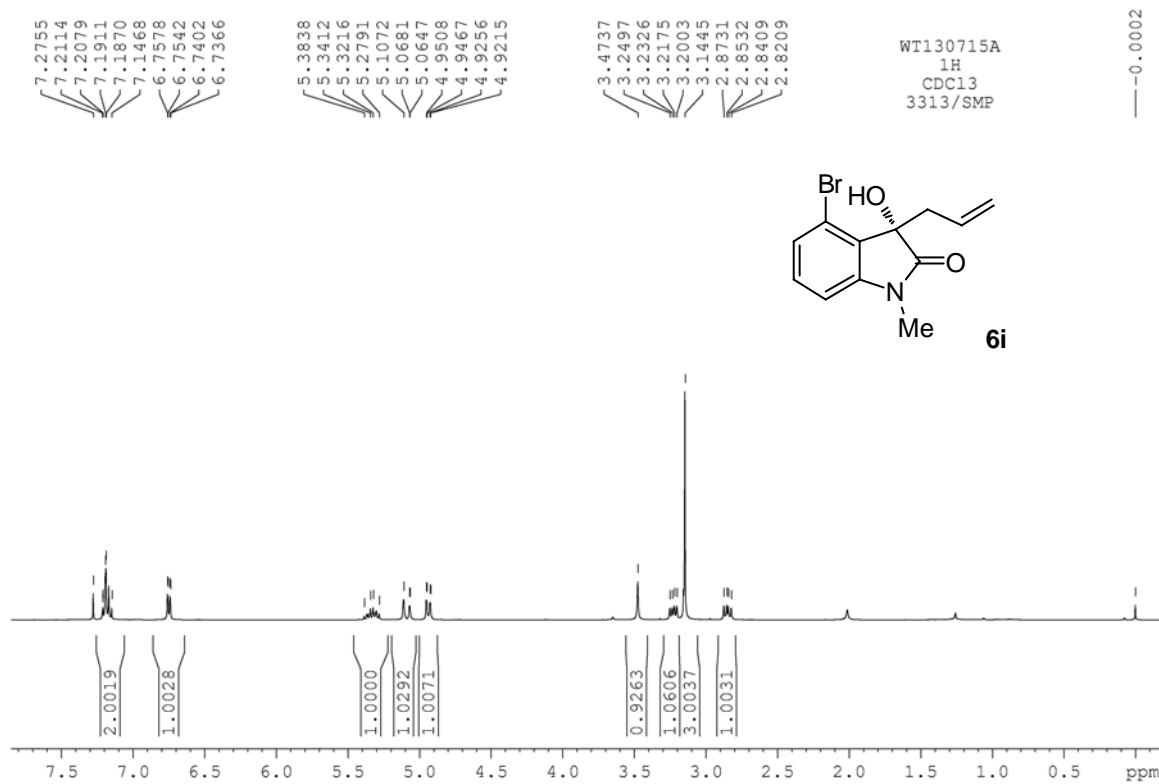
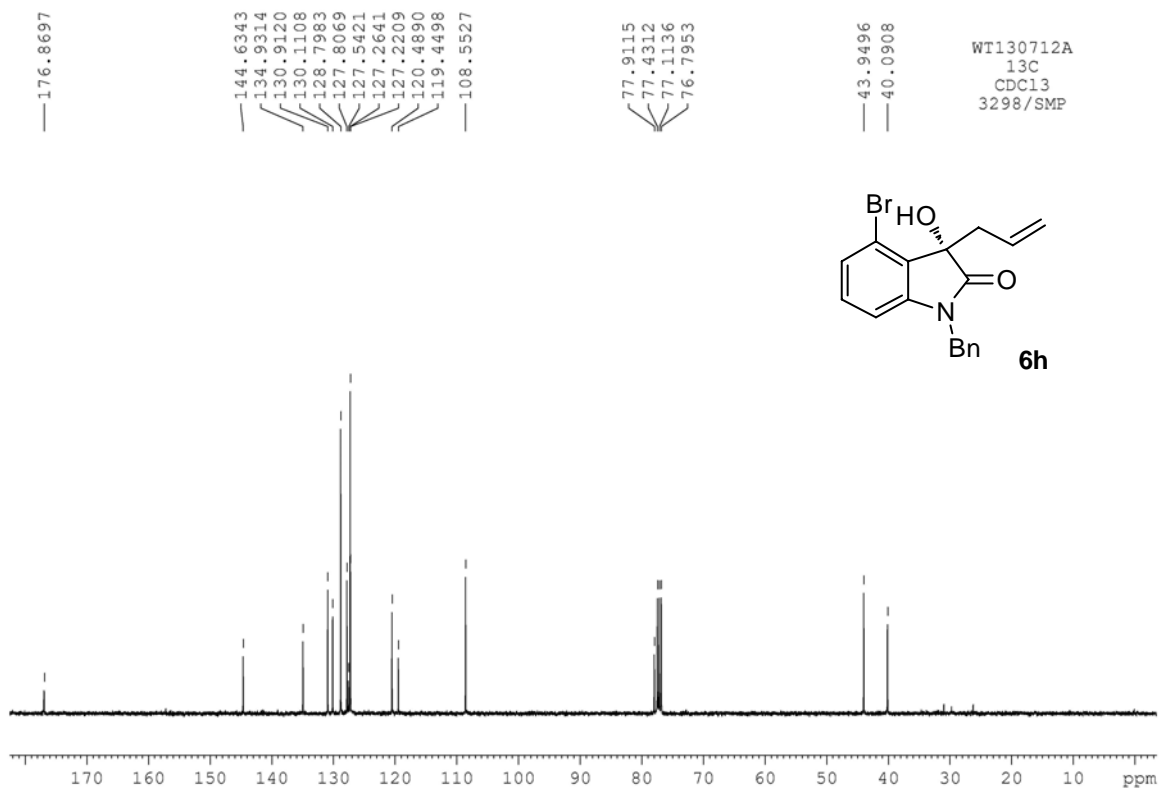


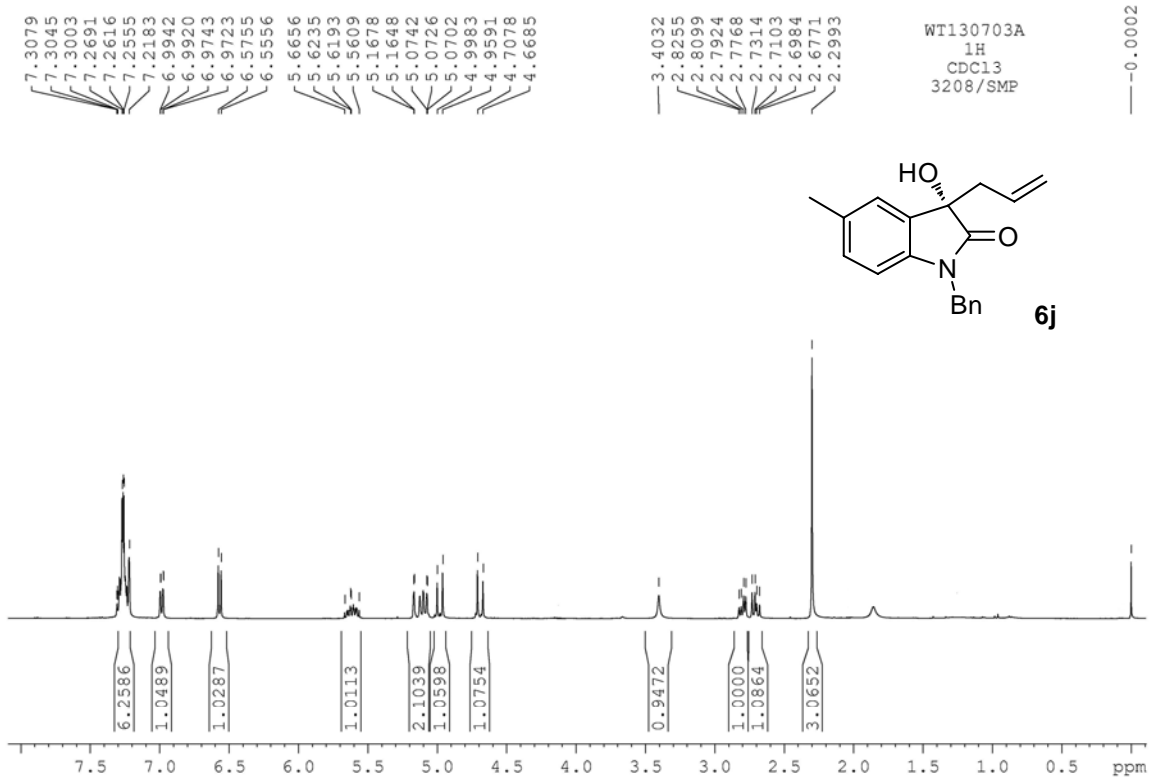
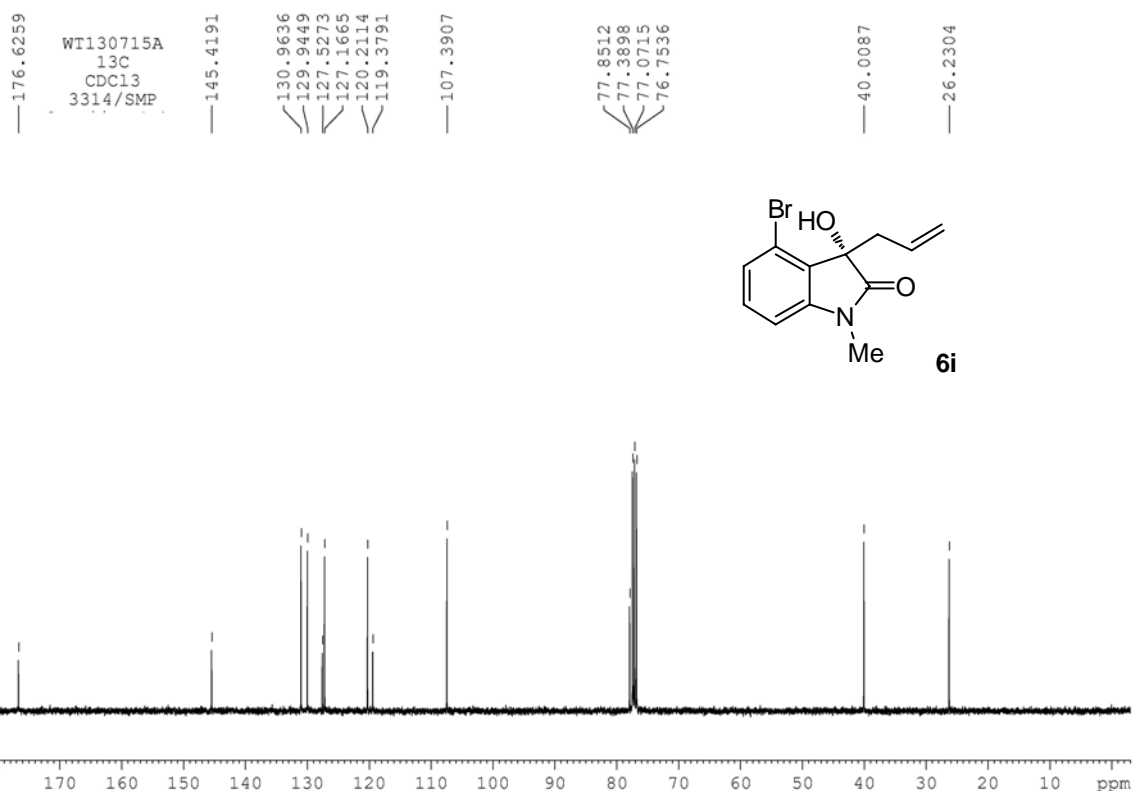


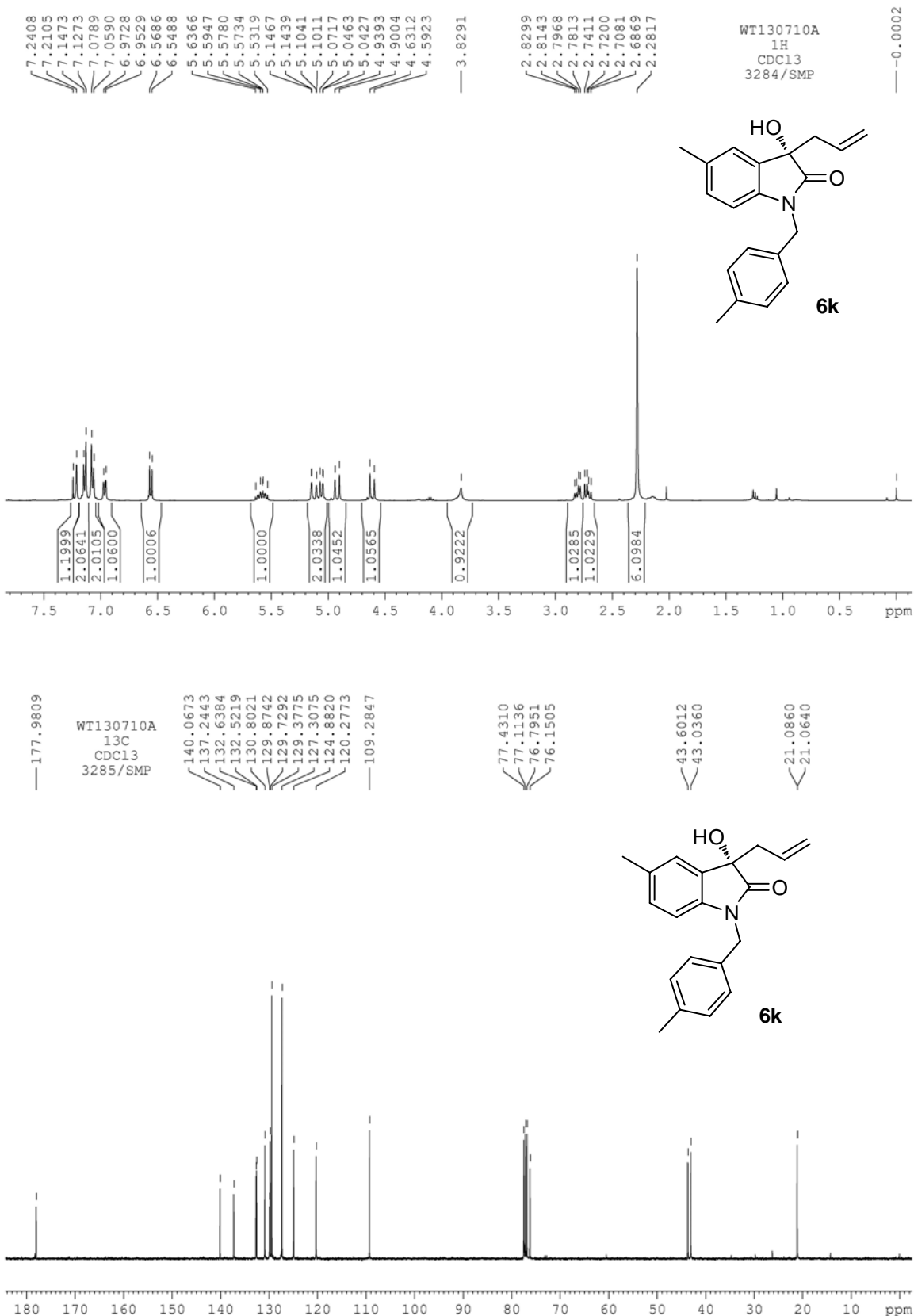


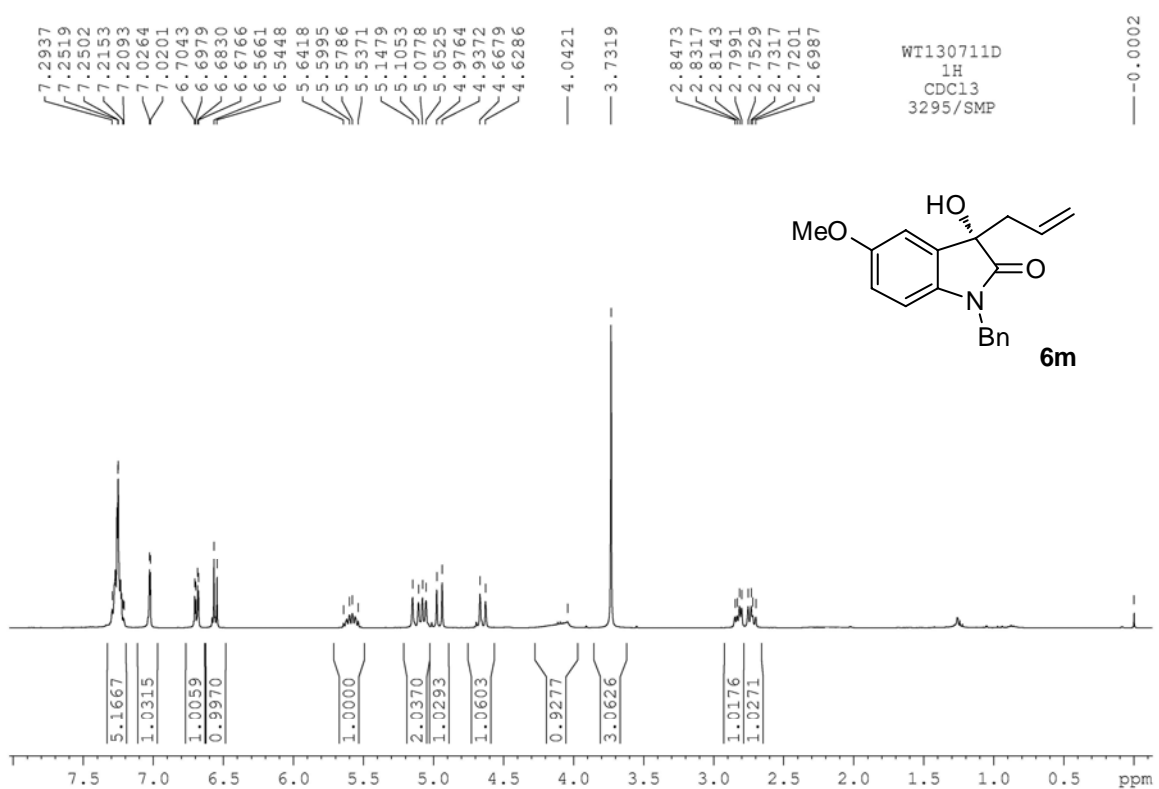
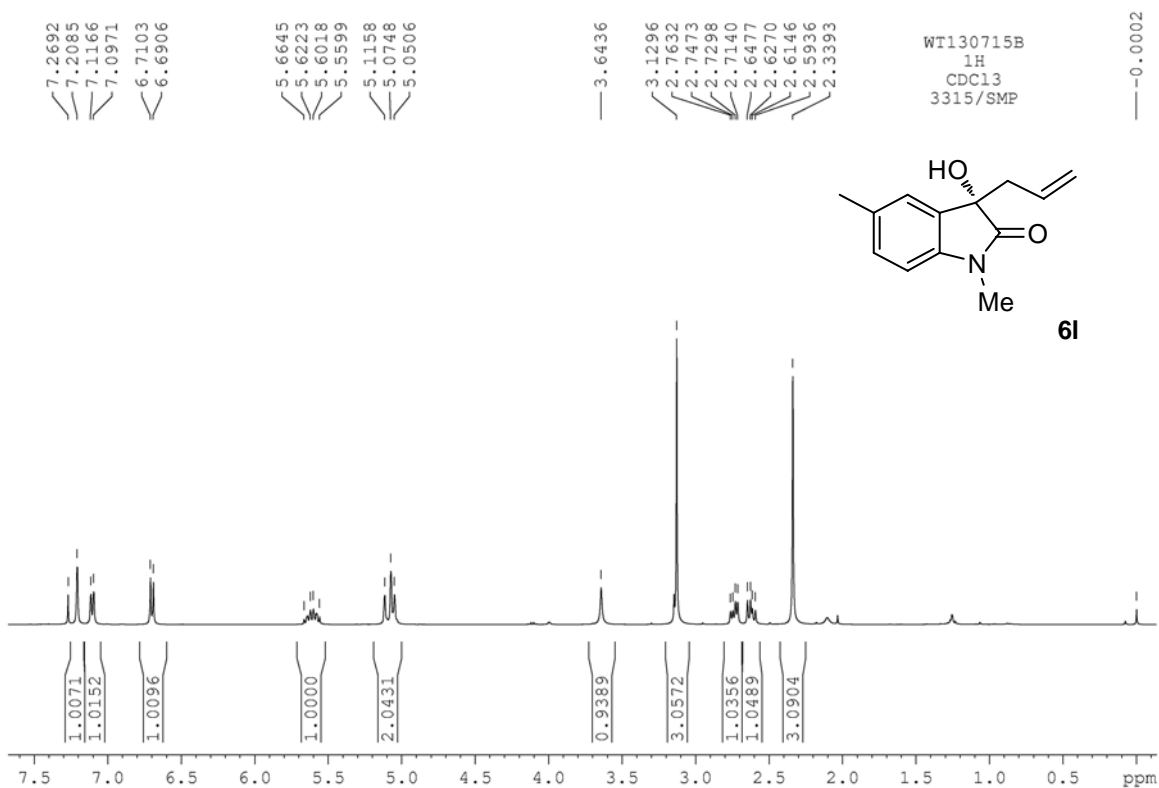


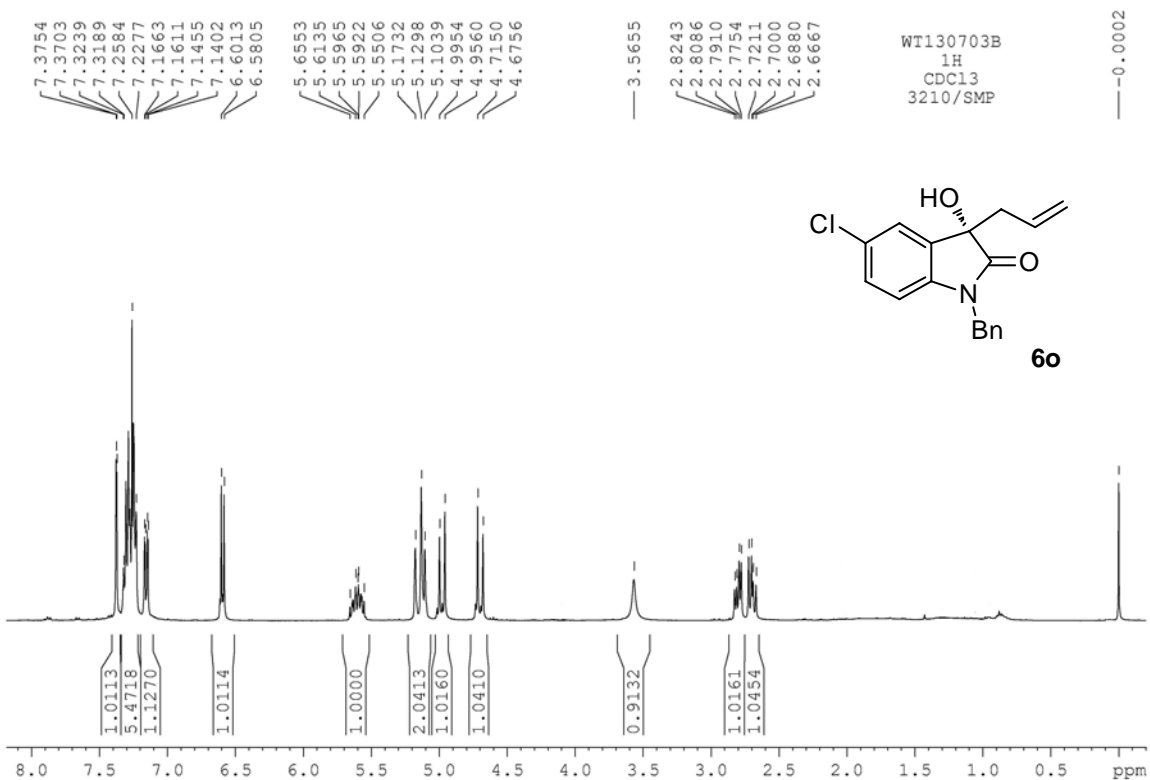
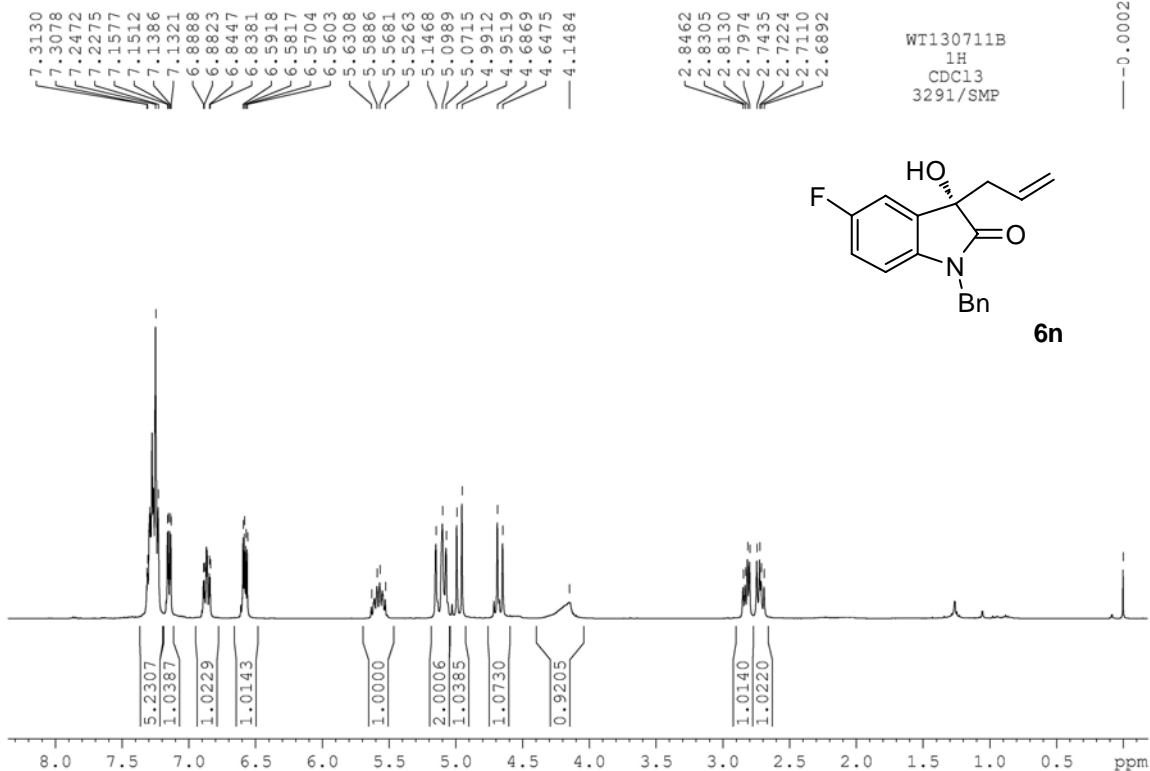


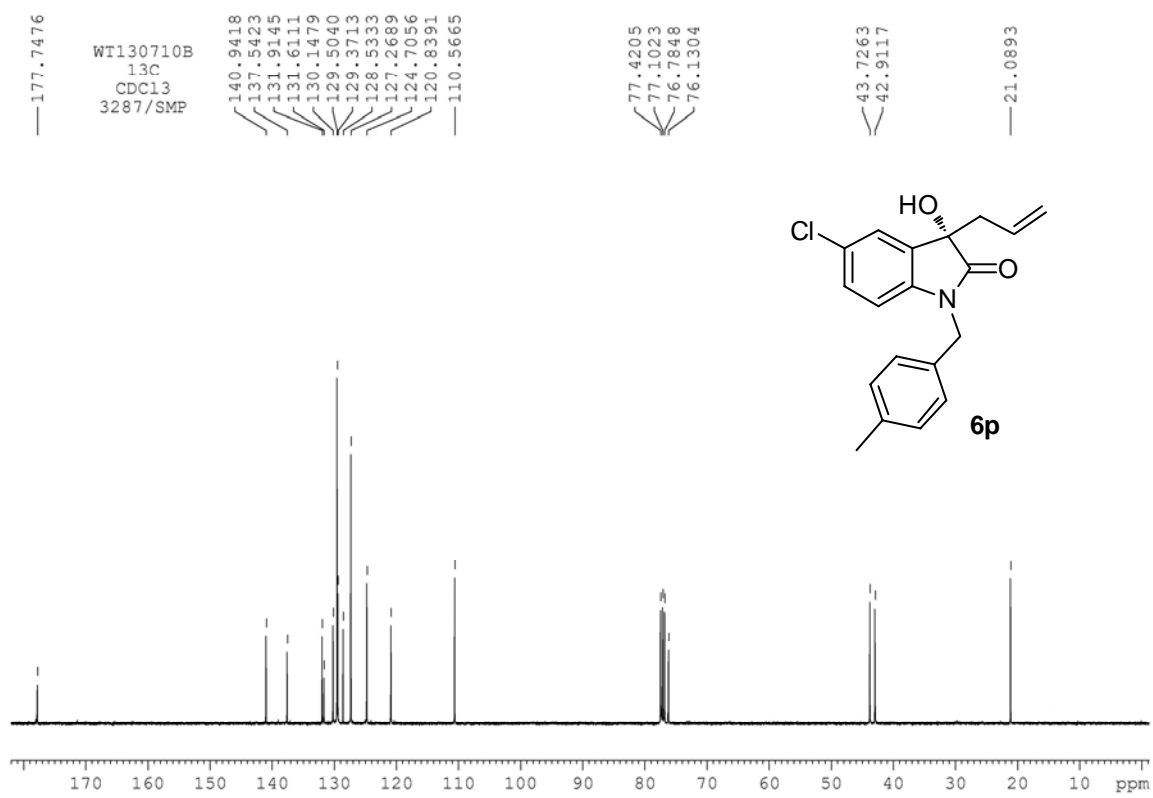
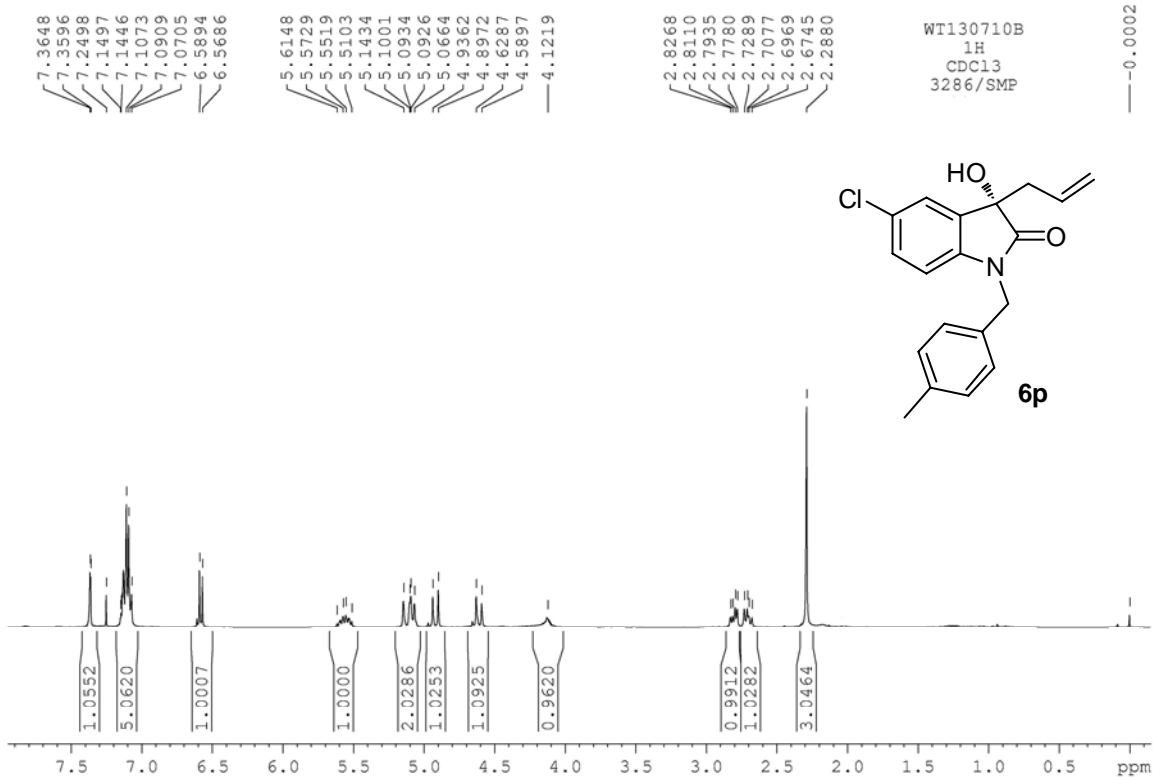


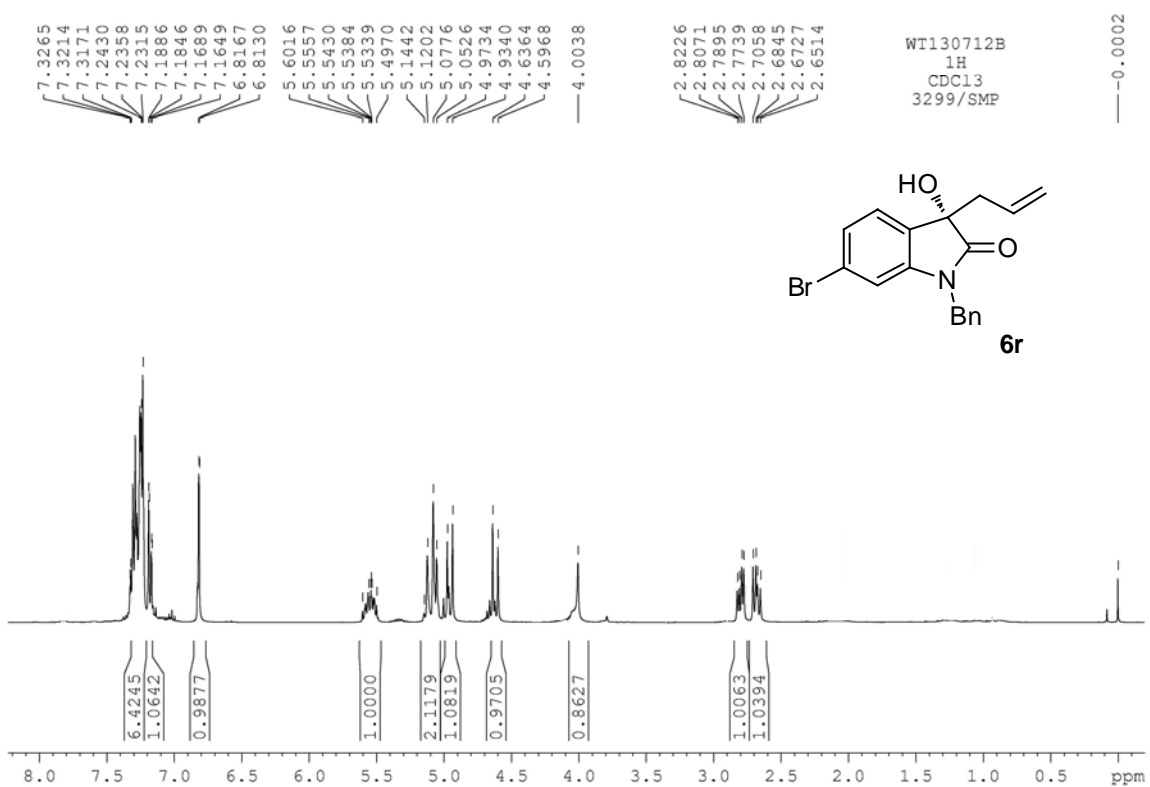
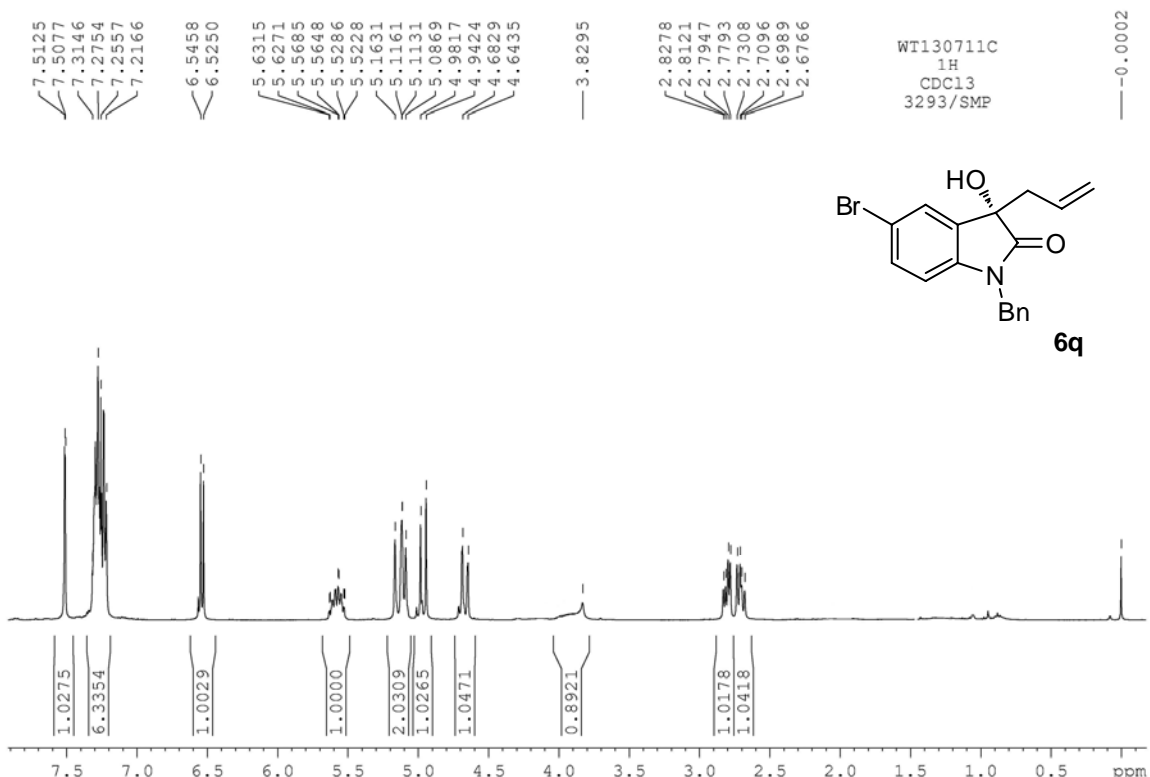


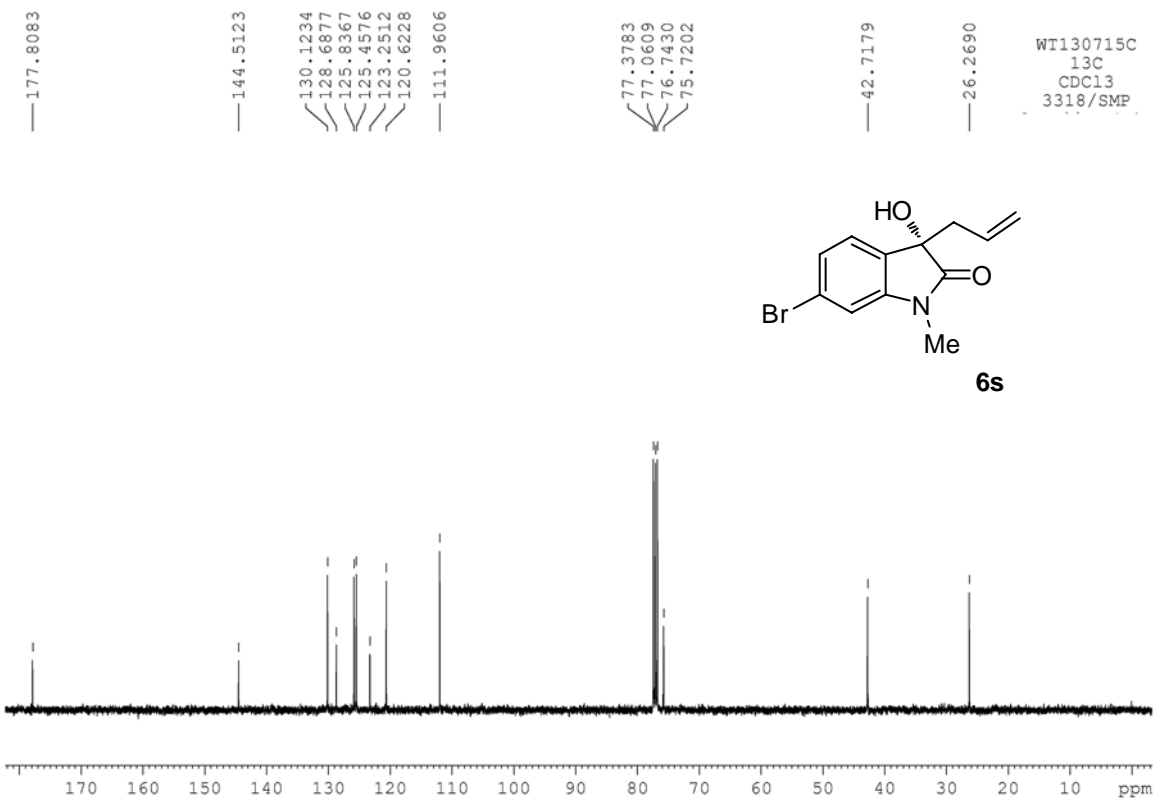
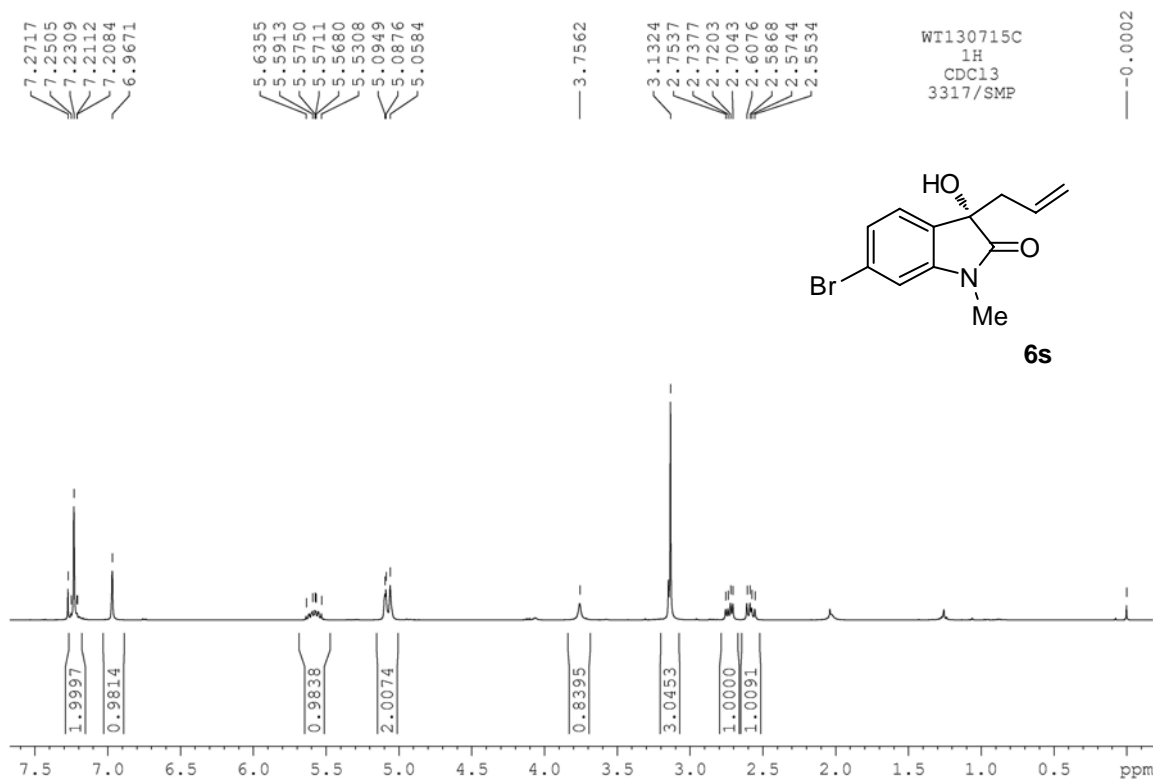


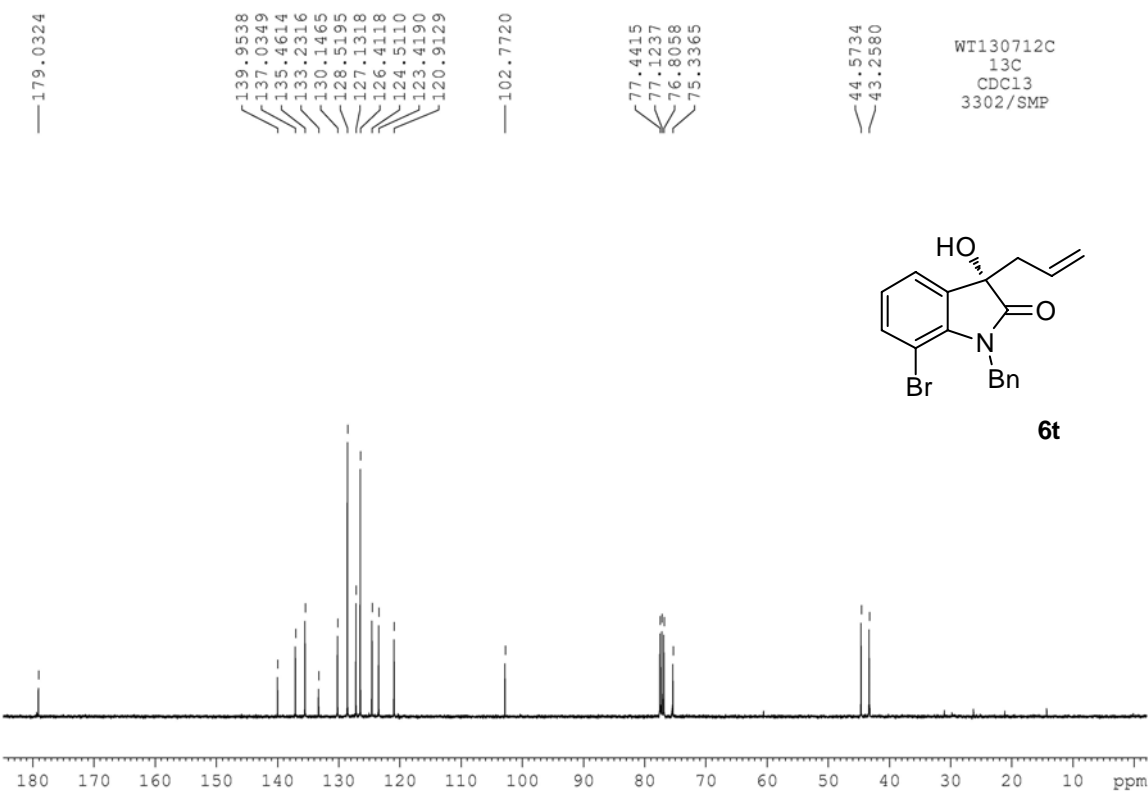
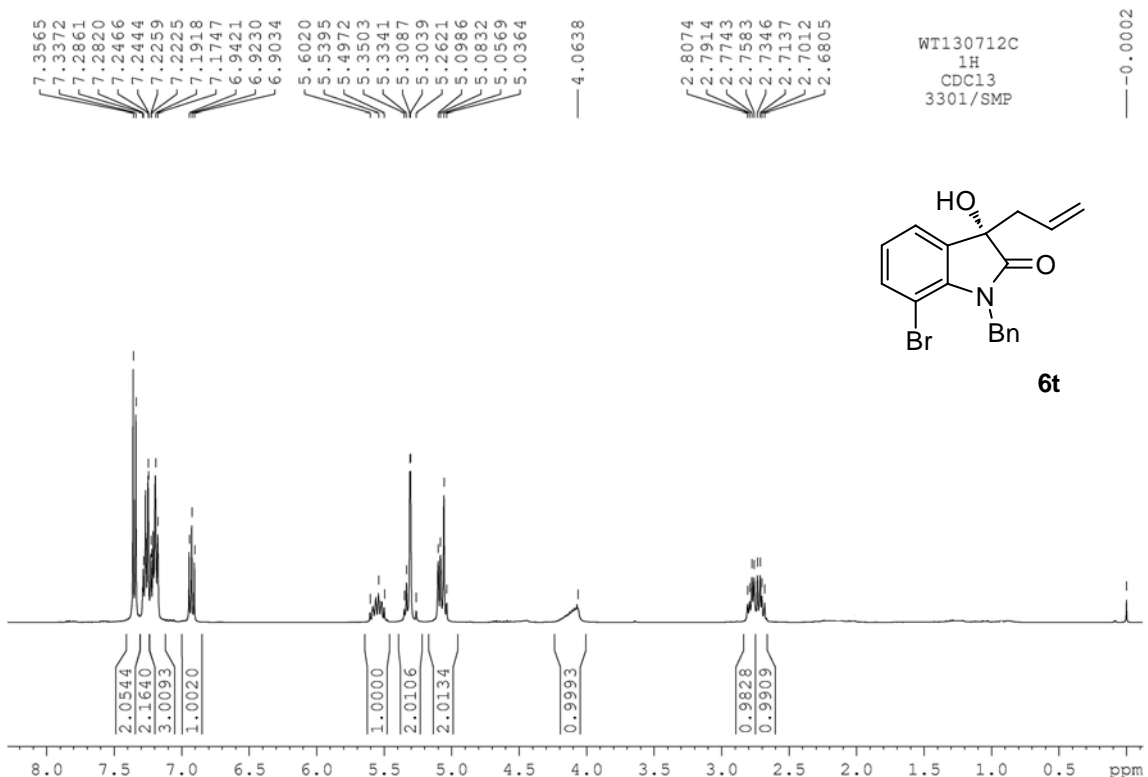


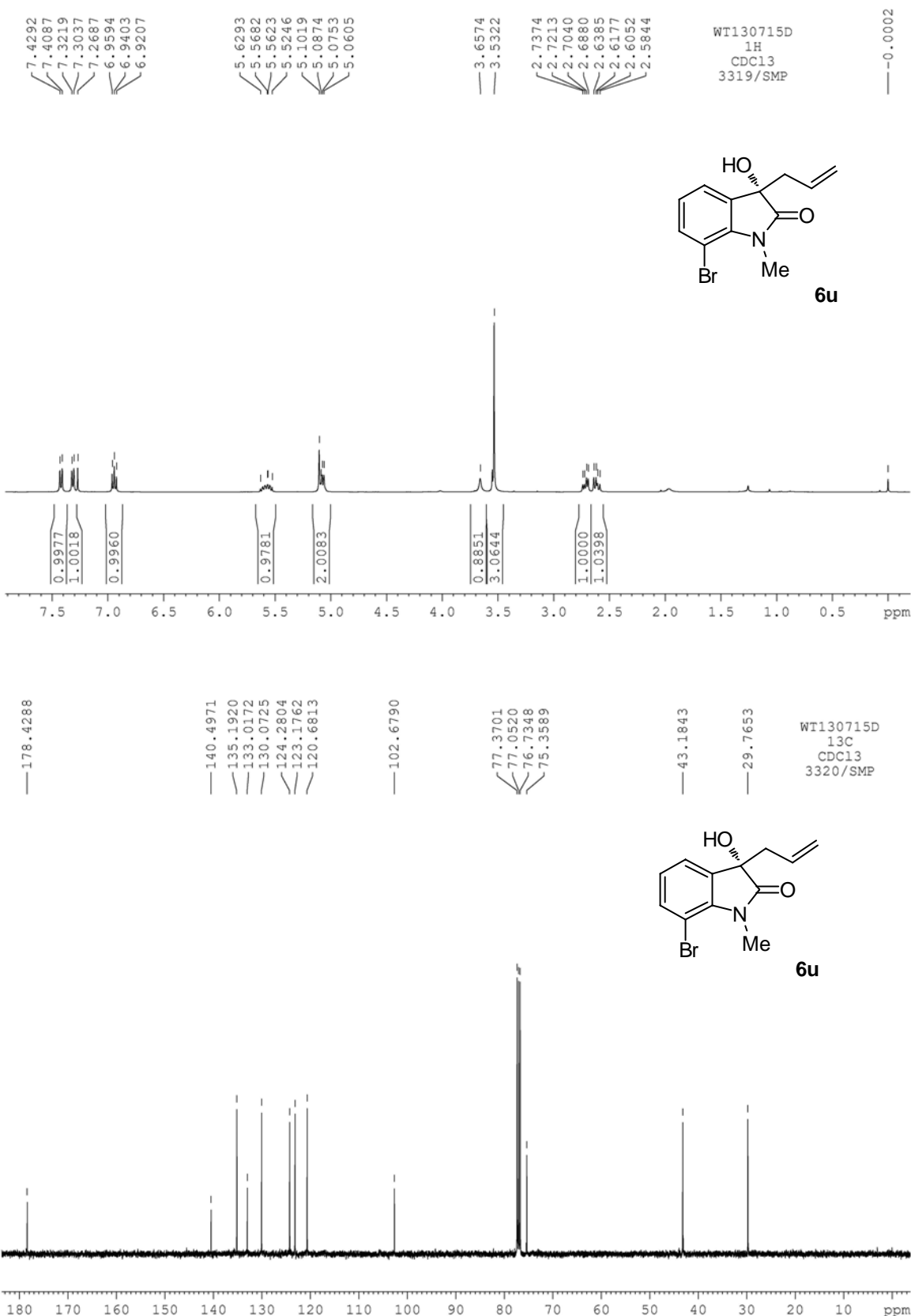


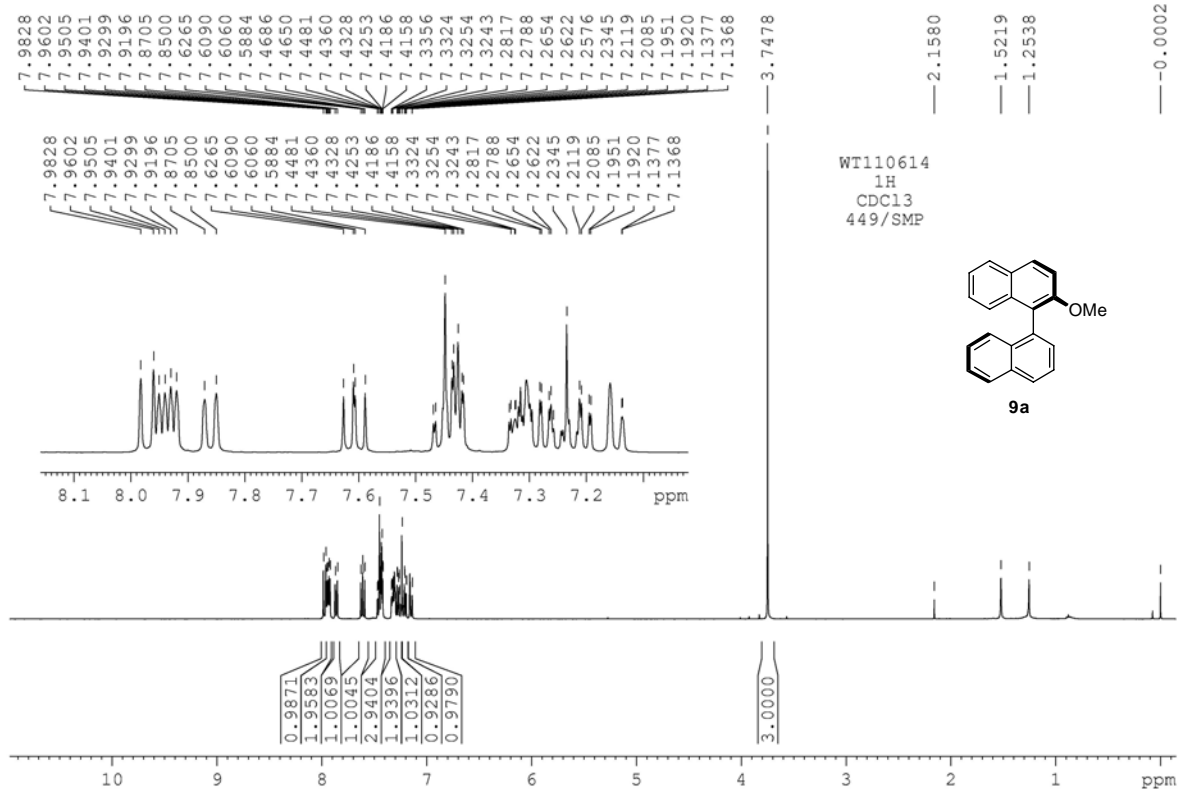


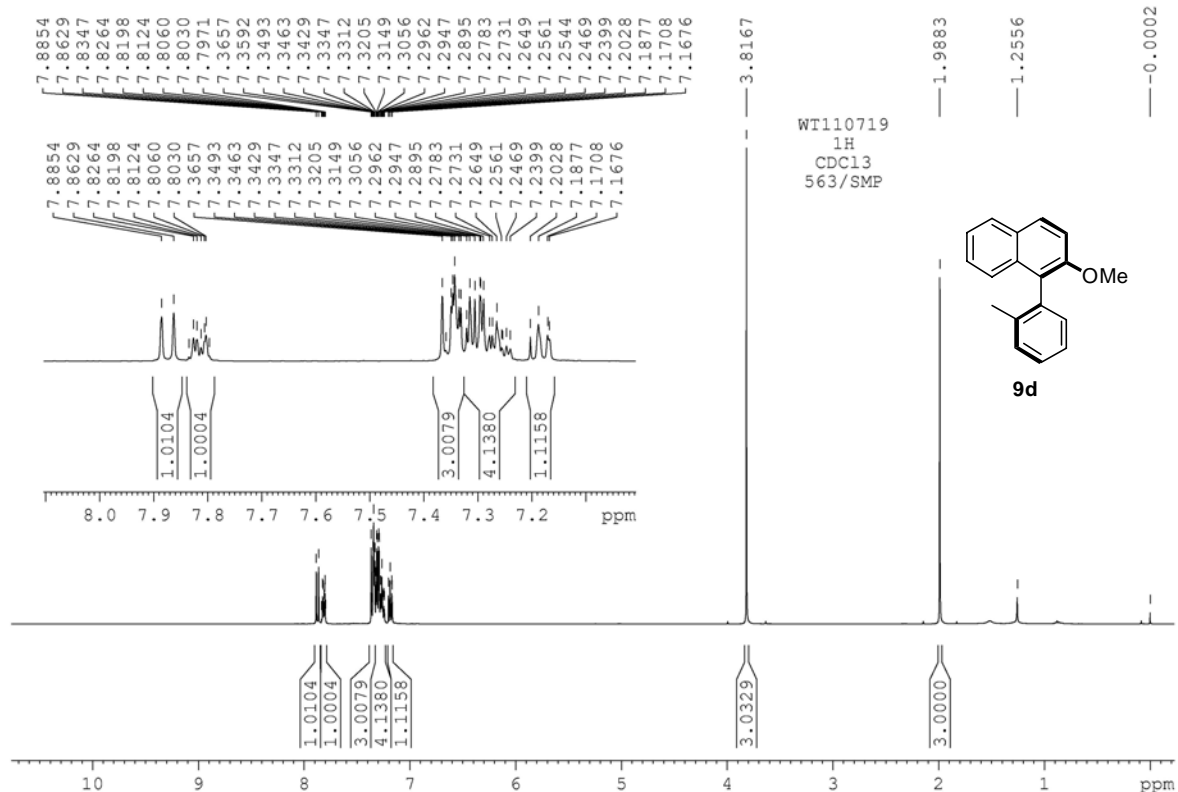
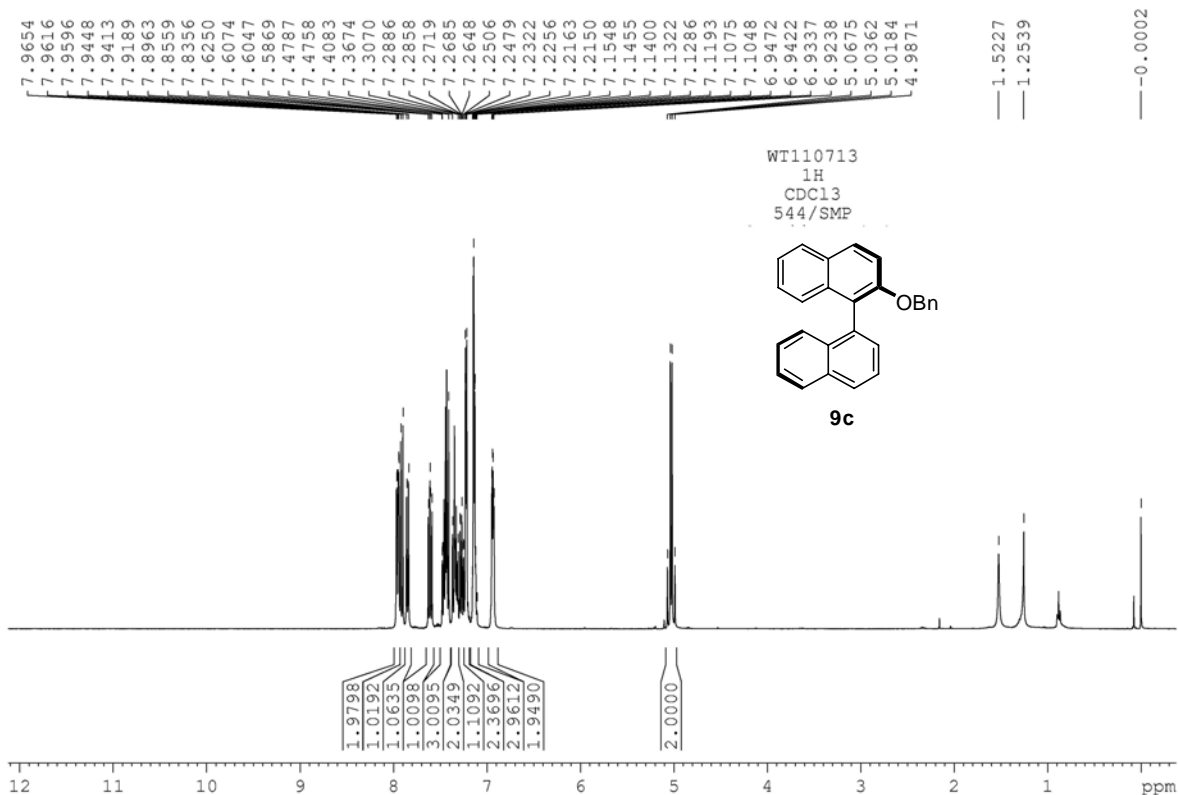


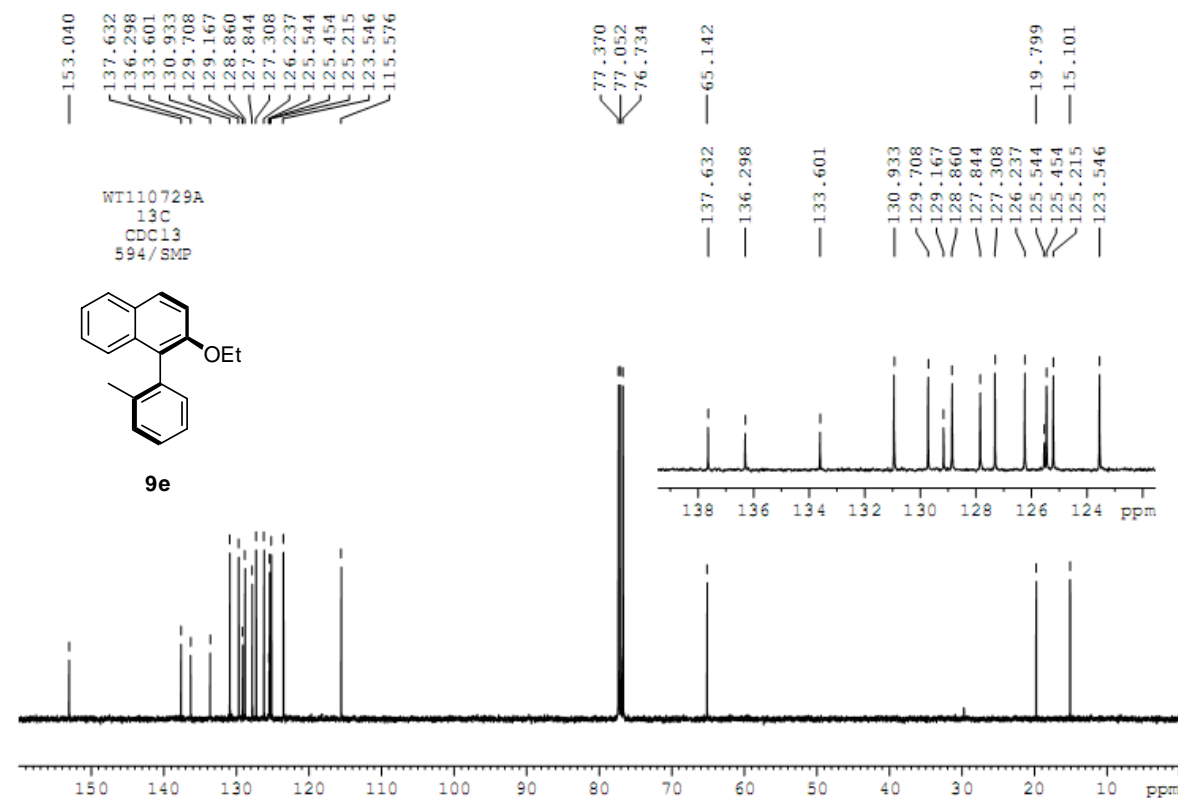
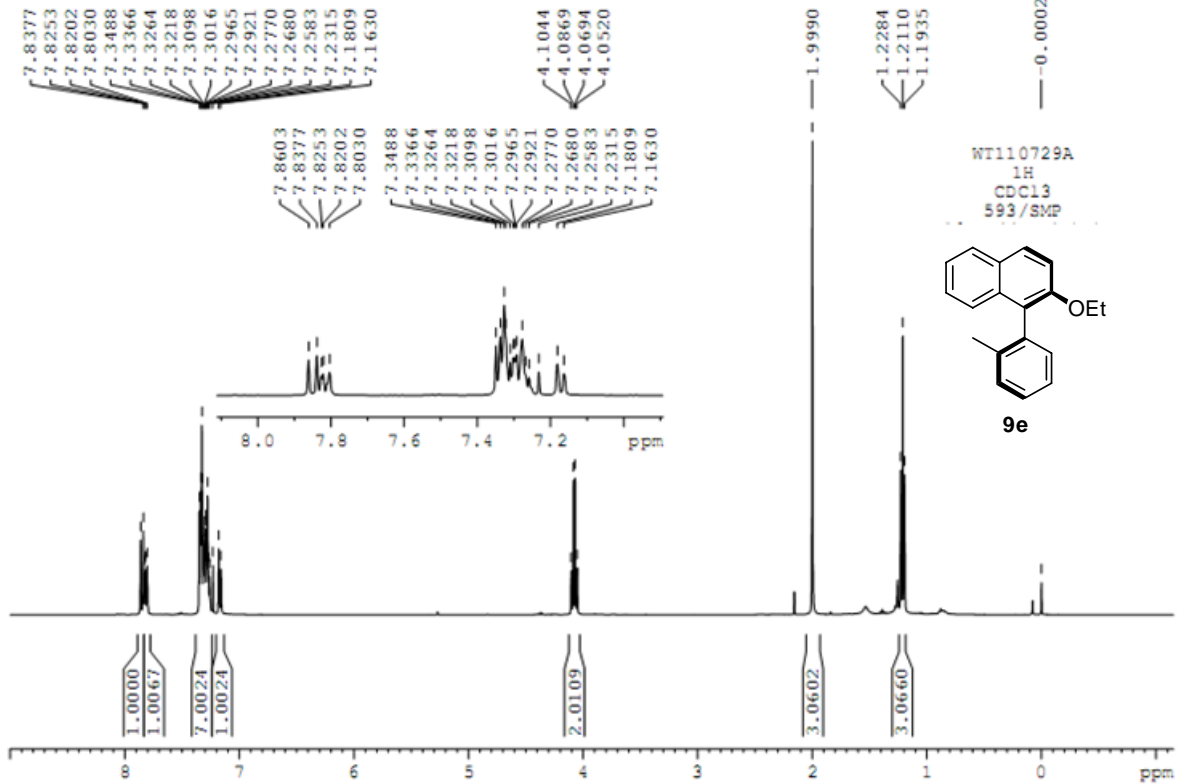


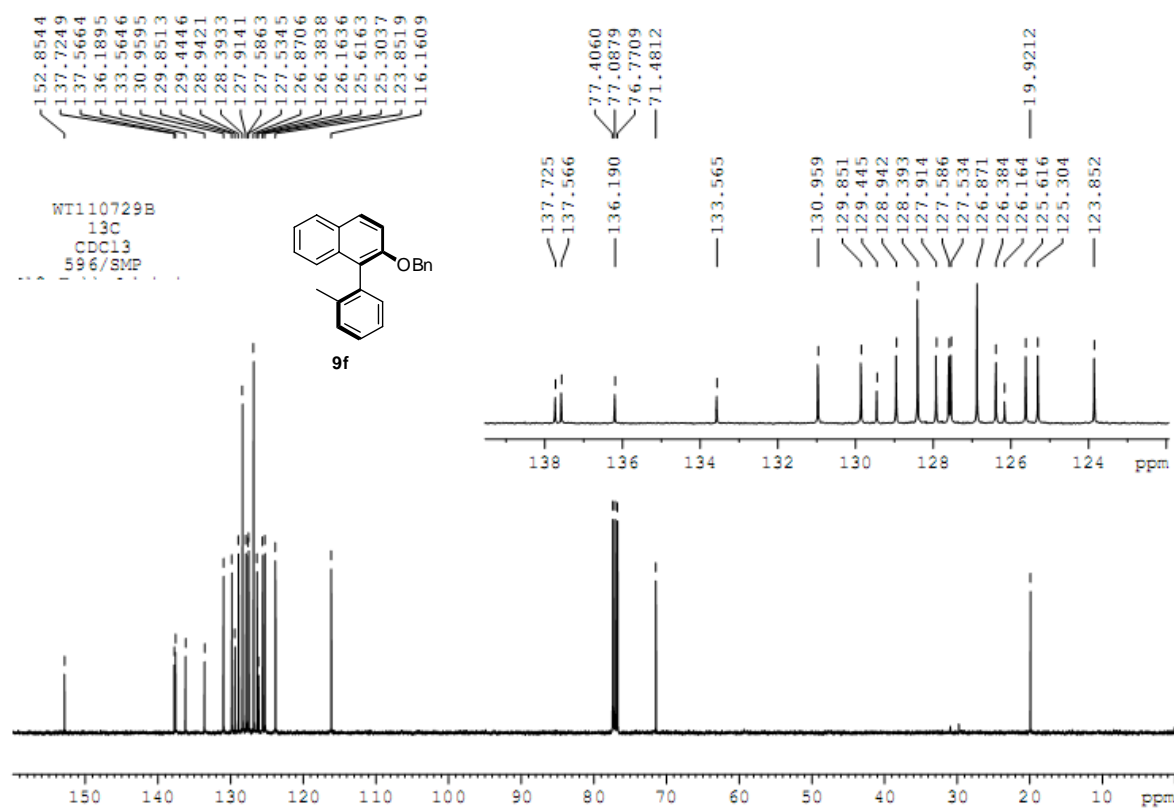
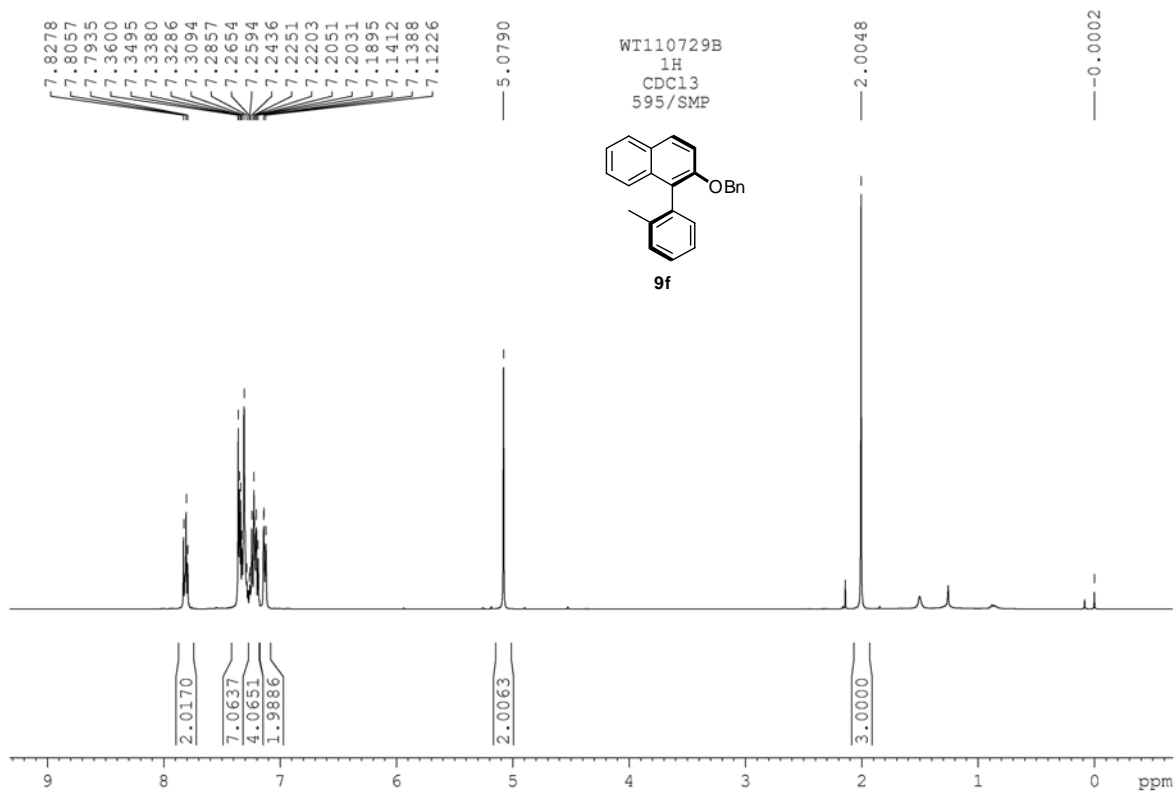


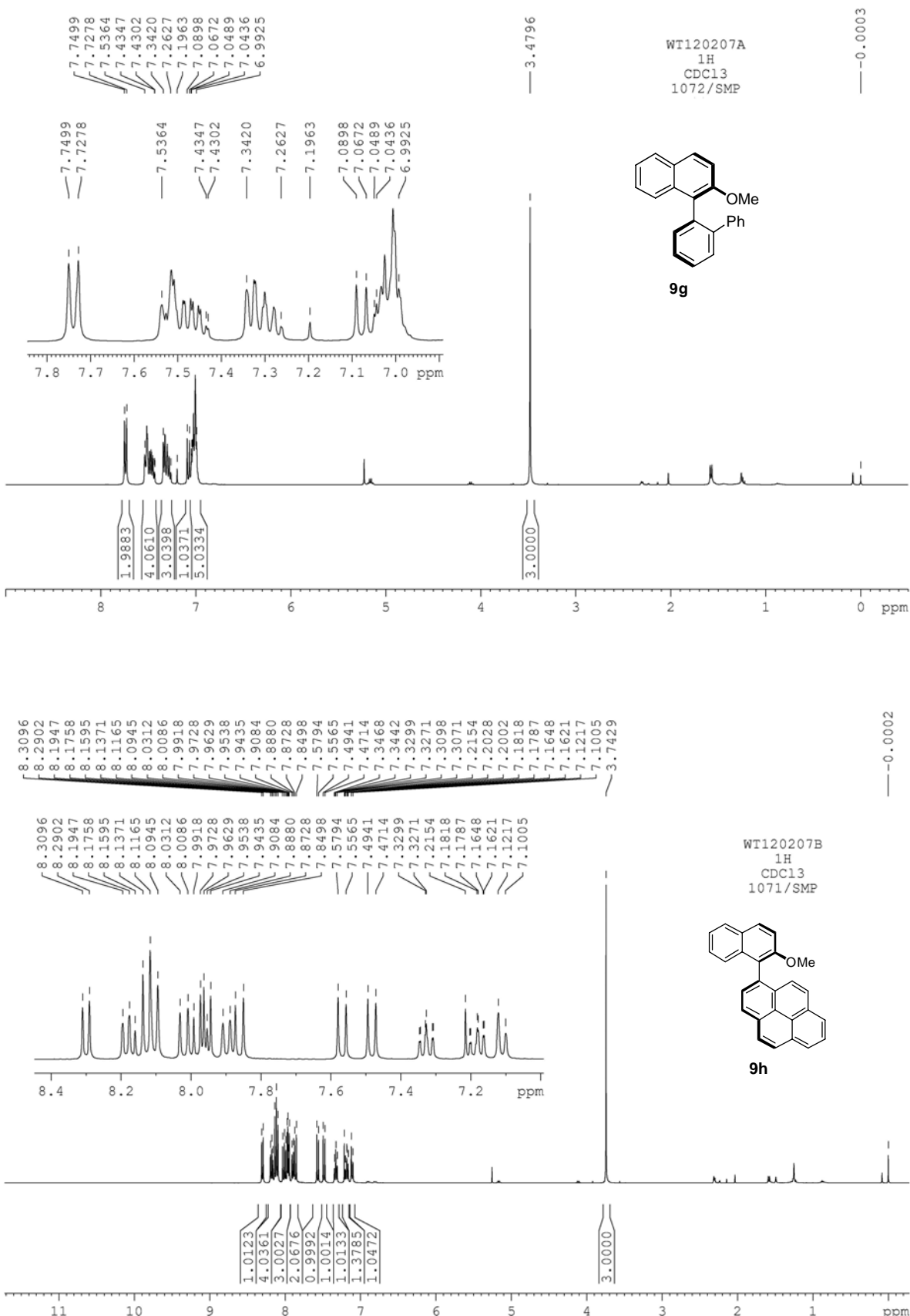


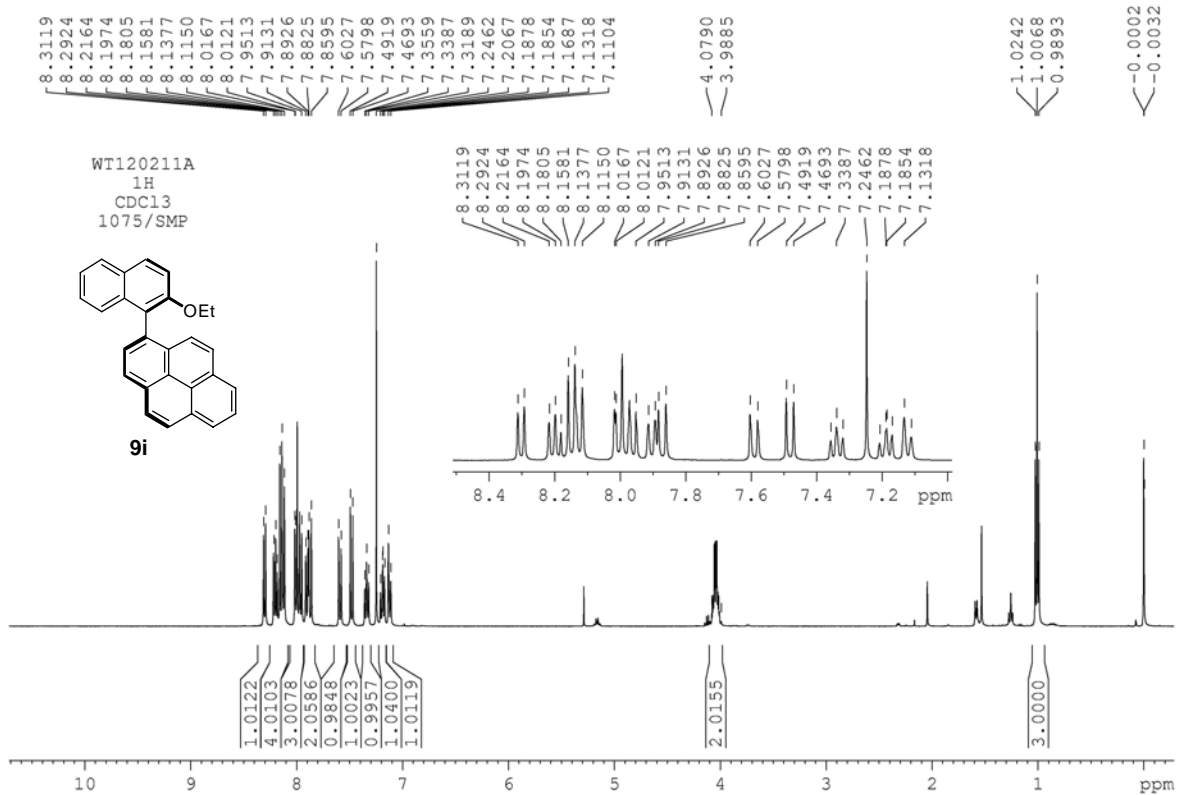
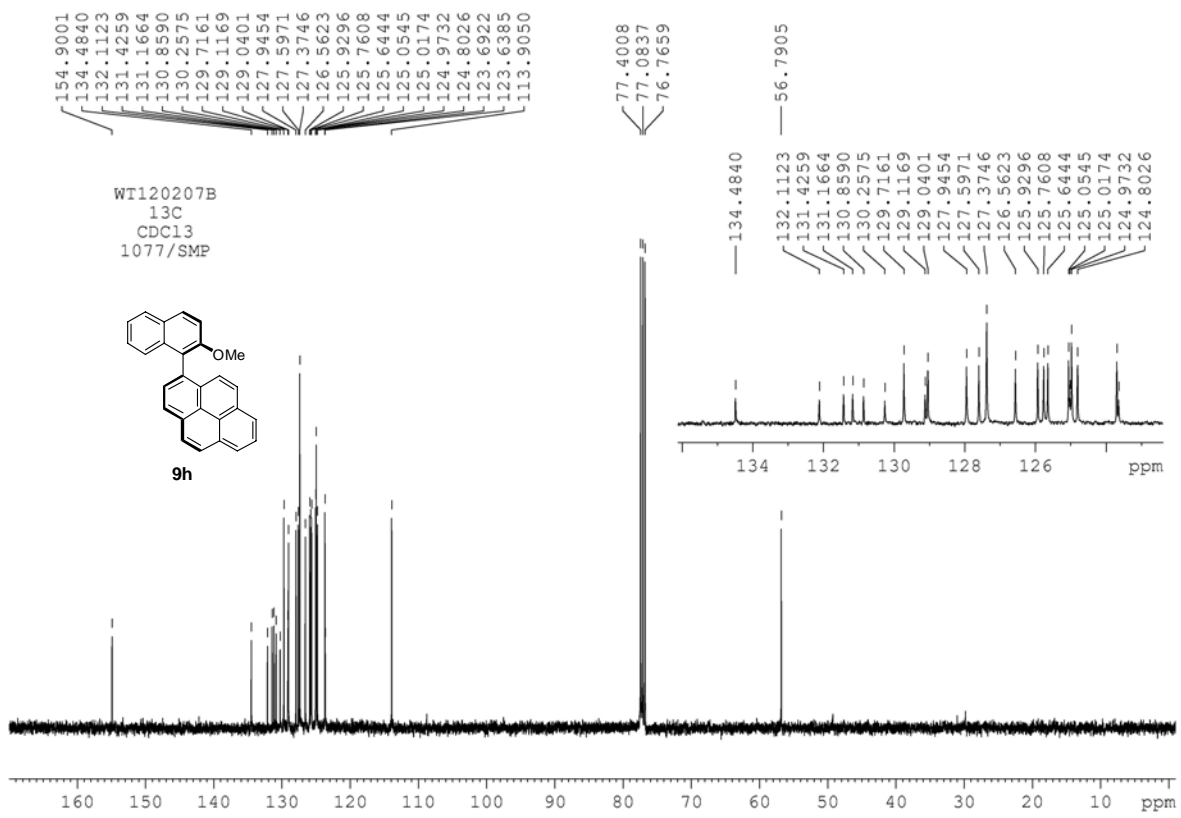


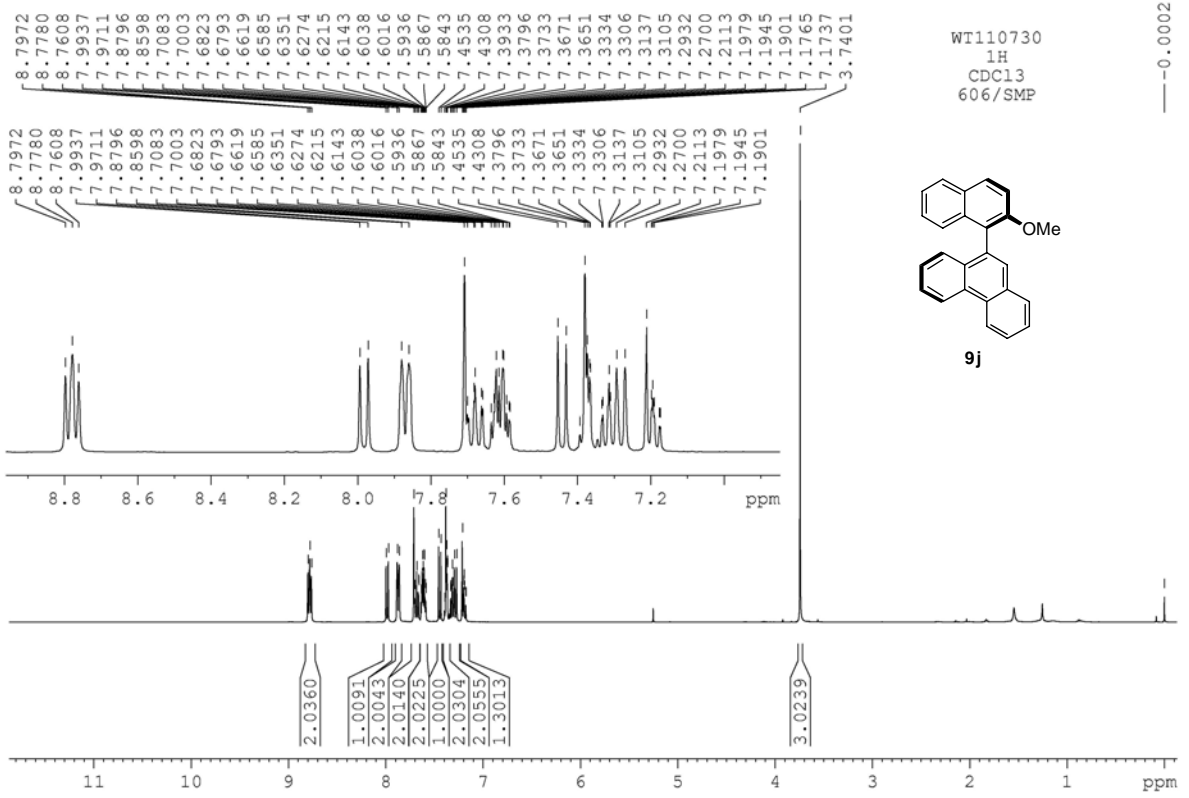
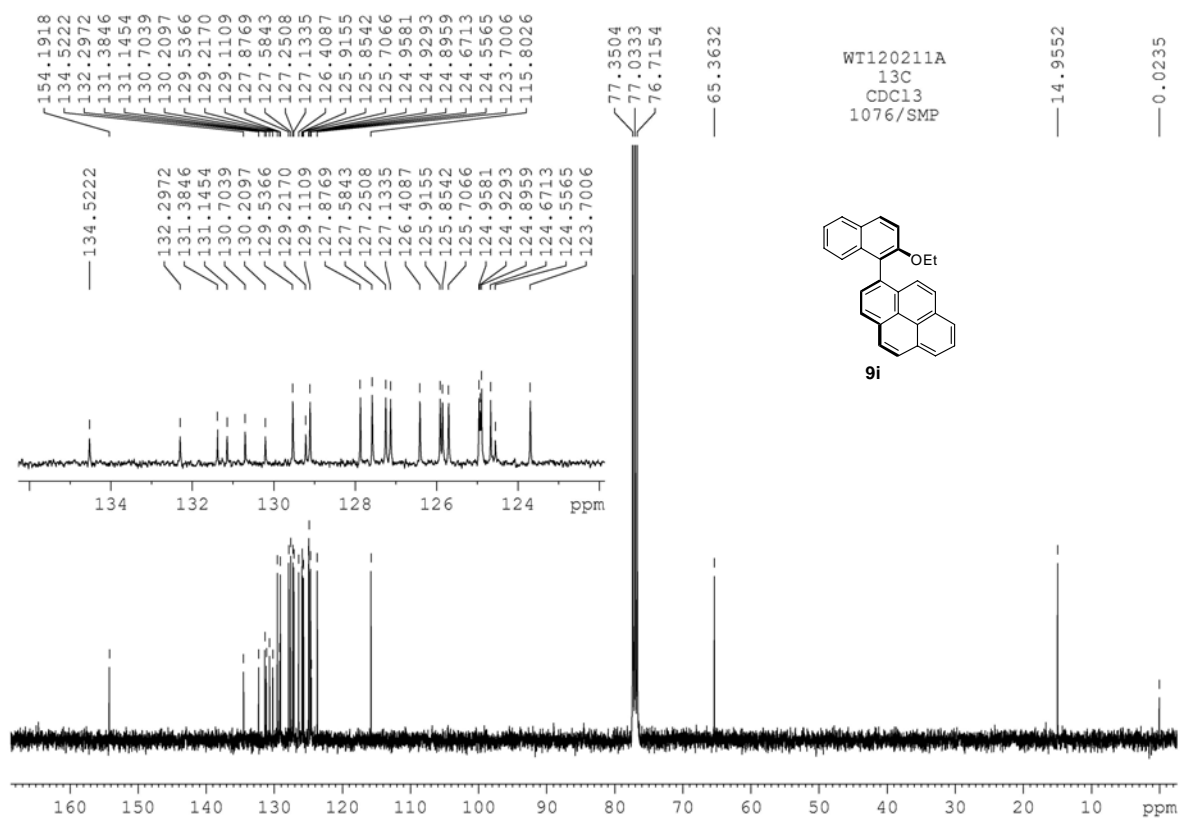


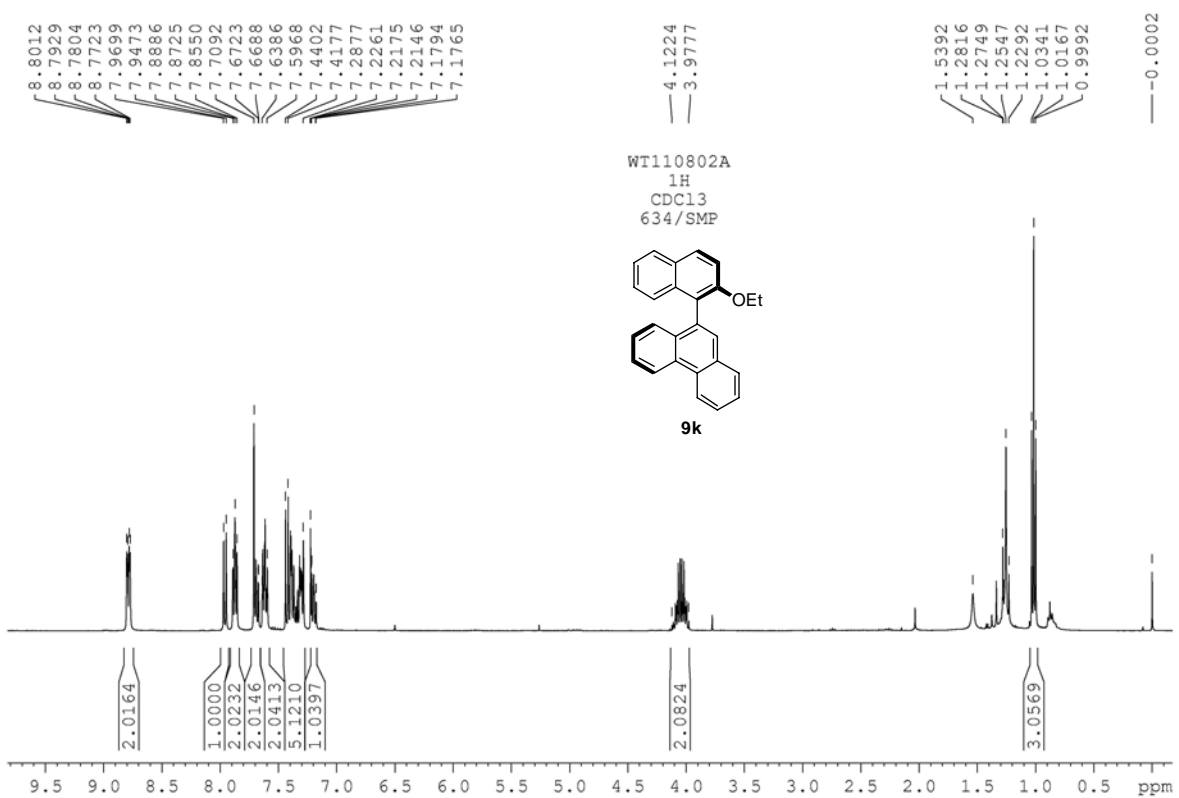
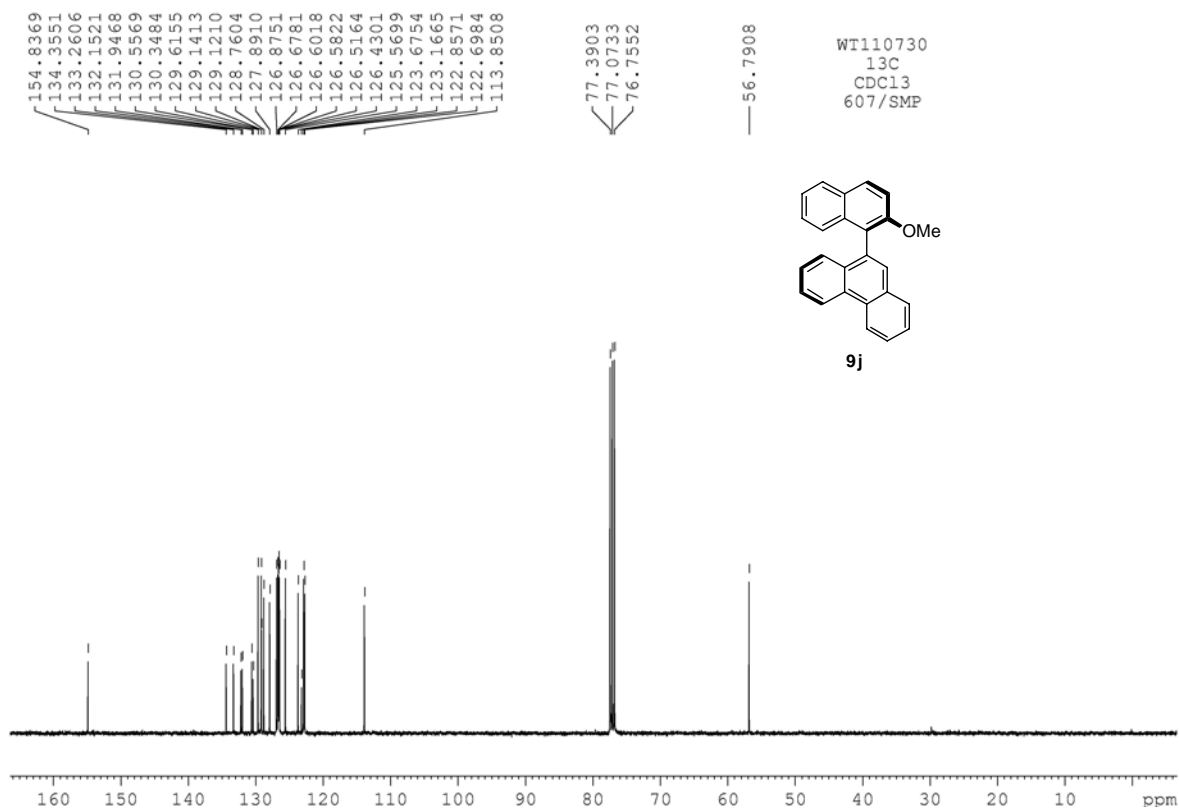


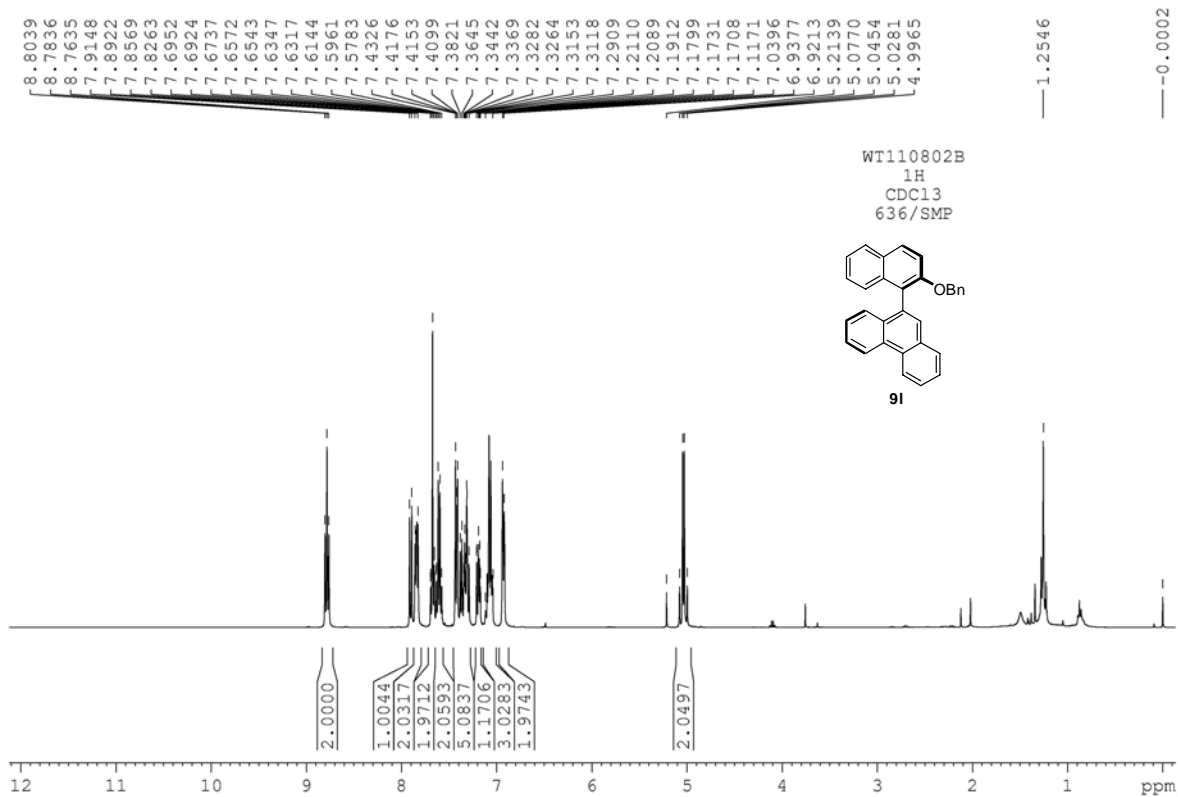
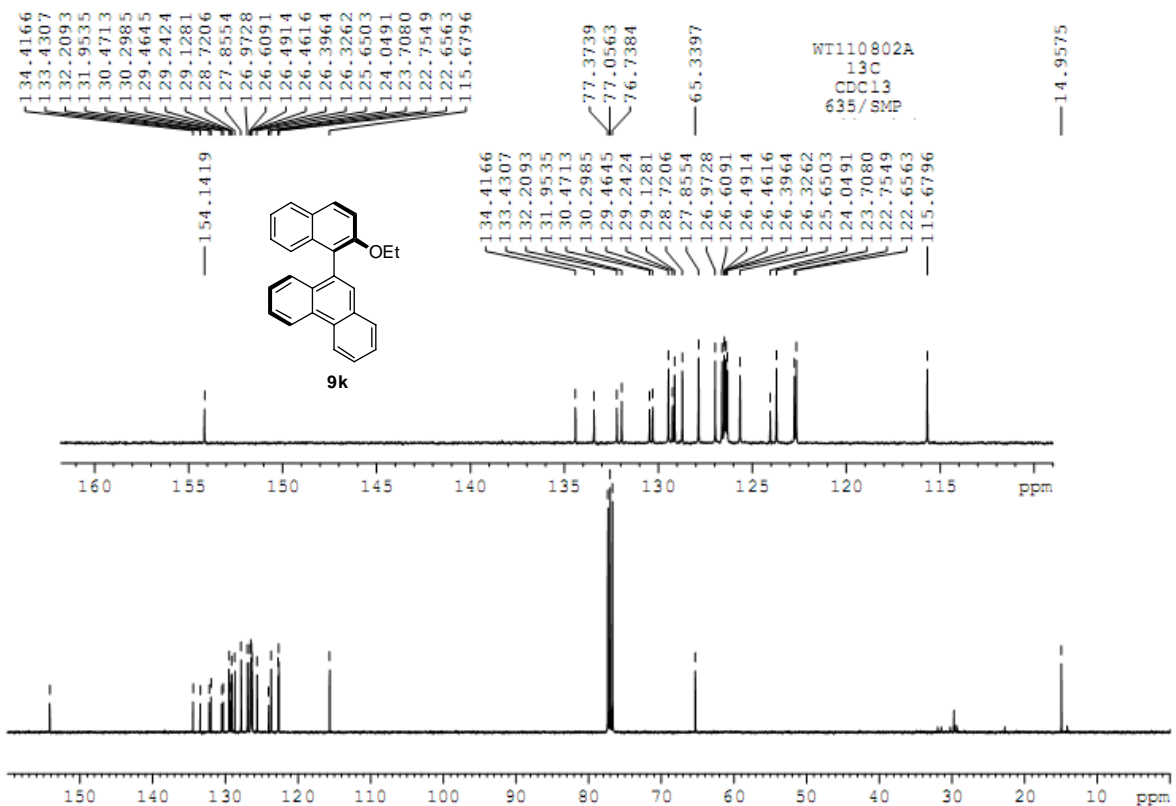


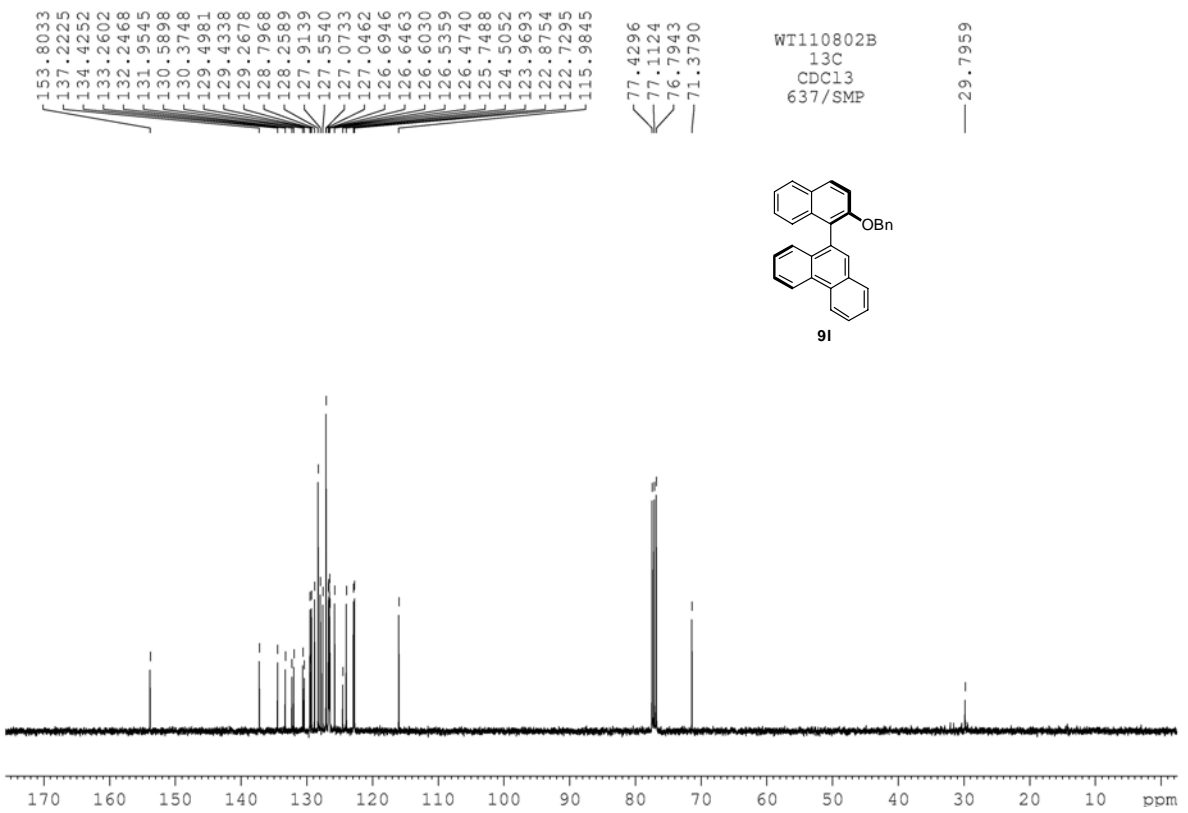




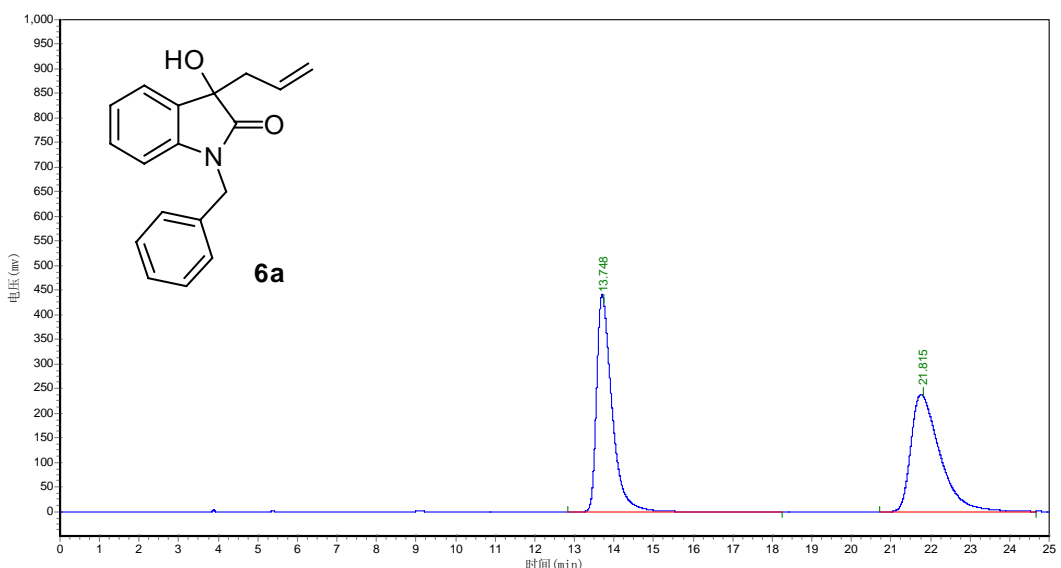




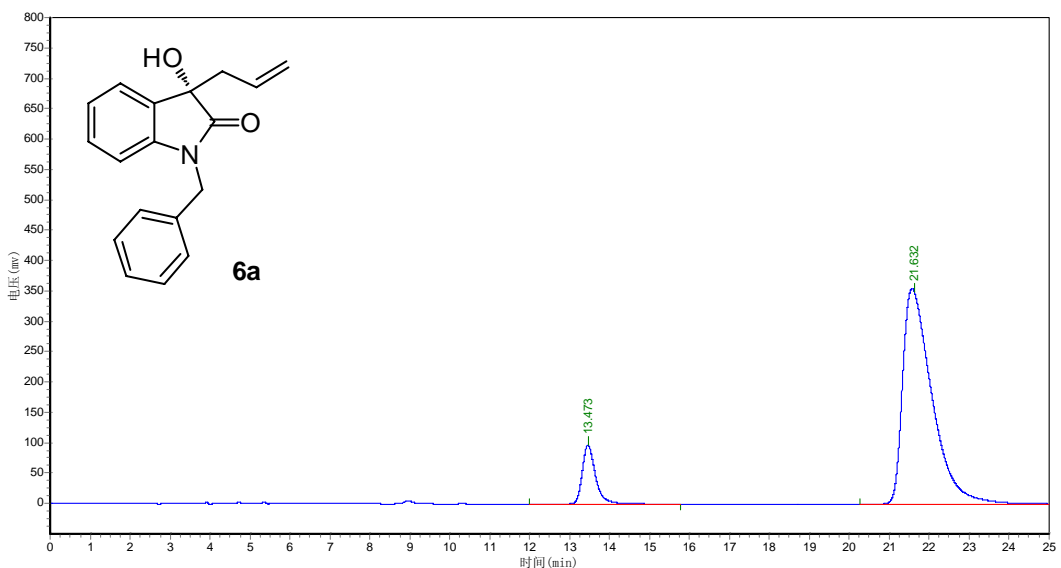




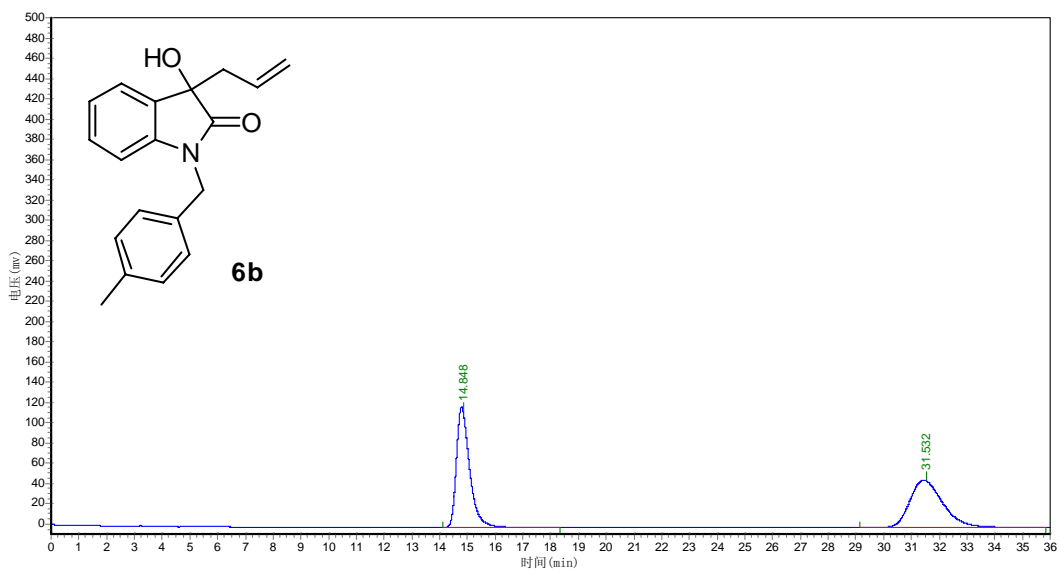
## HPLC Spectra of the Catalysis Products



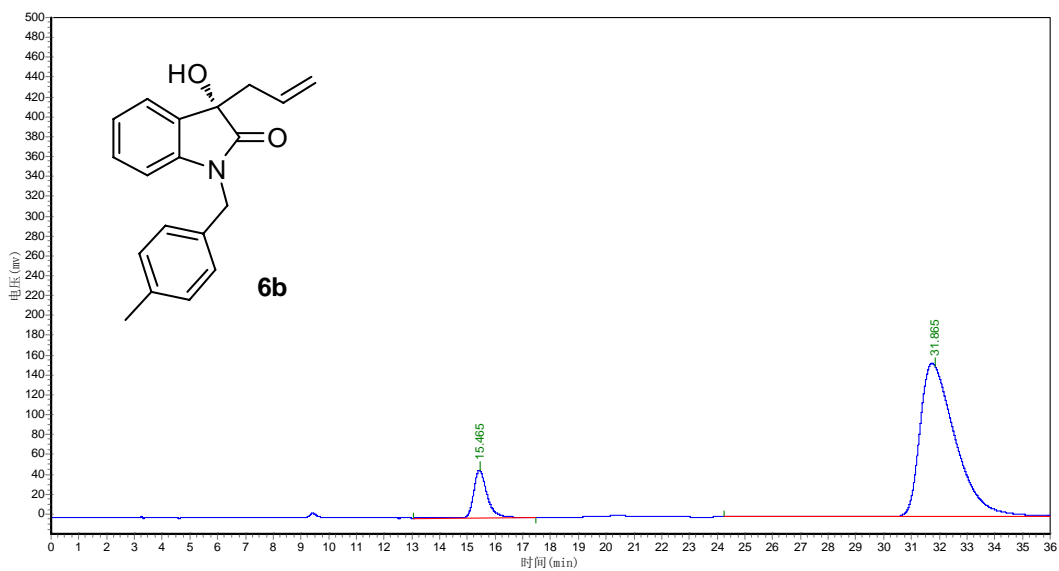
PeakNO.	Ret.Time	PeakHeight	PeakArea	Area%
1	13.748	435453.031	11848680.000	49.5216
2	21.815	237599.609	12077611.000	50.4784



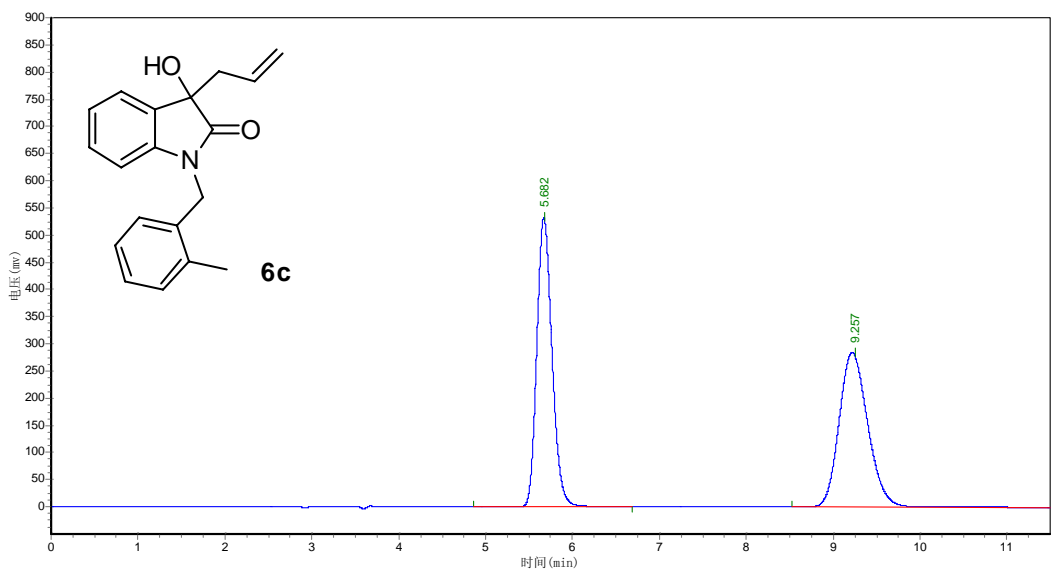
PeakNO.	Ret.Time	PeakHeight	PeakArea	Area%
1	13.473	93414.125	2220433.500	10.9524
2	21.632	353226.313	18053064.000	89.0476



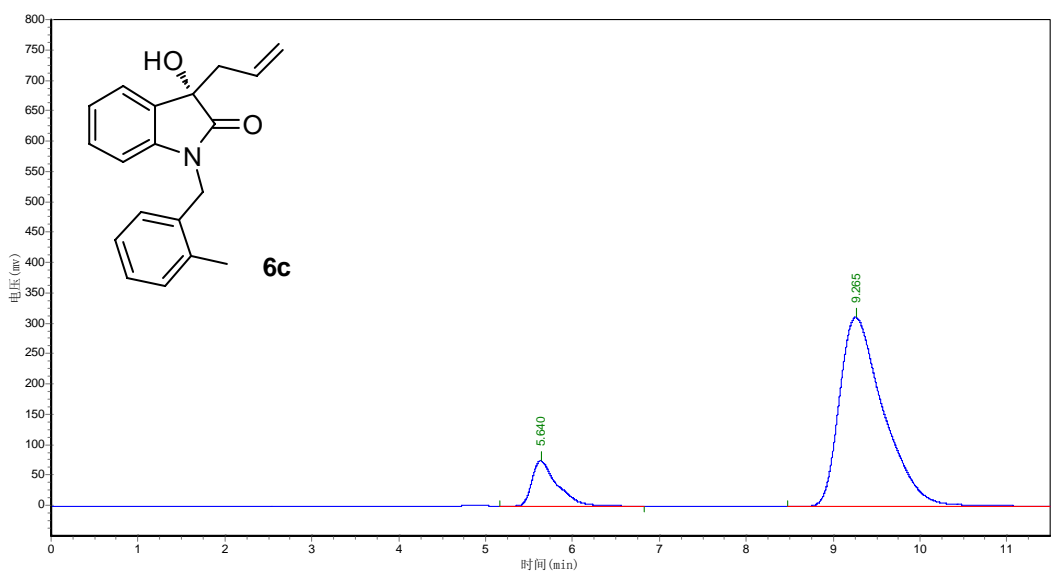
PeakNO.	Ret.Time	PeakHeight	PeakArea	Area%
1	14.848	117938.258	3939534.500	50.2363
2	31.532	46845.848	3902468.000	49.7637



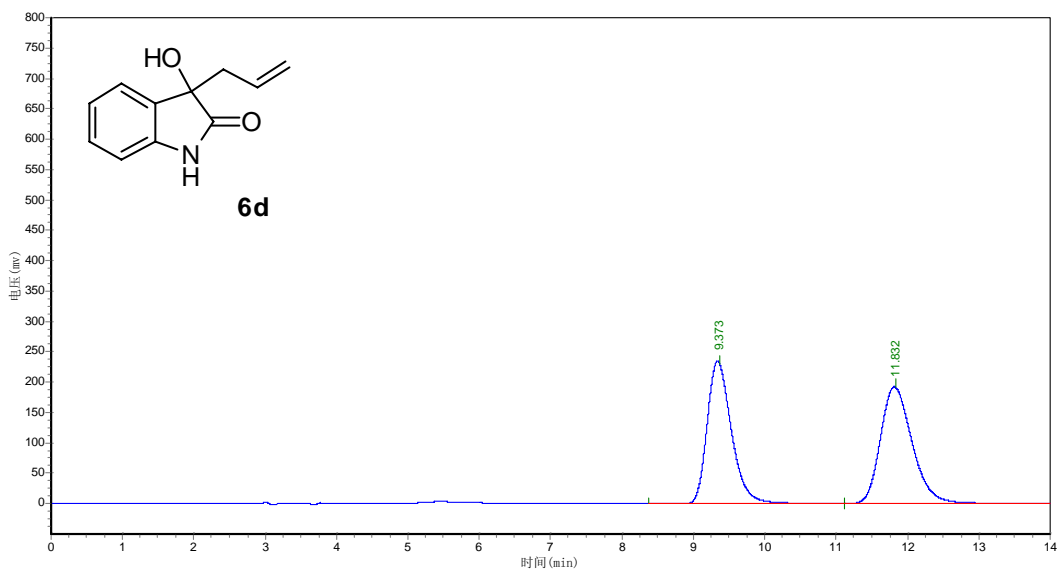
PeakNO.	Ret.Time	PeakHeight	PeakArea	Area%
1	15.465	46419.547	1567856.375	10.3593
2	31.865	152968.516	13566866.000	89.6407



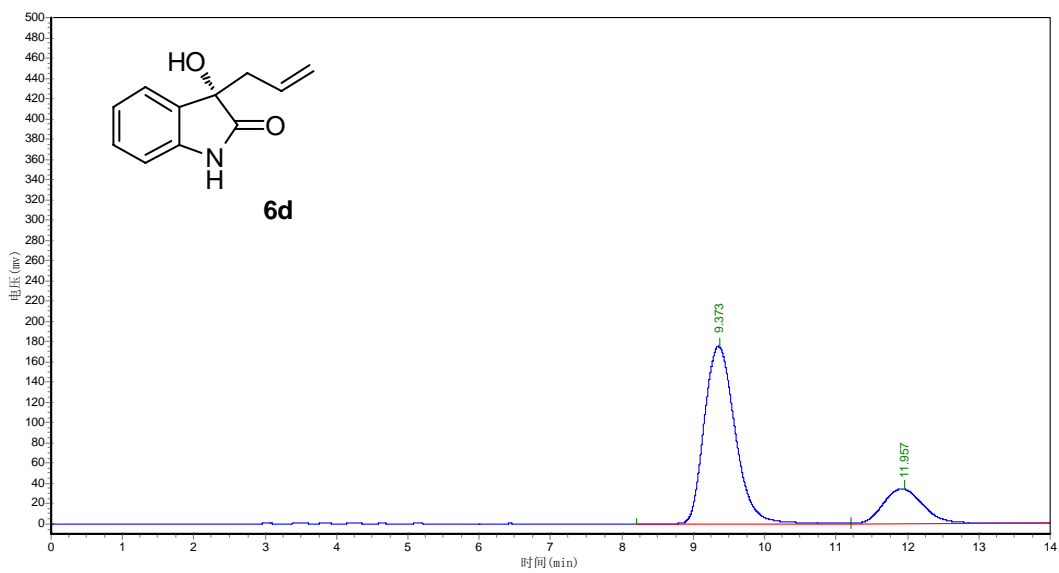
PeakNO.	Ret.Time	PeakHeight	PeakArea	Area%
1	5.682	457612.156	6502315.000	49.9723
2	9.257	279133.781	6509526.000	50.0277



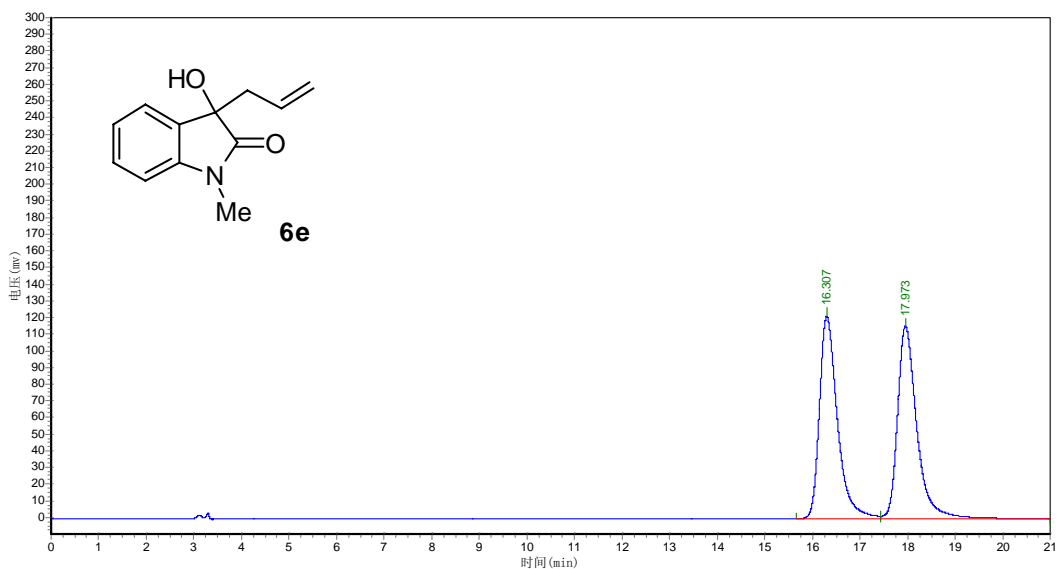
PeakNO.	Ret.Time	PeakHeight	PeakArea	Area%
1	5.640	74274.617	1486815.750	11.9485
2	9.265	311061.063	10956707.000	88.0515



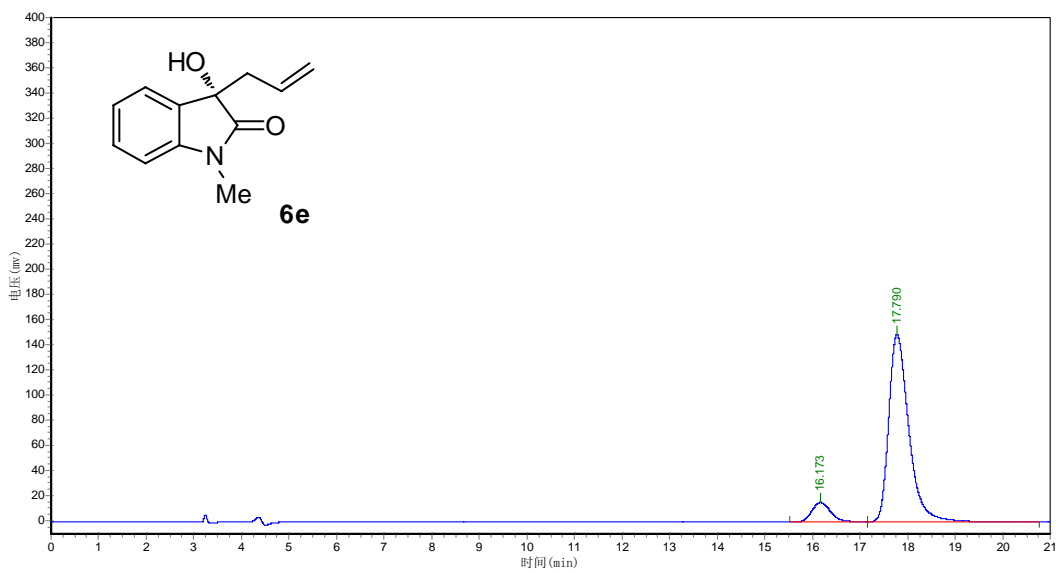
PeakNO.	Ret.Time	PeakHeight	PeakArea	Area%
1	9.373	232818.719	5581357.500	48.1657
2	11.832	191994.297	6006461.000	51.8343



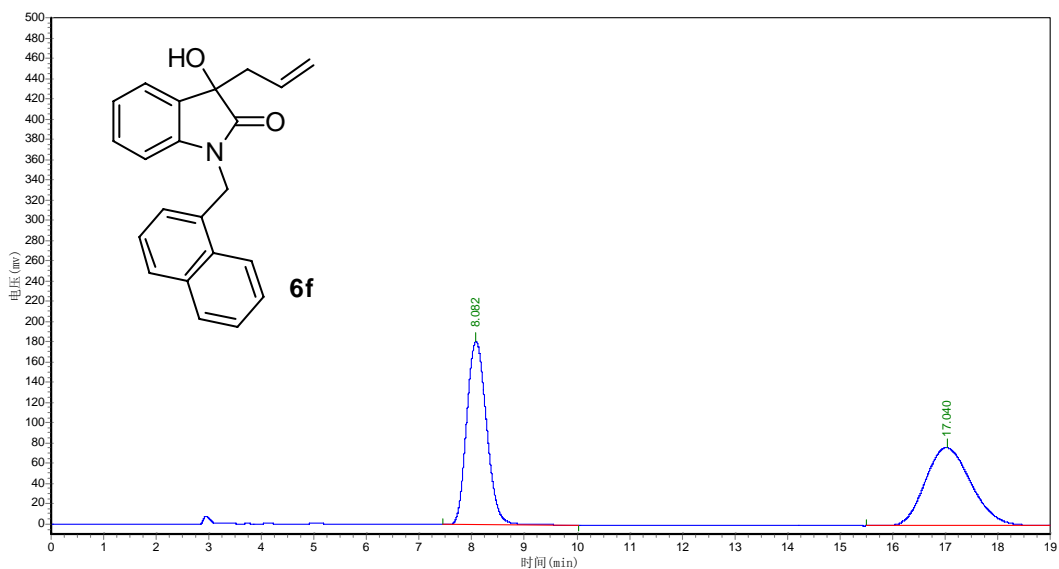
PeakNO.	Ret.Time	PeakHeight	PeakArea	Area%
1	9.373	174935.938	5258504.500	79.7376
2	11.957	34188.531	1336254.125	20.2624



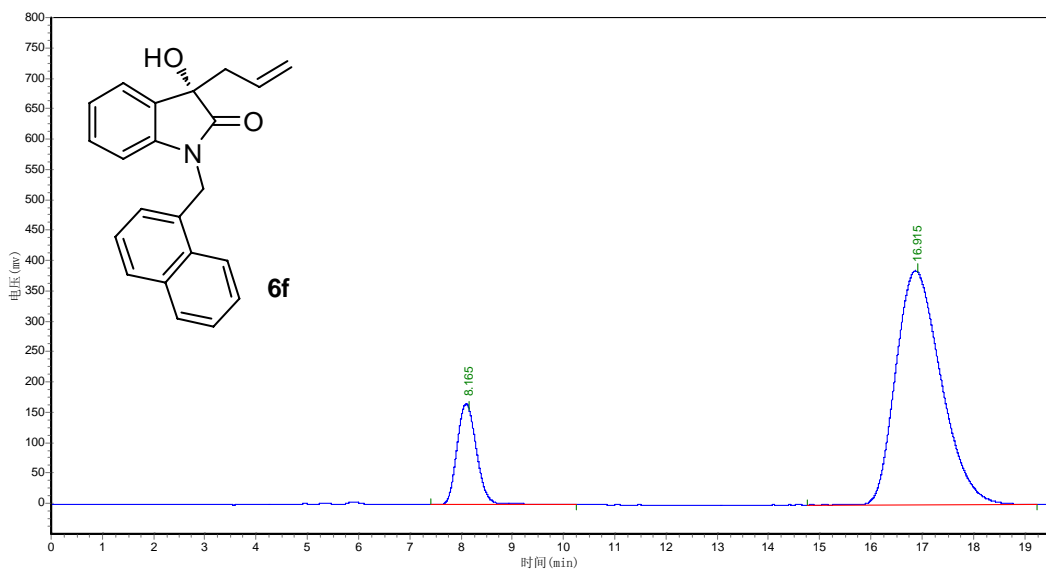
PeakNO.	Ret.Time	PeakHeight	PeakArea	Area%
1	16.307	121310.266	3188576.750	49.5872
2	19.973	115365.078	3241659.750	50.4128



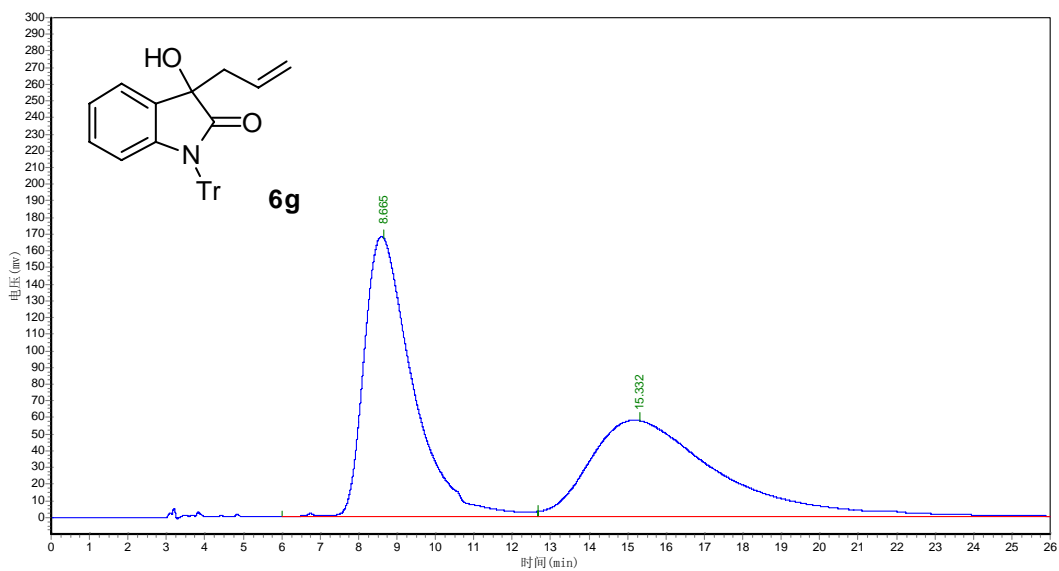
PeakNO.	Ret.Time	PeakHeight	PeakArea	Area%
1	16.173	15706.481	445244.844	9.2049
2	17.790	148909.203	4391781.500	90.7951



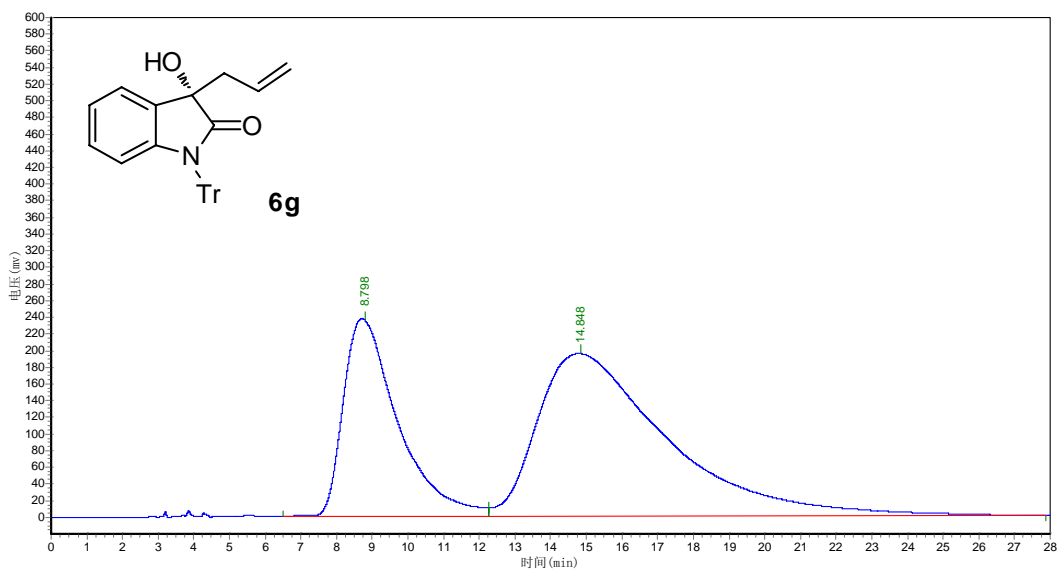
PeakNO.	Ret.Time	PeakHeight	PeakArea	Area%
1	8.082	179941.906	4776146.500	50.5080
2	17.040	77113.508	4680072.500	49.4920



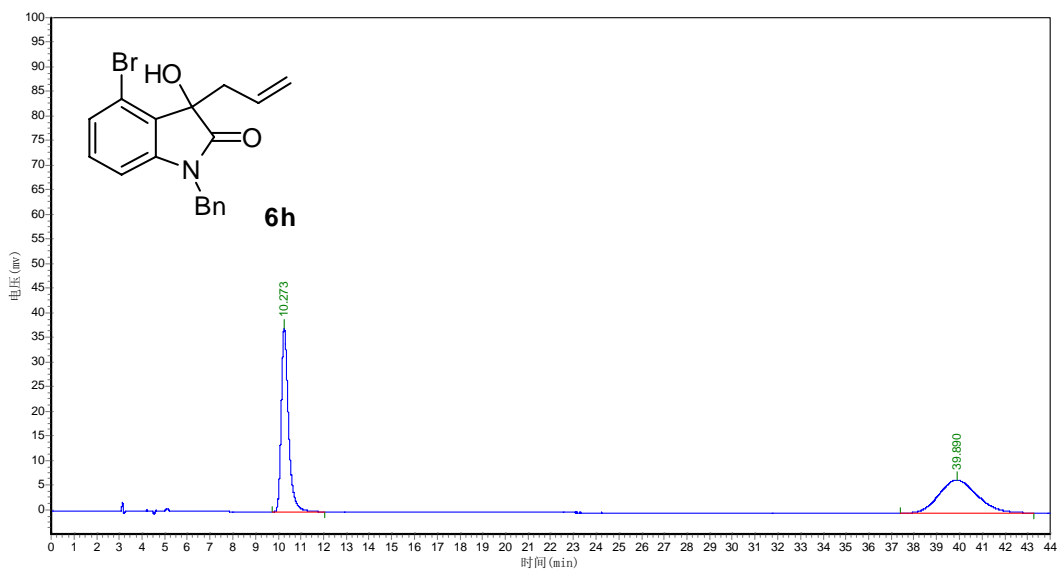
PeakNO.	Ret.Time	PeakHeight	PeakArea	Area%
1	8.165	162826.859	4420632.000	15.7954
2	16.915	384297.125	23566120.000	84.2046



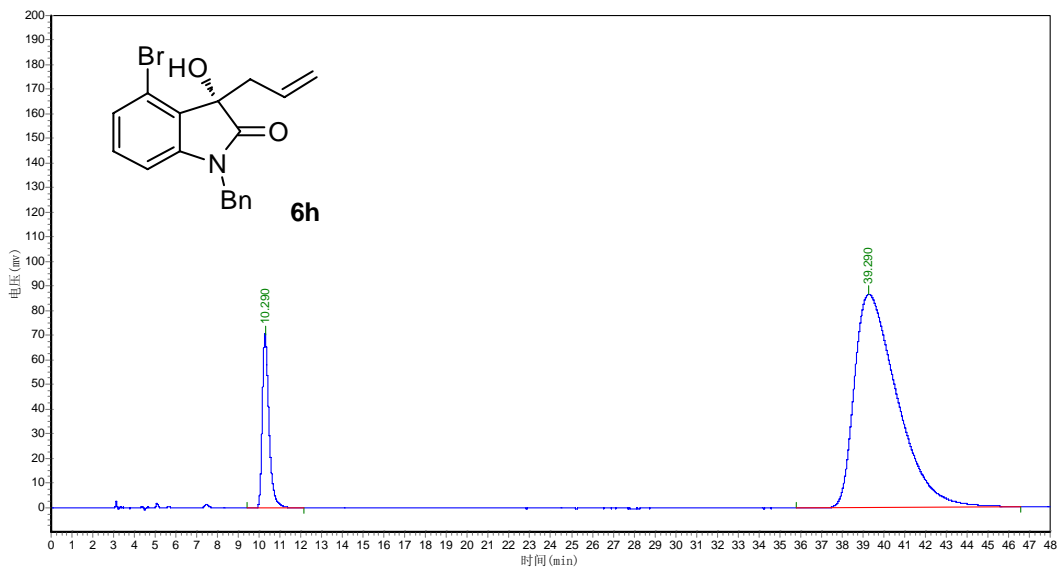
PeakNO.	Ret.Time	PeakHeight	PeakArea	Area%
1	8.665	161888.703	14796688.000	52.7314
2	15.332	57601.969	13263776.000	47.2686



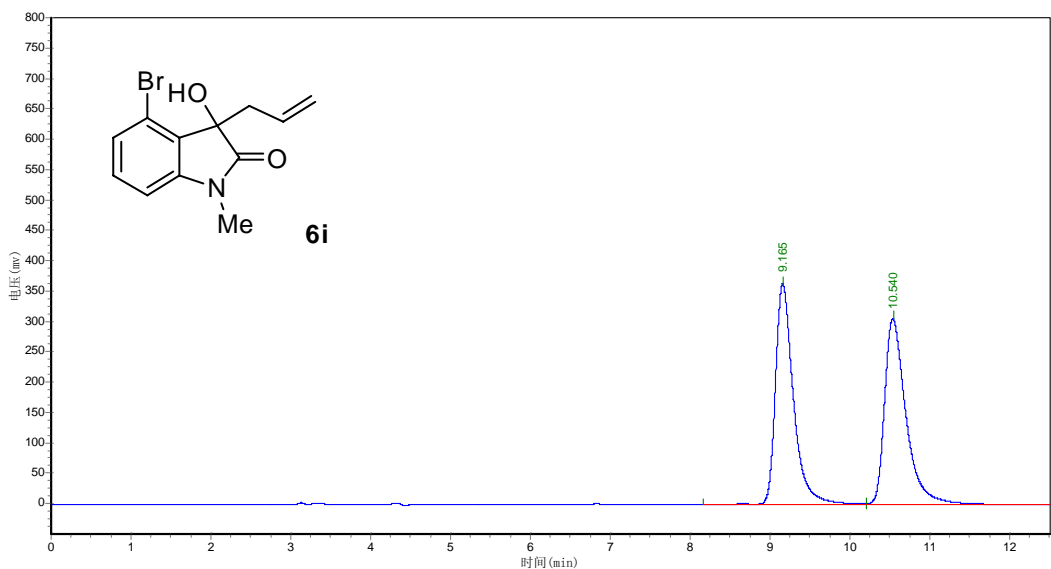
PeakNO.	Ret.Time	PeakHeight	PeakArea	Area%
1	8.798	237231.781	25359674.000	33.9400
2	14.848	195366.219	49359464.000	66.0600



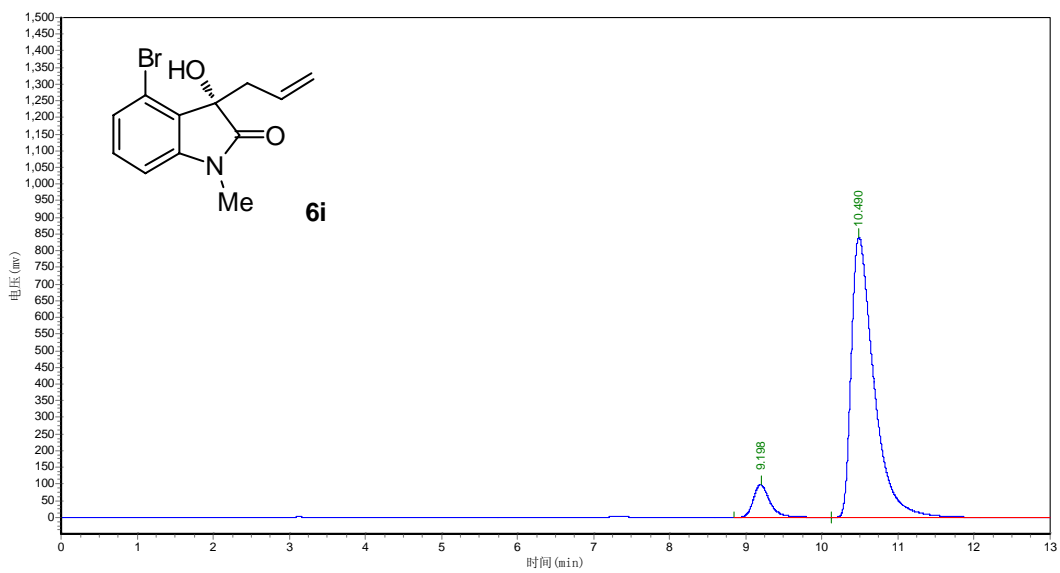
PeakNO.	Ret.Time	PeakHeight	PeakArea	Area%
1	10.273	37374.000	836698.500	51.0917
2	39.890	6742.313	800942.875	48.9083



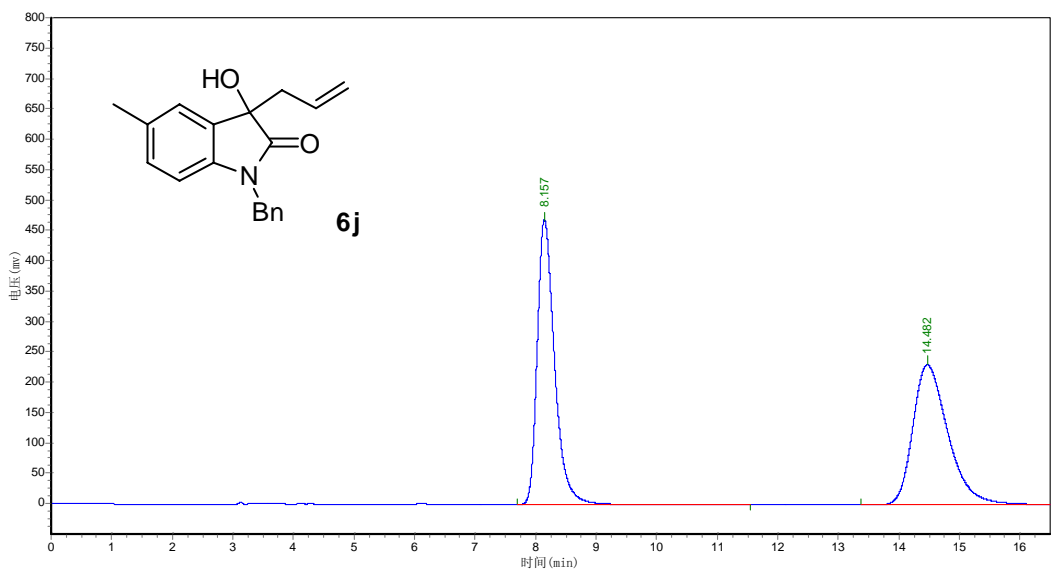
PeakNO.	Ret.Time	PeakHeight	PeakArea	Area%
1	10.290	70323.711	1586164.000	11.3357
2	39.290	86800.375	12406421.000	88.6643



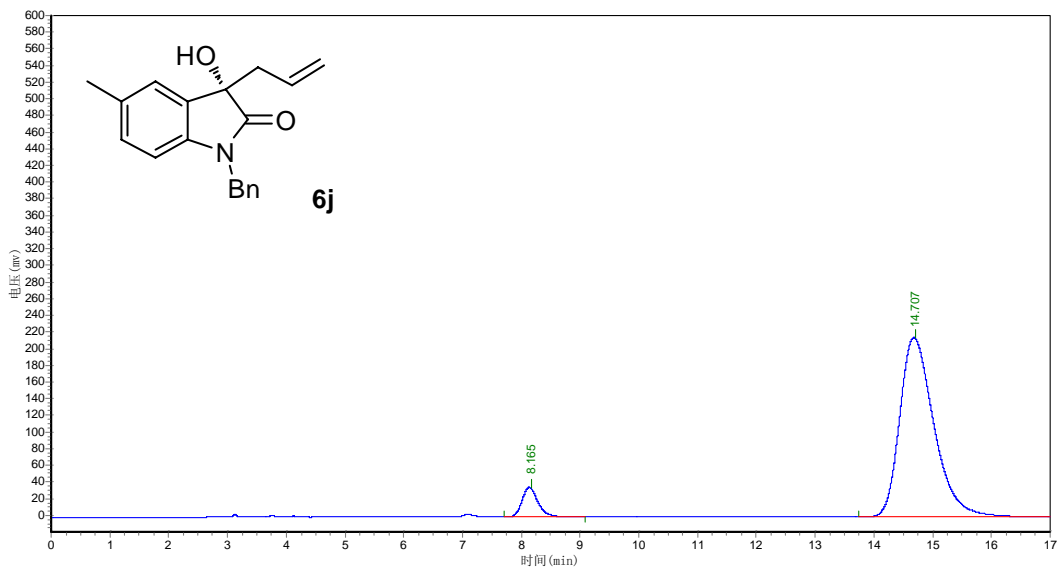
PeakNO.	Ret.Time	PeakHeight	PeakArea	Area%
1	9.165	358324.188	5674352.500	49.9648
2	10.540	302539.594	5682345.000	50.0352



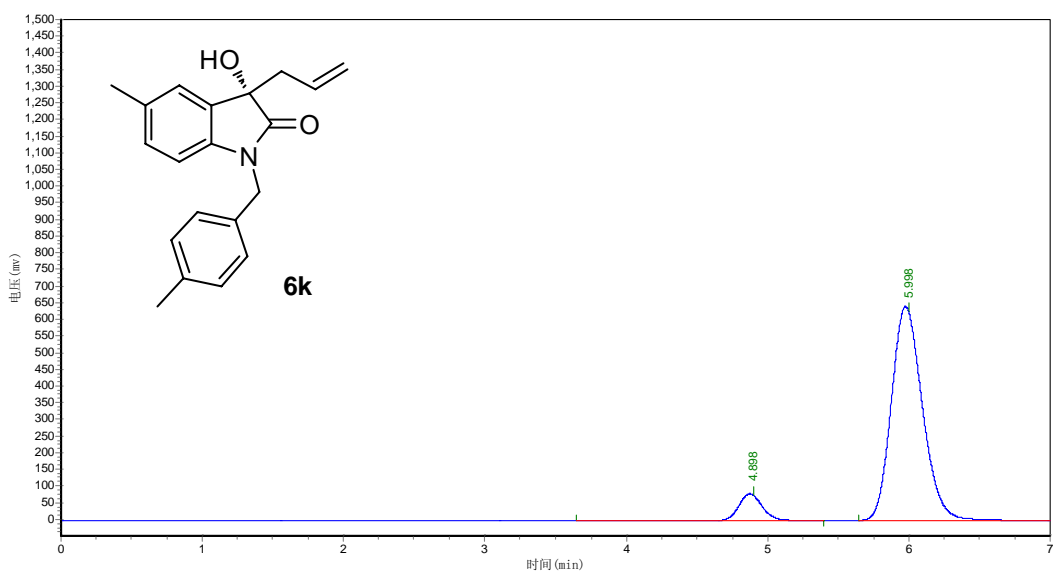
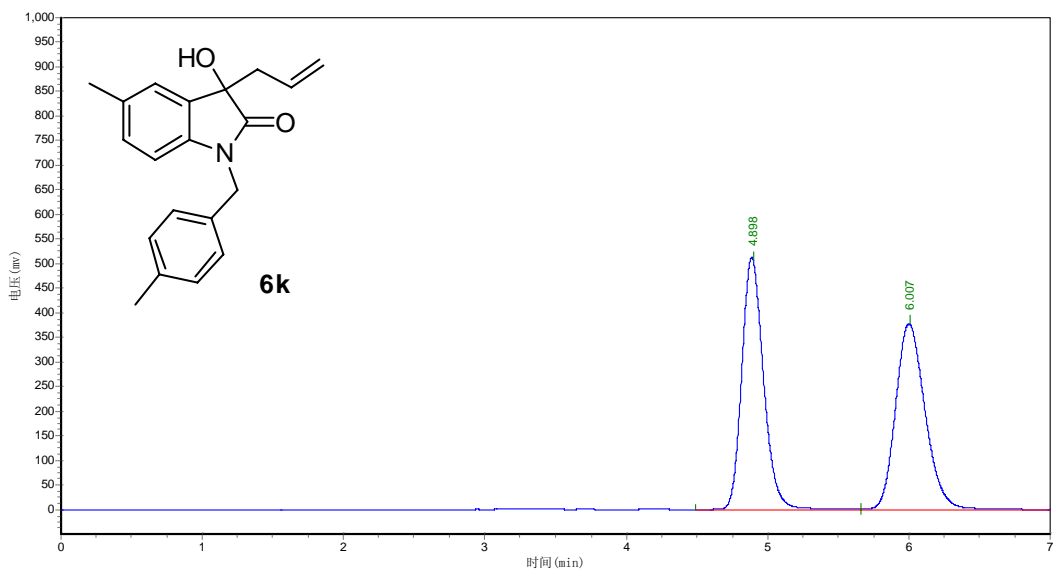
PeakNO.	Ret.Time	PeakHeight	PeakArea	Area%
1	9.198	98180.859	1501473.000	7.9798
2	10.490	841130.188	17314460.000	92.0202

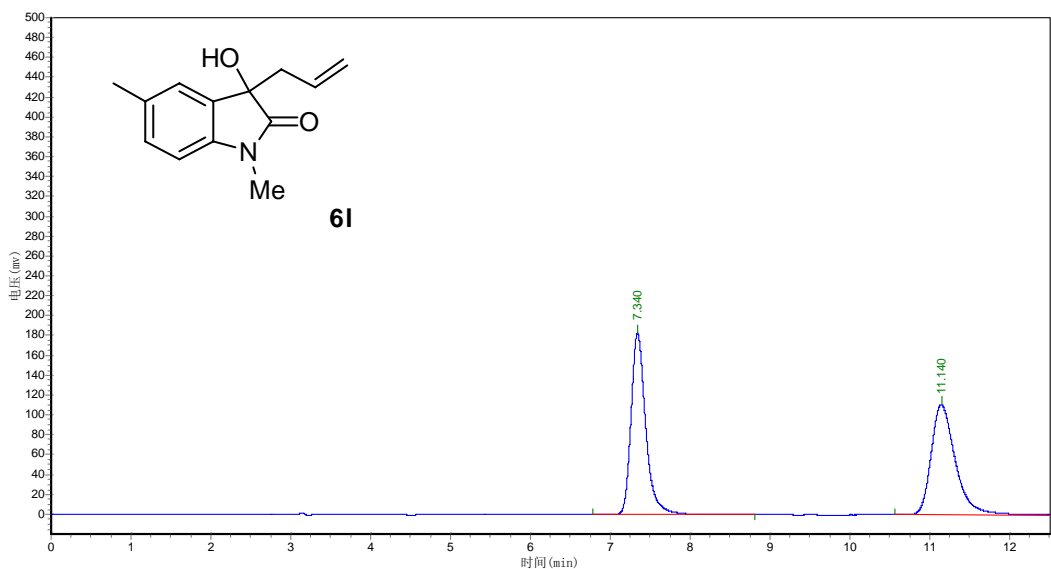


PeakNO.	Ret.Time	PeakHeight	PeakArea	Area%
1	8.157	435905.781	9323303.000	50.0332
2	14.482	226776.141	9309918.000	49.9668

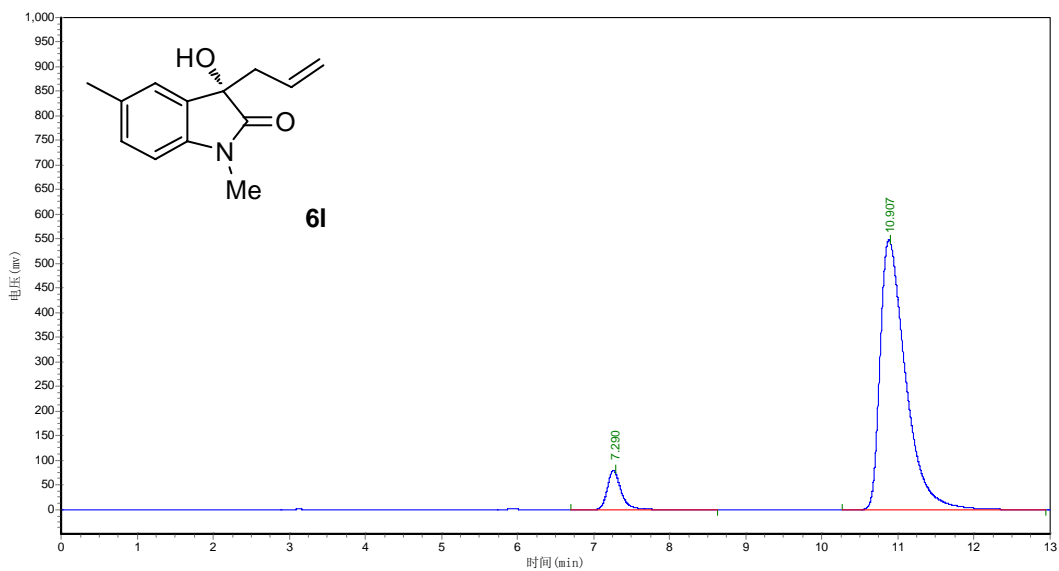


PeakNO.	Ret.Time	PeakHeight	PeakArea	Area%
1	8.165	35064.000	667083.375	7.0799
2	14.707	215273.672	8755143.000	92.9201

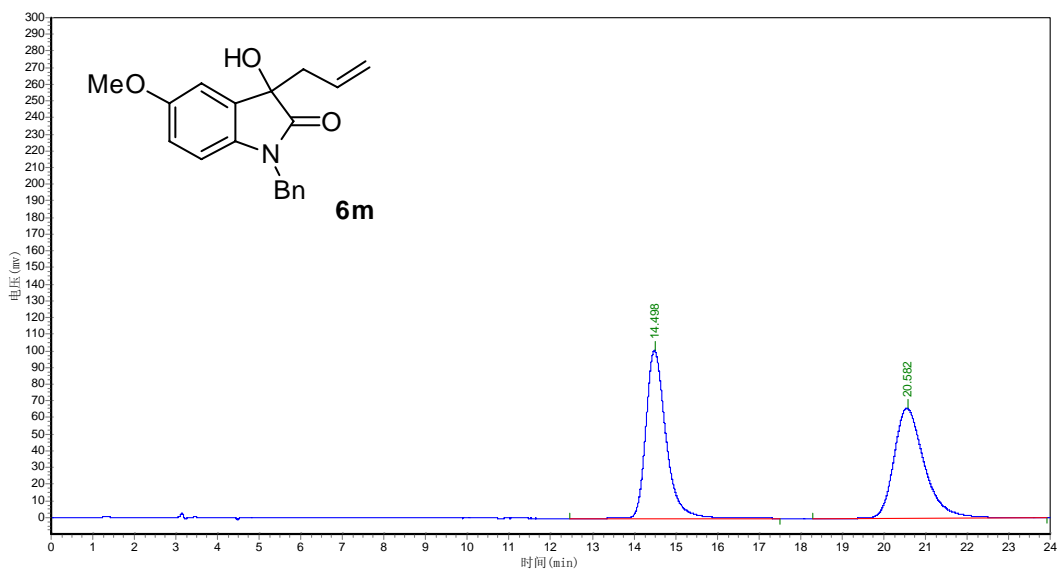




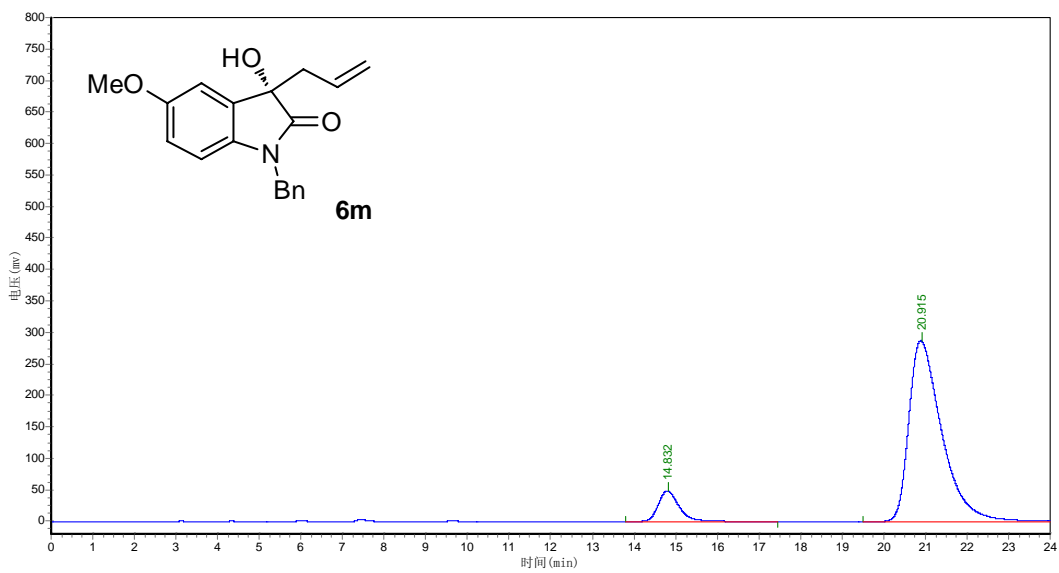
PeakNO.	Ret.Time	PeakHeight	PeakArea	Area%
1	7.340	182888.375	2345038.250	50.0488
2	11.140	110971.047	2340468.250	49.9512



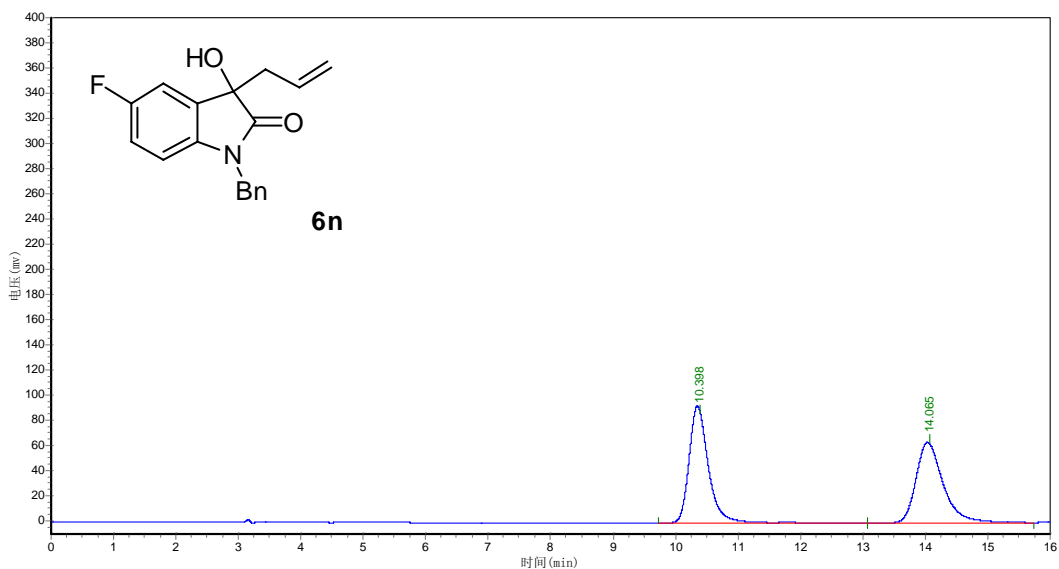
PeakNO.	Ret.Time	PeakHeight	PeakArea	Area%
1	7.290	77879.094	1011647.563	7.3505
2	10.907	544764.563	12751247.000	92.6495



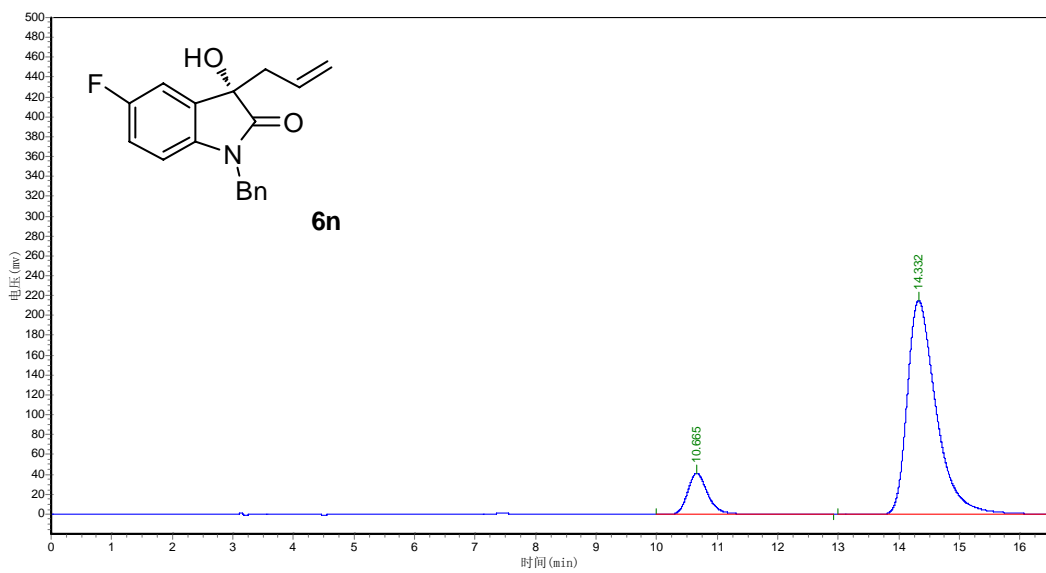
PeakNO.	Ret.Time	PeakHeight	PeakArea	Area%
1	14.498	100314.609	3345486.500	50.0534
2	20.582	65947.039	3338350.000	49.9466



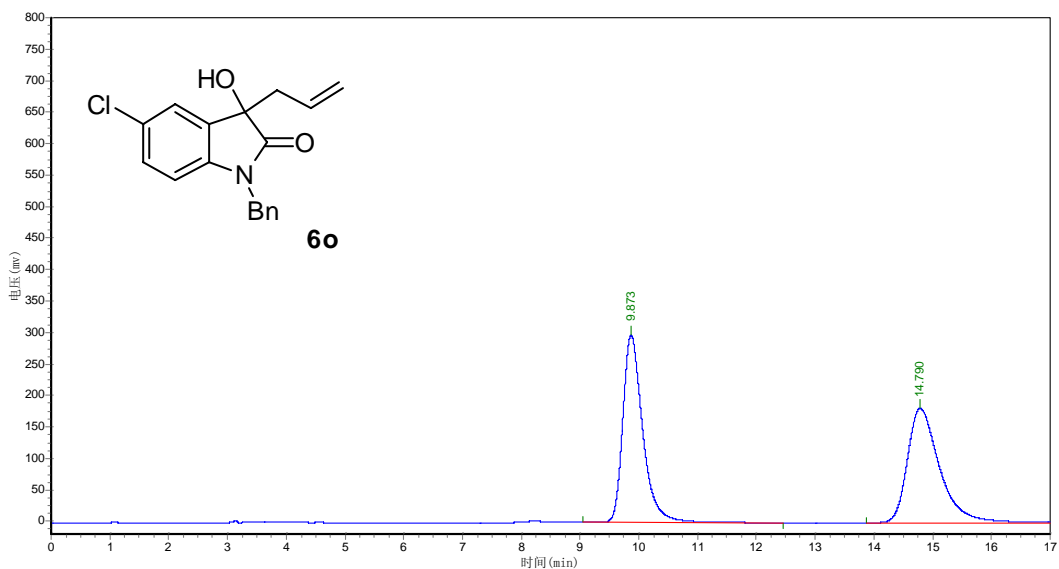
PeakNO.	Ret.Time	PeakHeight	PeakArea	Area%
1	14.832	48379.602	1684058.625	9.6608
2	20.915	286879.000	15747899.000	90.3392



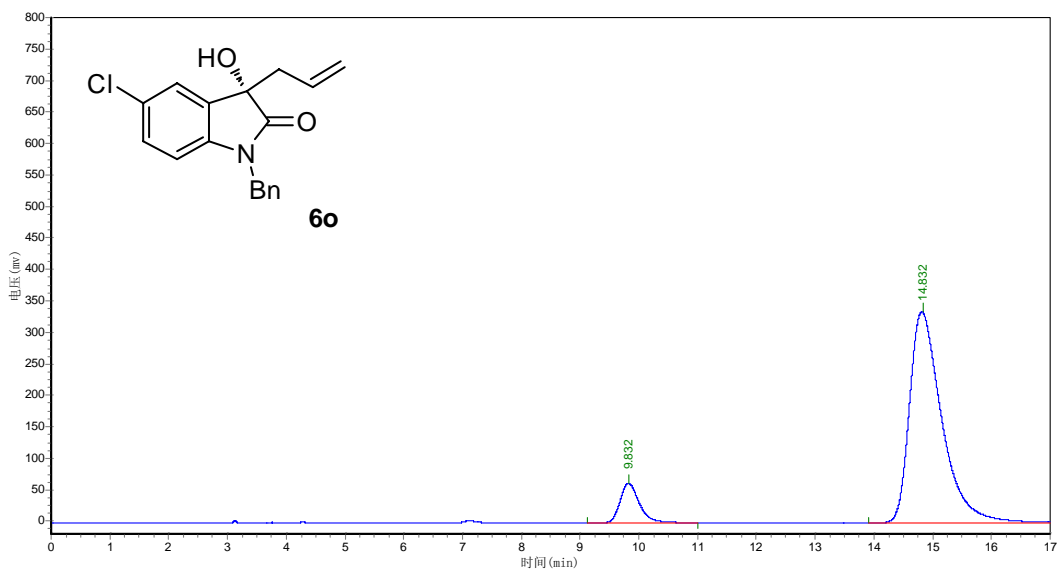
PeakNO.	Ret.Time	PeakHeight	PeakArea	Area%
1	10.398	91169.000	1993330.375	50.7155
2	14.065	63442.000	1937088.750	49.2845



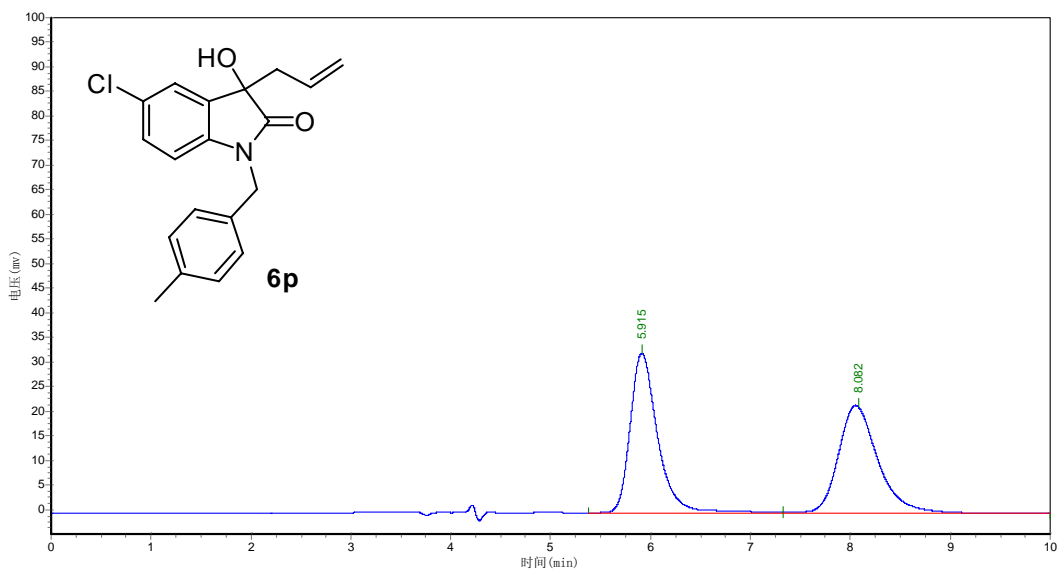
PeakNO.	Ret.Time	PeakHeight	PeakArea	Area%
1	10.665	41068.086	970142.500	11.8760
2	14.332	214600.750	7198789.000	88.1240



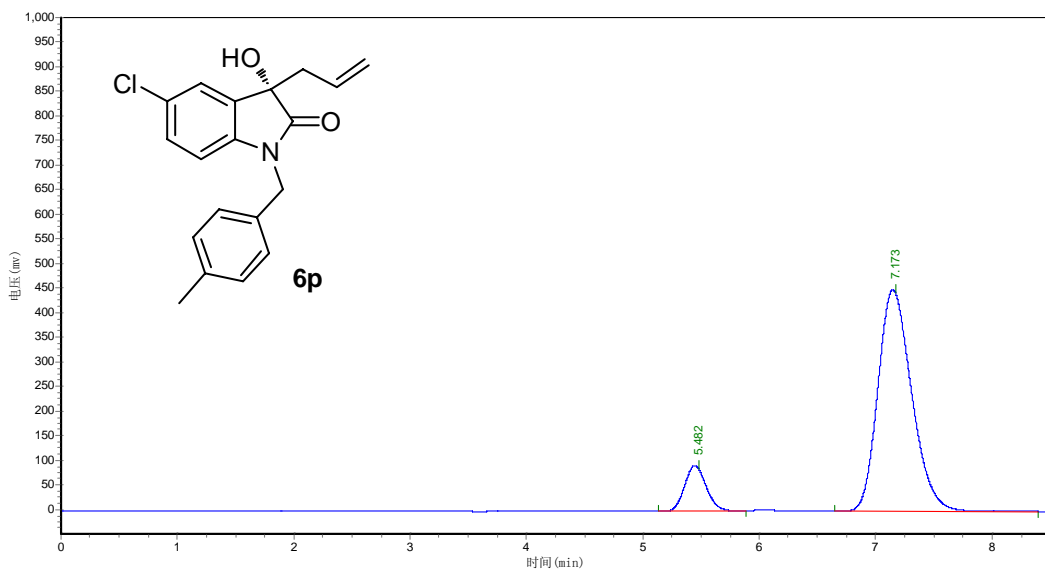
PeakNO.	Ret.Time	PeakHeight	PeakArea	Area%
1	9.873	294339.719	6985419.500	50.1838
2	14.790	180632.500	6934243.500	49.8162



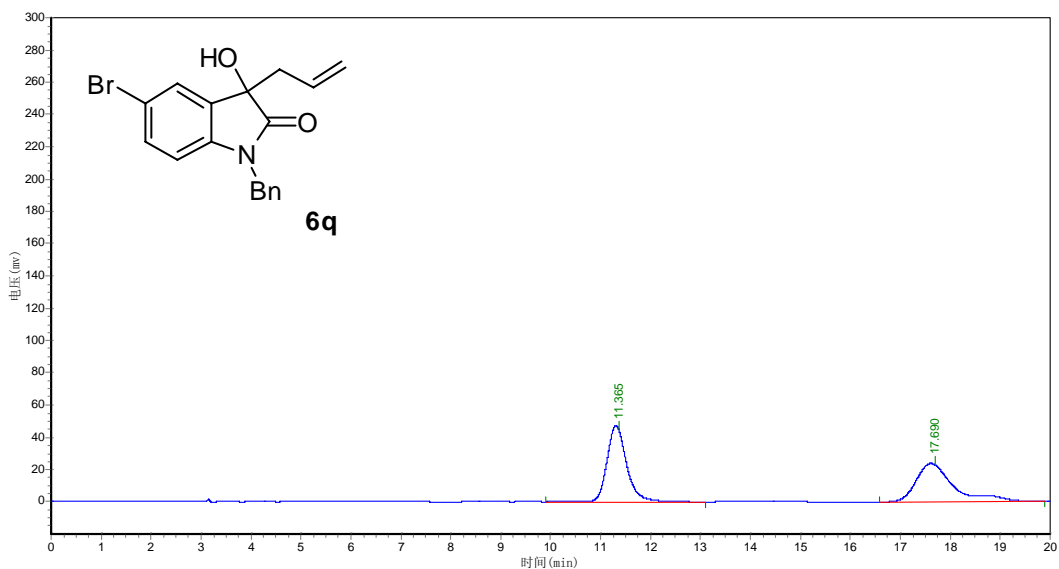
PeakNO.	Ret.Time	PeakHeight	PeakArea	Area%
1	9.832	62636.777	1437535.375	10.0646
2	14.832	335039.000	12845596.000	89.9354



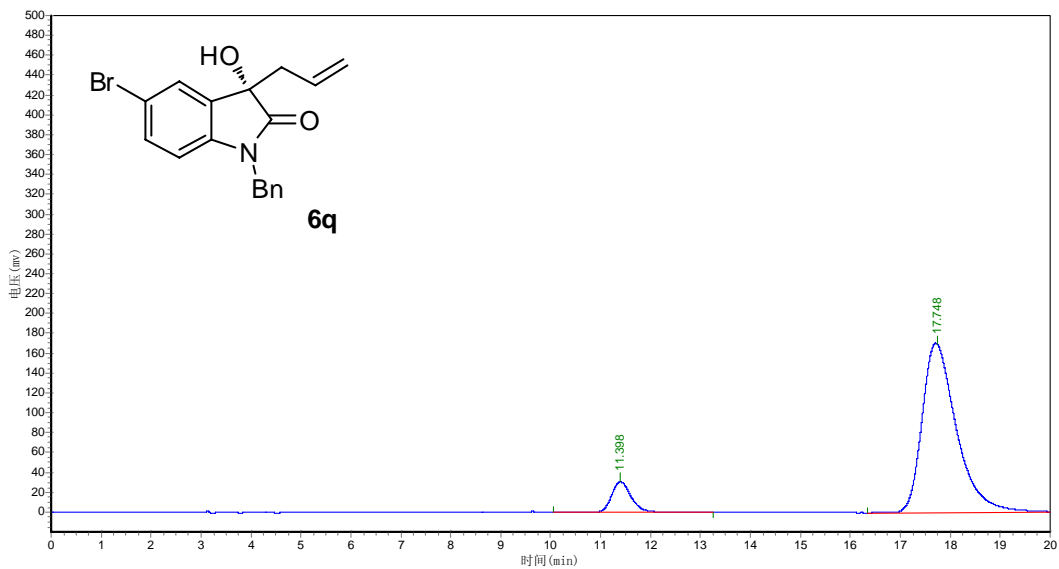
PeakNO.	Ret.Time	PeakHeight	PeakArea	Area%
1	5.915	32010.783	631603.625	50.8768
2	8.082	21863.918	609834.625	49.1232



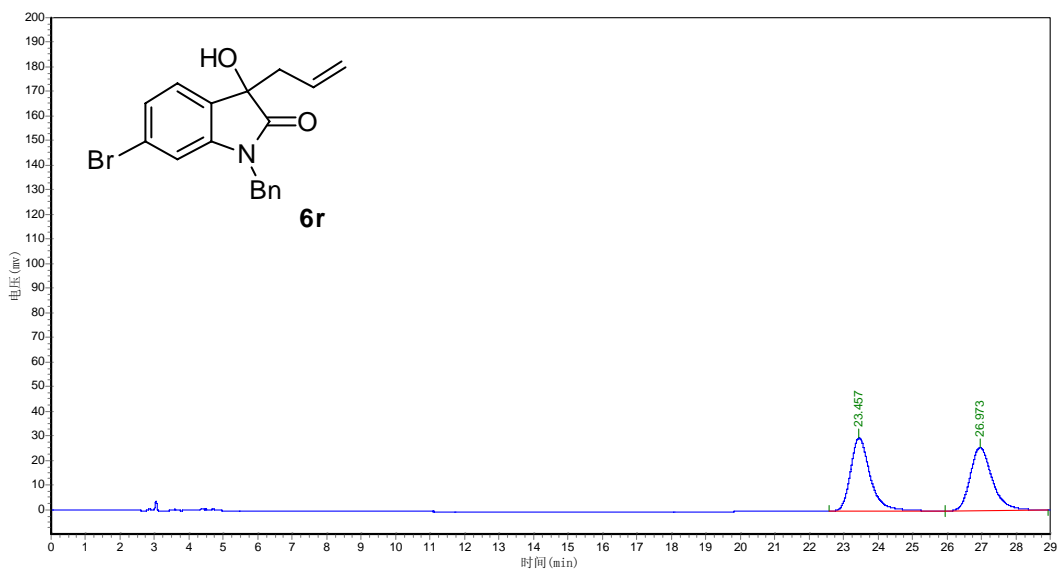
PeakNO.	Ret.Time	PeakHeight	PeakArea	Area%
1	5.482	90607.766	1193568.000	11.6055
2	7.173	447060.594	9090935.000	88.3945



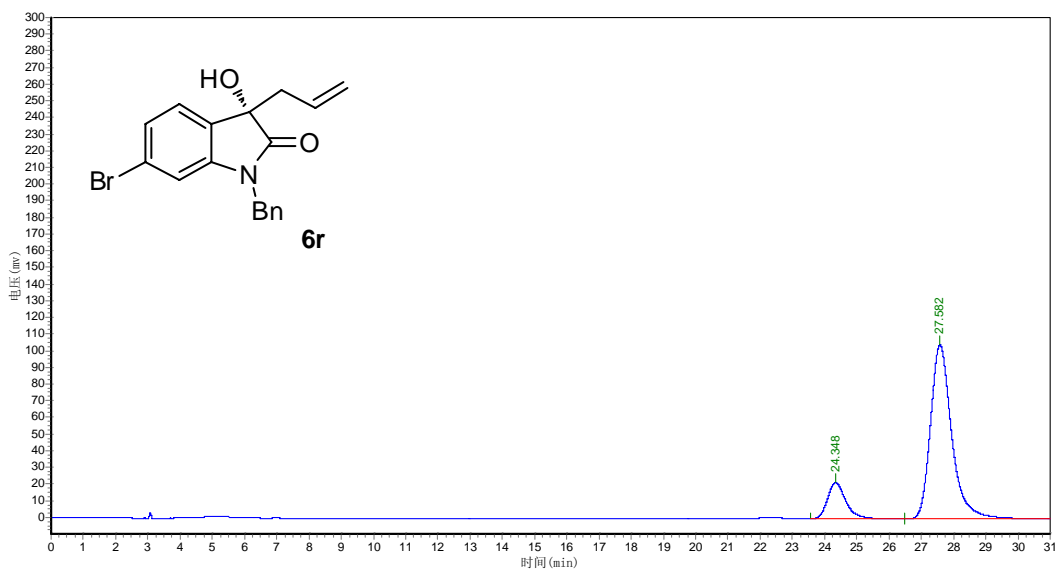
PeakNO.	Ret.Time	PeakHeight	PeakArea	Area%
1	11.365	46536.086	1286158.000	50.9487
2	17.690	23590.000	1238258.125	49.0513



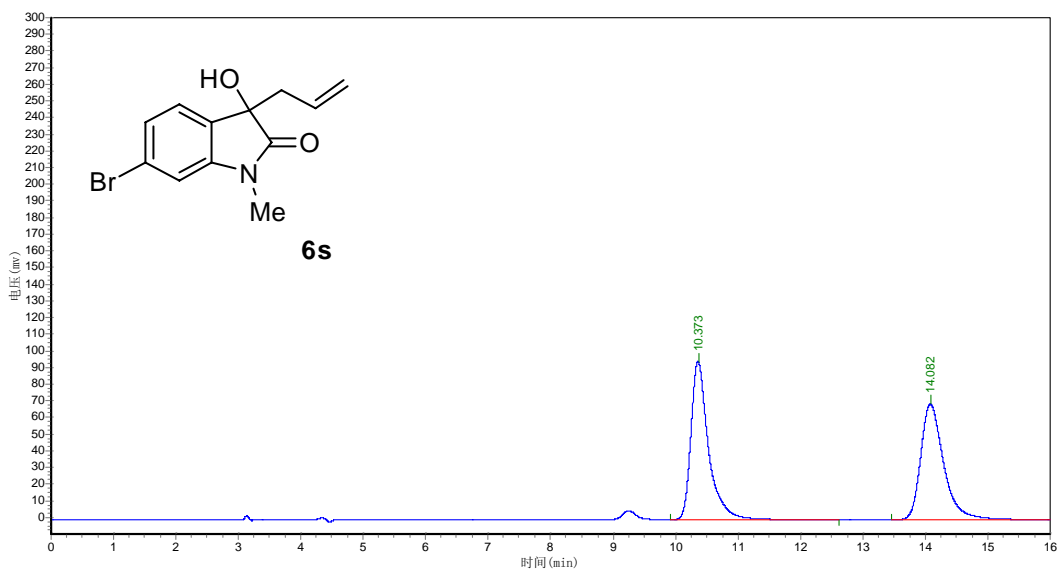
PeakNO.	Ret.Time	PeakHeight	PeakArea	Area%
1	11.398	30748.344	868963.375	9.5887
2	17.748	170258.859	8193376.000	90.4113



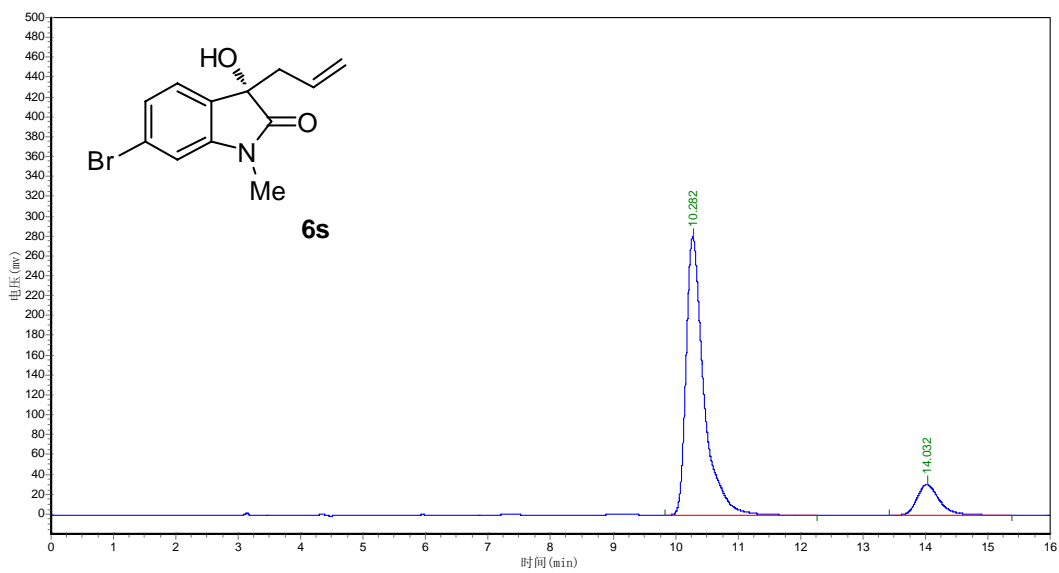
PeakNO.	Ret.Time	PeakHeight	PeakArea	Area%
1	23.457	29760.367	1176750.500	50.8366
2	26.973	25693.797	1138212.250	49.1634



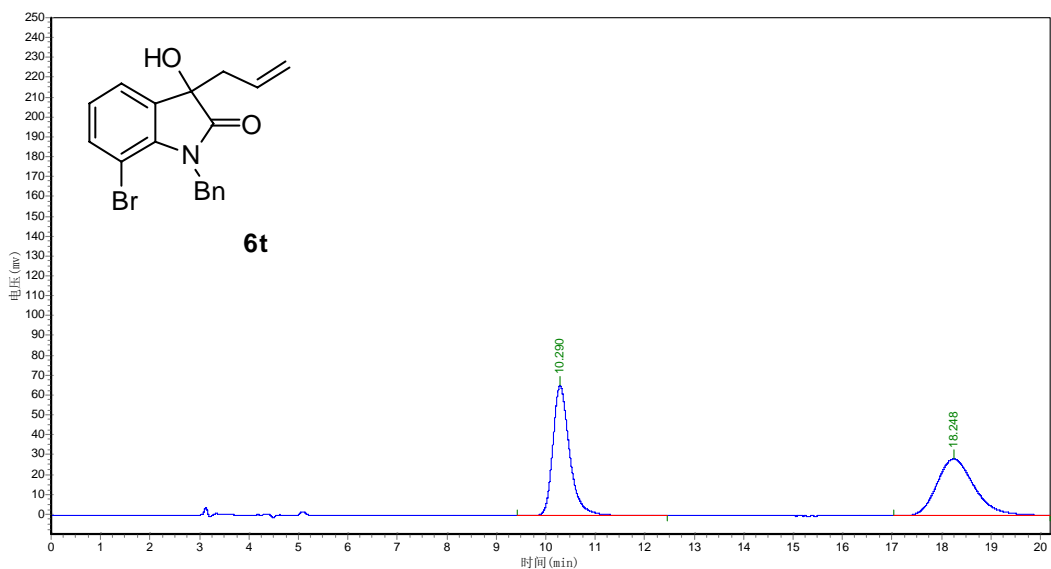
PeakNO.	Ret.Time	PeakHeight	PeakArea	Area%
1	24.348	21652.305	858483.875	15.1748
2	27.582	104353.813	4798808.500	84.8252



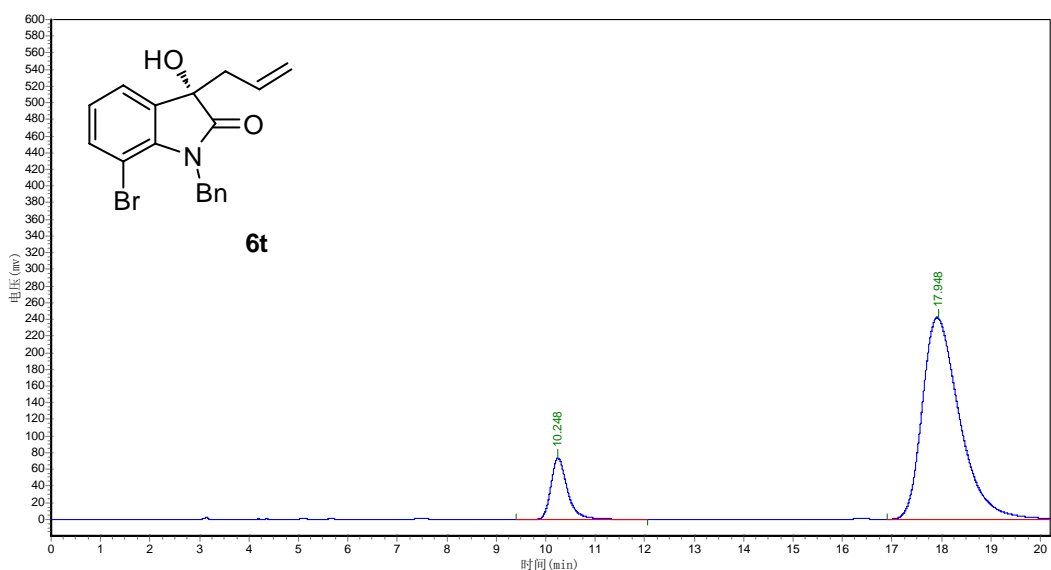
PeakNO.	Ret.Time	PeakHeight	PeakArea	Area%
1	10.373	94354.859	1861904.500	51.1402
2	14.082	68676.156	1778883.000	48.8598



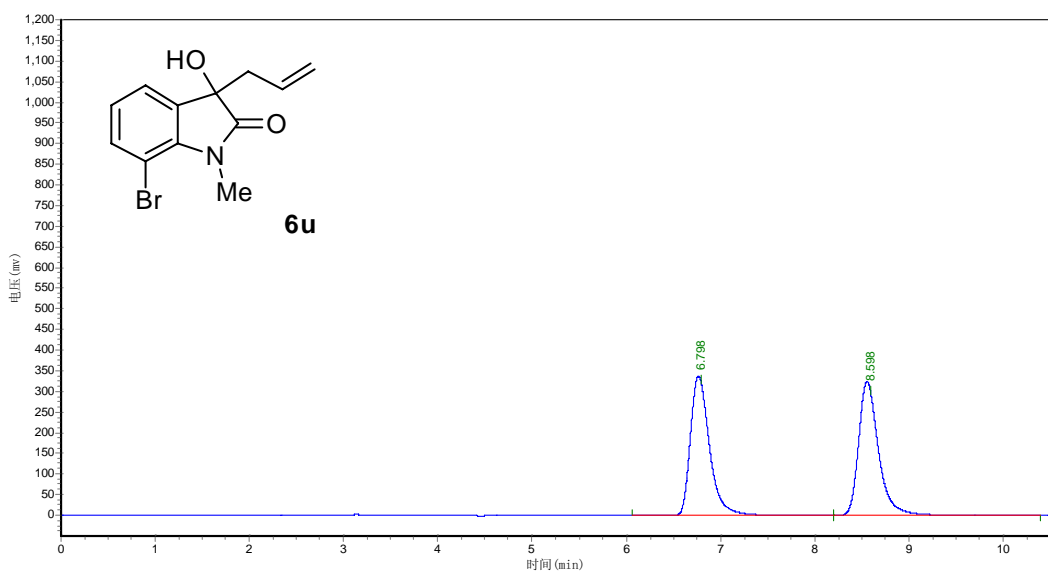
PeakNO.	Ret.Time	PeakHeight	PeakArea	Area%
1	10.282	280275.563	5549502.000	87.8031
2	14.032	30788.014	770893.500	12.1969



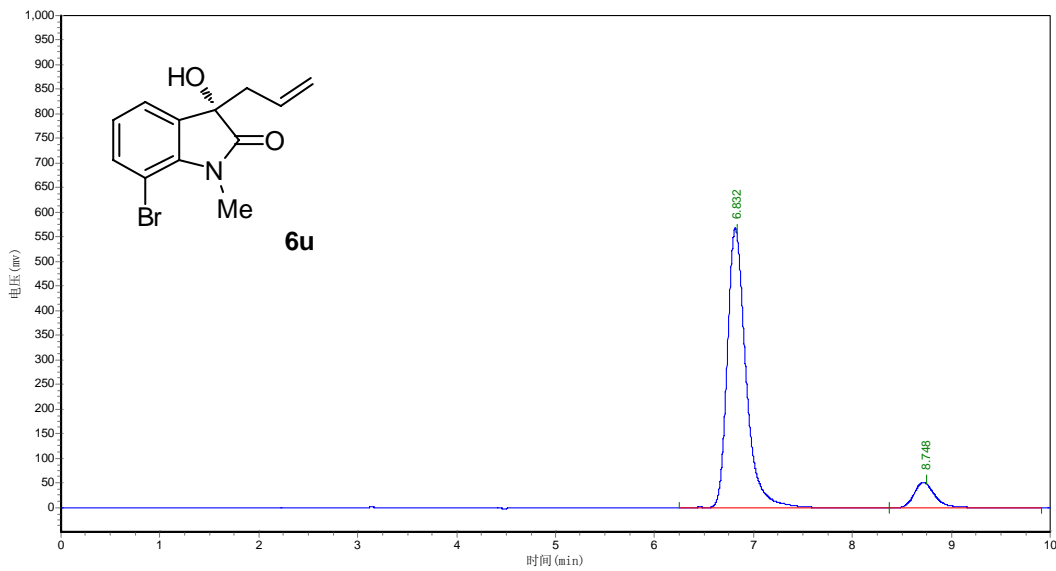
PeakNO.	Ret.Time	PeakHeight	PeakArea	Area%
1	10.290	64529.590	1545542.500	50.8803
2	18.248	28454.408	1492064.125	49.1197



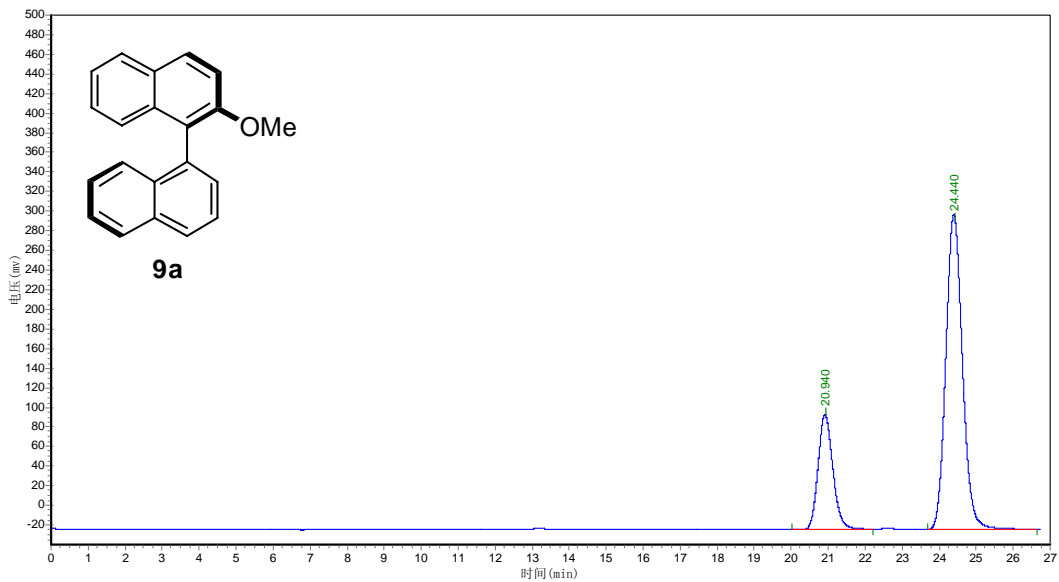
PeakNO.	Ret.Time	PeakHeight	PeakArea	Area%
1	10.248	72021.719	1697211.000	11.8081
2	17.948	242865.047	12676030.000	88.1919



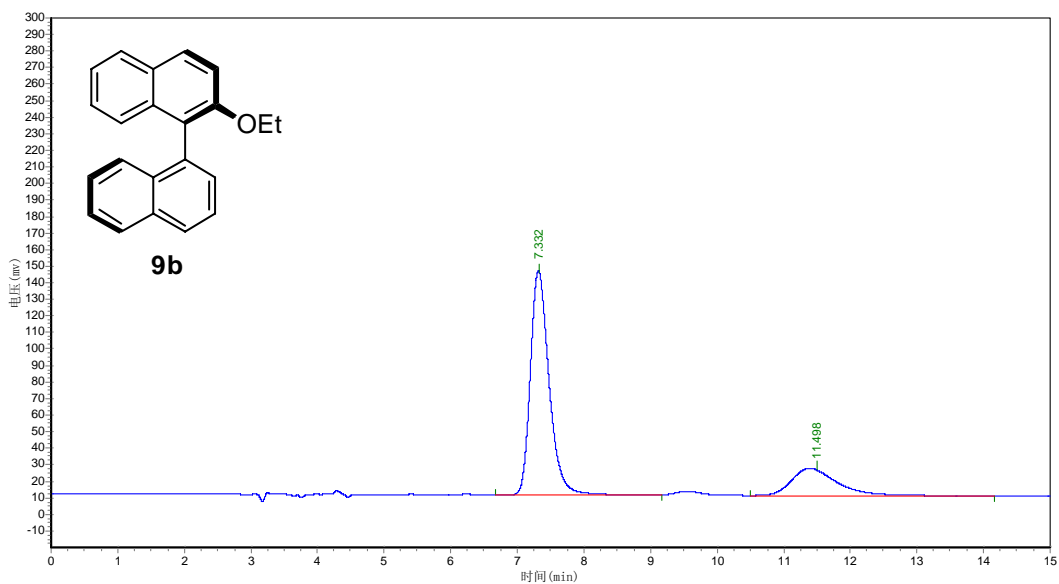
PeakNO.	Ret.Time	PeakHeight	PeakArea	Area%
1	6.798	329890.813	4792507.500	50.546
2	8.598	316043.406	4782059.500	49.9454



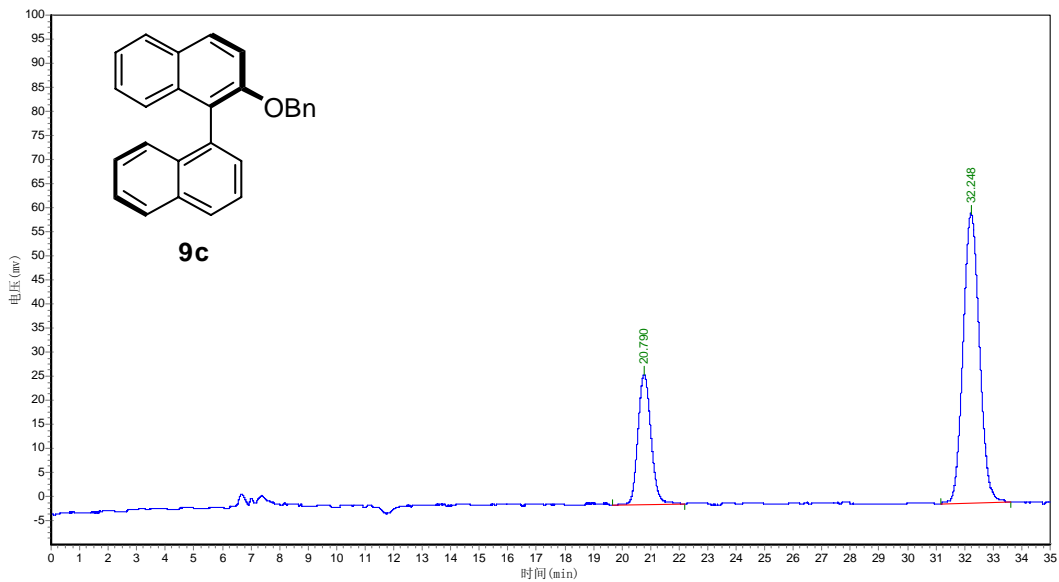
PeakNO.	Ret.Time	PeakHeight	PeakArea	Area%
1	6.832	560885.000	7461302.000	90.5709
2	8.748	51464.953	776780.188	9.4291



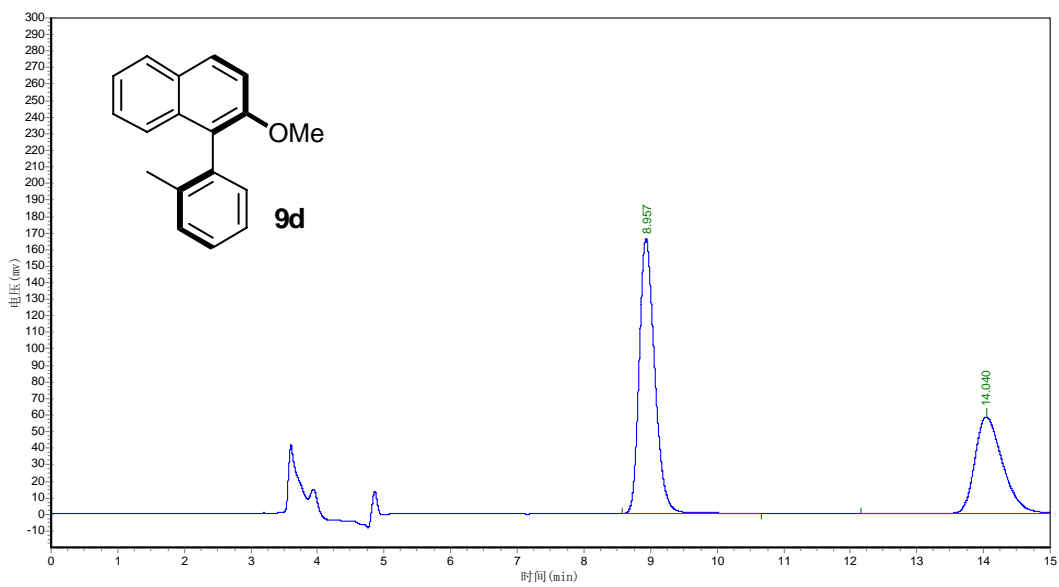
PeakNO.	Ret.Time	PeakHeight	PeakArea	Area%
1	20.940	113030.000	3240603.000	24.4637
2	24.440	309526.375	10005961.000	75.5363



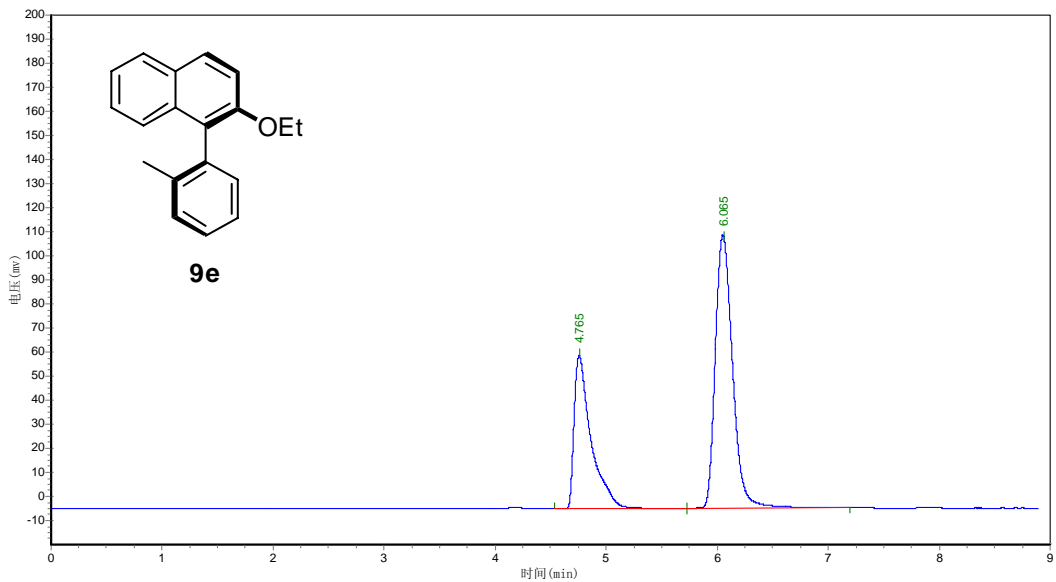
PeakNO.	Ret.Time	PeakHeight	PeakArea	Area%
1	7.332	135253.109	2665170.500	75.7229
2	11.498	16414.688	783910.750	22.2725



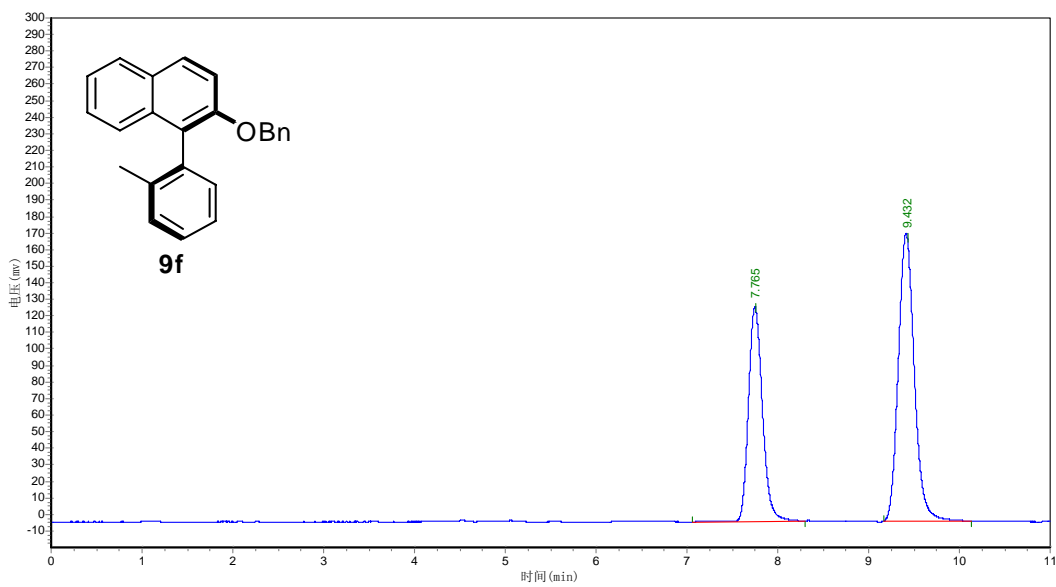
PeakNO.	Ret.Time	PeakHeight	PeakArea	Area%
1	20.790	26889.443	866877.063	24.4957
2	32.248	60158.680	2404885.250	75.5043



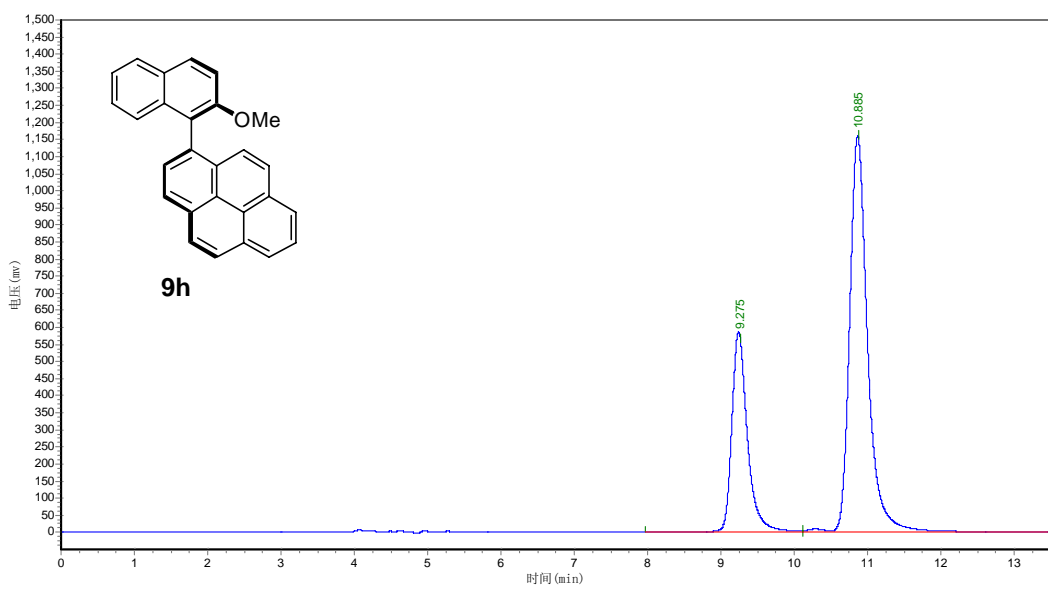
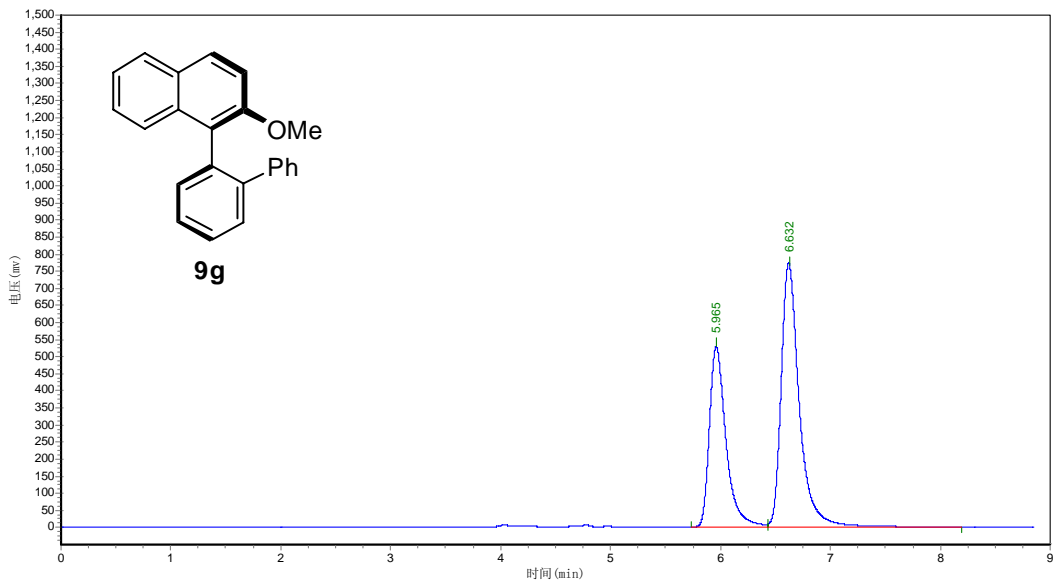
PeakNO.	Ret.Time	PeakHeight	PeakArea	Area%
1	8.957	163812.078	2688827.500	61.5748
2	14.040	58177.691	1677937.250	38.4252

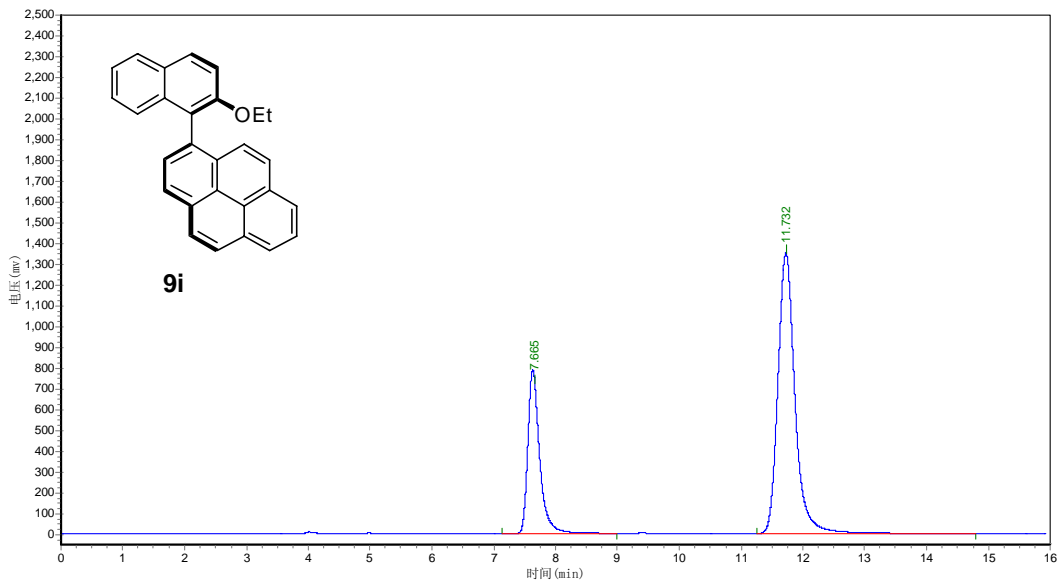


PeakNO.	Ret.Time	PeakHeight	PeakArea	Area%
1	4.765	59606.332	677907.375	35.4598
2	6.065	106107.336	1233857.000	64.5402

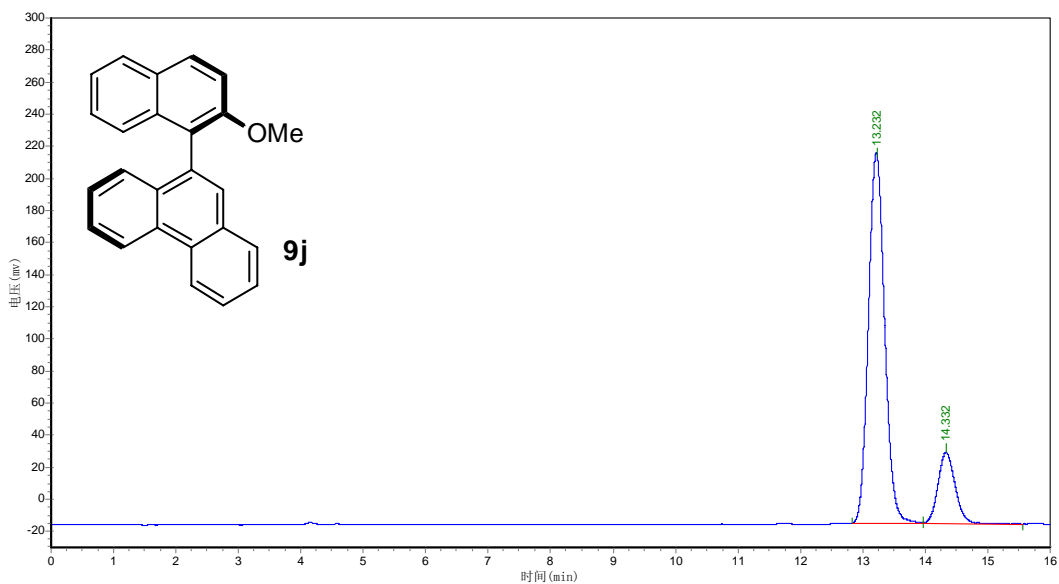


PeakNO.	Ret.Time	PeakHeight	PeakArea	Area%
1	7.765	122264.805	1413330.125	39.5027
2	9.432	167760.375	2164474.750	60.4973

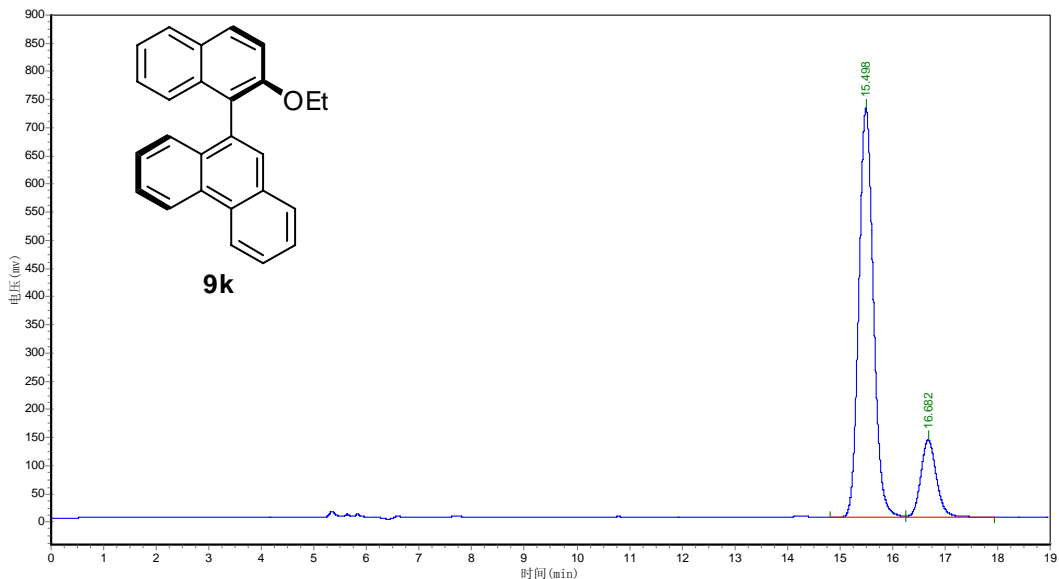




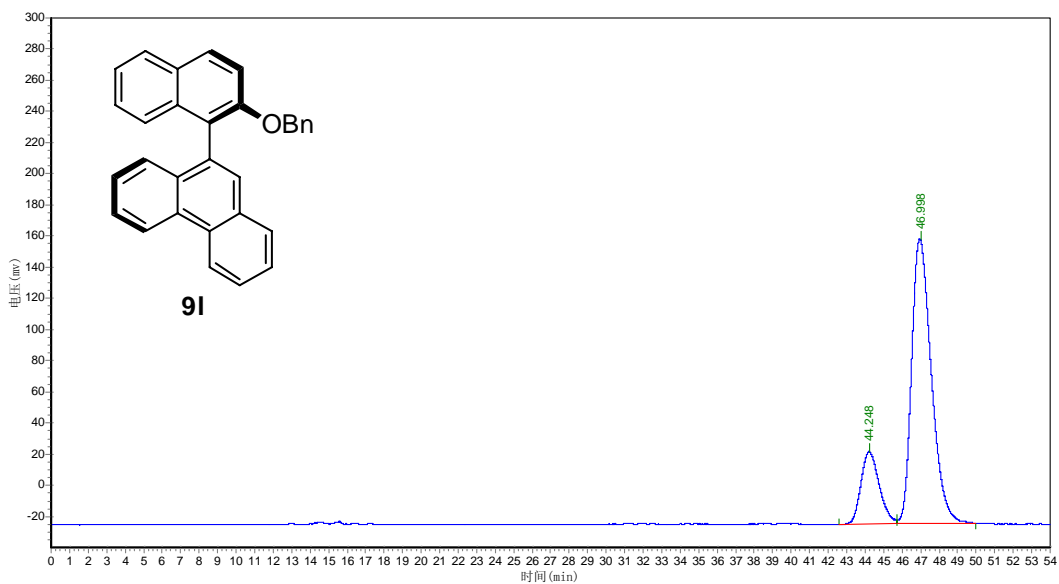
PeakNO.	Ret.Time	PeakHeight	PeakArea	Area%
1	7.665	643408.000	10396649.000	28.6495
2	11.732	1223090.625	25892460.000	71.3505



PeakNO.	Ret.Time	PeakHeight	PeakArea	Area%
1	13.232	230307.609	4192408.750	83.6917
2	14.332	44062.535	871393.000	16.3083



PeakNO.	Ret.Time	PeakHeight	PeakArea	Area%
1	15.498	726574.125	13942462.000	83.7169
2	16.682	137071.453	2811909.250	16.2831



PeakNO.	Ret.Time	PeakHeight	PeakArea	Area%
1	44.248	46322.242	3189235.750	19.0490
2	46.998	182892.156	13553059.000	80.9510